Diploma Thesis

Forces on mobile optical elements in a ring cavity

Institute of Physics
at University of Potsdam

Author:
Marc Herzog
(matriculation number: 710157)

Supervisor and first assessor:
PD Dr. Carsten Henkel

Second assessor:
Prof. Dr. Martin Wilkens

April 2008

Abstract

We consider a partially reflecting micro-mechanical mirror in thermal equilibrium placed into a ring cavity of circumference L, which is pumped by two external lasers that excite degenerate counterpropagating plane wave modes. The mirror of arbitrary reflectivity couples these modes, whereby optomechanical forces are exerted on the mirror, which can be identified as radiation pressure and dipole force. These can be exploited for trapping and cooling of the mirror motion in order to further approach the quantum regime of macroscopic objects. First, we investigate the effect of the micro-mirror on the cavity fields. In particular, the eigenmodes and eigenfrequencies of the composite system "ring cavity + mirror" are derived, which are given by even and odd mode functions corresponding to a lower and higher resonance frequency, respectively. Moreover, the eigenfrequencies are found to depend on the mirror reflectivity, but not on the mirror position, as opposed to the case of linear cavities with a movable end mirror. Second, we derive the various parts of the optomechanical force acting on the mirror (conservative and friction force) and study their dependence on the system parameters. Finally, the limit temperatures achievable with the particular setup are estimated and discussed.

Kurzdarstellung

Wir betrachten in dieser Arbeit einen teilreflektierenden, mikromechanischen Spiegel im thermischen Gleichgewicht, welcher sich in einem optischen Ringresonator vom Umfang L befindet. Dieser wird mittels zweier externer Pumplaser getrieben, die entartete, in entgegengesetzte Richtungen propagierende Moden von ebenen elektromagnetischen Wellen anregen. Der Spiegel mit beliebiger Reflektivität koppelt nun diese Moden, wodurch optomechanische Kräfte auf ihn einwirken und diese können als Strahlungsdruck und Dipolkraft identifiziert werden. Die auftretenden Kräfte können als Falle und als Kühlung für die Bewegung des Spiegels verwendet werden, um somit dem Quantenregime von makromechanischen Objekten näher zu kommen. Zuerst untersuchen wir die Effekte des Mikrospiegels auf die Resonatorfelder. Insbesondere werden die Eigenmoden und Eigenfrequenzen des zusammengesetzten Systems "Ringresonator + Spiegel" hergeleitet, welche durch gerade und ungerade Modenfunktionen beschrieben sind, die jeweils eine niedrigere bzw. höhere Eigenfrequenz besitzen. Desweiteren hängen die Eigenfrequenzen von der Reflektivität des Spiegels ab, jedoch nicht von seiner Position, was somit im Gegensatz zu linearen Resonatoren mit beweglichen Endspiegeln steht. Als zweites ermitteln wir die verschiedenen Komponenten der optomechanischen Kraft (konservative Kraft und Reibungskraft) und untersuchen deren Abhängigkeit von den Systemparametern. Schlussendlich wird die Grenztemperatur, die mit diesem speziellen Aufbau erreicht werden kann, abgeschätzt und diskutiert.

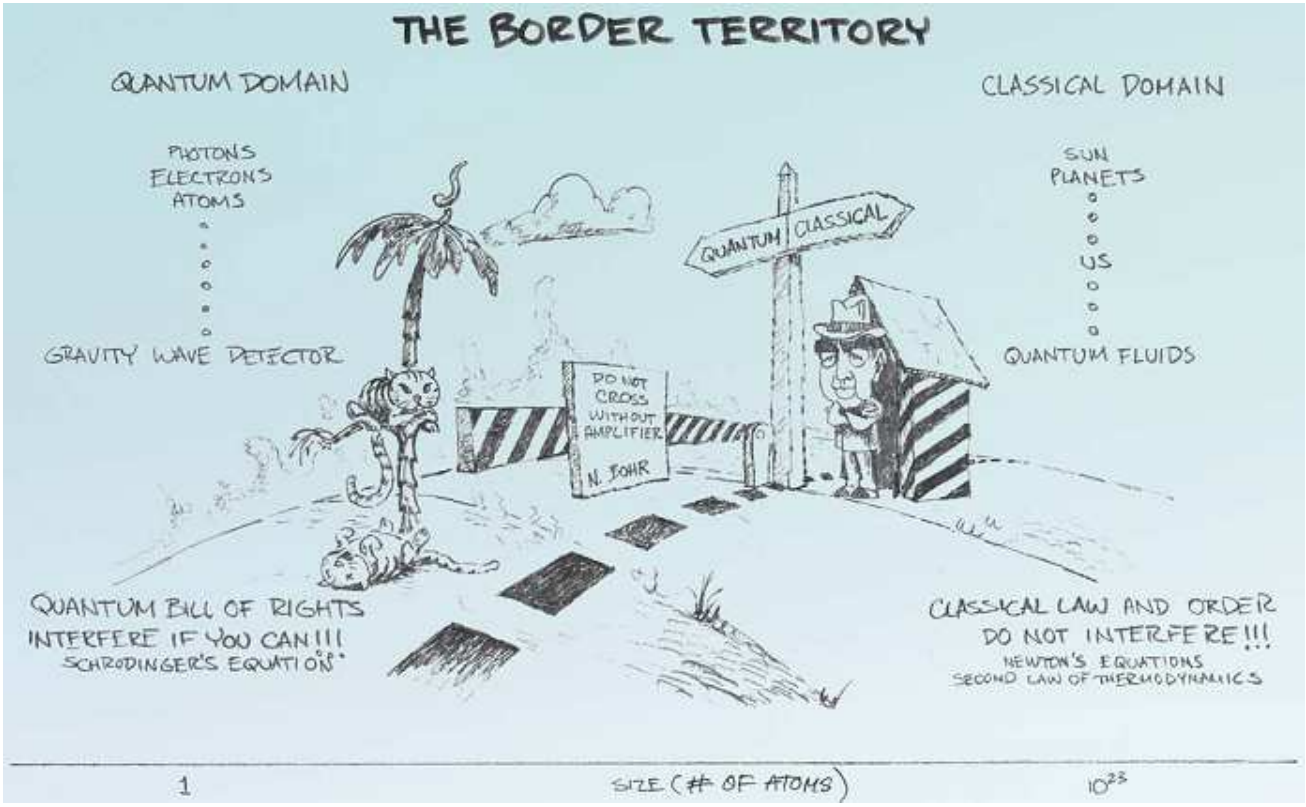

Figure 1: Caricature of the actually blurred border between the quantum and the classical world. It separates the laws of quantum and classical physics and is not yet clearly understood and hence of great research interest (from reference [1]).

Acknowledgements

I would like to thank all persons who directly and indirectly have participated in this thesis. I owe special thanks to my supervisor PD Dr. Carsten Henkel, who was always willing to help to overcome all the small and big obstacles on the way to this thesis. I am also grateful for inspiring discussions with Francesco Intravaia and Timo Felbinger, who also gave great computational support. Of course, thanks to all of the rest of the Quantum optics group, especially to secretary Marlies Path, who was always there to solve any problem whatsoever. Last but not least, special thanks for a lot of mental support to Peggy and my family.

Contents

Chapter 1

Introduction

Superposition of states and entanglement are "*the* characteristic trait of quantum mechanics" [2] and at the same time distinguishes it from the laws of classical physics. The preparation of superposition and entanglement of microscopic systems such as photons, atoms and ions has already been experimentally realized, mainly for the purposes of information processing and manipulation [3, 4, 5]. Probably the most famous phrase in this topic is the "Schrödinger cat", which describes a cat being in a superposition of being dead and alive. Such state should in principle be possible by the laws of quantum mechanics, however, one has never observed such macroscopic superposition states in nature. More and more research effort is therefore expended on preparing macroscopic superposition states and entanglement using micro- and nano-mechanical oscillators [6, 7, 8, 9, 10]. One of the motivations is to gain more insight into the fundamental structure of the physical reality, for instance, in setting or exploring the mark between the classical and quantum world (cf. fig. 1). In this mesoscopic regime one may hope to adjust the size of the system, and thus, interpolate between quantum and classical [11]. But there are also many promising applications such as in nanotechnology, quantum state engineering and high-precision measurements like gravitational wave detection [7, 9].

The fact that one has so far not observed macroscopic superposition states reflects the difference between the quantum and the classical world. There exists, however, the so called *decoherence* theory, which explains the appearance of a classical reality from an underlying quantum world [1, 12]. The suppression of quantum mechanical interferences and superpositions is due to the coupling of the macroscopic object to its environment. The larger the object becomes, the harder it is to isolate it from its environment, and the effect of the coupling is that the object's degrees of freedom are "measured" by the environment, thereby leading to a collapse of the quantum mechanical wave function of the object. The result is that only a few states (compared to the object's Hilbert space) survive this collapse and those are the classical ones observed in "everyday life" (e.g. coherent states in case of harmonic oscillators). This destruction of superpositions ("cat is dead *and* alive"), leaving only classical mixtures ("cat is dead *or* alive"), is represented by the decay of the off-diagonal elements (coherences) of the object's density matrix ρ with time. For example, consider a particle in a superposition state consisting of two narrow gaussian wavepackets separated by Δx in position phase space. The typical time

scale of decoherence, τ_D, for Quantum Brownian motion can then be estimated by [1, 12]

$$\tau_d^{-1} = D_p \left(\frac{\Delta x}{\hbar} \right)^2, \qquad D_p = 2m\gamma k_B T \tag{1.1}$$

where D_p is the momentum diffusion coefficient due to random force fluctuations induced by the environment at temperature T and the quantities m and γ are the object's mass and dissipation rate, respectively. To illustrate the effect, imagine a harmonic oscillator of mass $m \sim 10^{11}\,\mathrm{kg}$, resonance frequency $\Omega_m \sim 10^5\,\mathrm{Hz}$ and quality $Q_m \sim 10^6$, which are typical values we will use in this thesis. If such an oscillator was prepared in a superposition at room temperature with a spatial splitting of *only* an optical wavelength, e.g. $\Delta x \sim 10^{-6}\,\mathrm{m}$, the decoherence rate would be $\tau_D^{-1} \sim 10^{23}\,\mathrm{Hz}$, that is, the superposition would almost immediately decay into a classical mixture and macroscopic superpositions are thus next to impossible to prepare [11].

As one can see from the definition of D_p, this can only be improved if one drastically decreases m, $\gamma = \Omega_m/Q_m$ and the temperature T. On one hand, this is a challenging task for nanofabrication and material science. However, one can also employ optomechanical forces such as radiation pressure to approach the quantum regime and to increase the lifetime of quantum states of macroscopic objects. This is done by coupling the mechanical object to electromagnetic degrees of freedom, for example, by using coated micro- or nano-mechanical oscillators as one end mirror of a linear cavity [6, 13, 14, 15, 16] or as a mirror inside a linear cavity, effectively splitting it in two [7, 9, 10]. The technical challenge is integrating sensitive micro-mechanical elements (typically small, light and flexible) into high-finesse cavities (more rigid and massive) without compromising either [10, 17]. For example, for very light/thin mechanical oscillators, it is hard to achieve reflectivities close to unity, which is essential for a large cavity finesse. Therefore, experiments with partially reflecting mirrors (PRM) are also considered [10]. In such experiments, optomechanical trapping and cooling of the micro-mechanical objects is achieved for a suitable choice of parameters like cavity detuning and pump laser power. All experiments using linear cavities have in common, that the motion of the micro-mirror changes the length of the cavity and, thus, its resonance frequencies. The trapping and cooling effects of the cavity fields are mainly related to this particular feature.

In this thesis we consider a ring cavity, similar to the one used in [18], supporting two degenerate travelling plane wave modes, which are driven in general by independent pump lasers. Moreover, a micro-mechanical oscillator with arbitrary reflectivity is placed into the beam line of the cavity fields in order to generate optomechanical forces acting on it. Due to the translational symmetry along the ring coordinate, the eigenfrequencies of the ring cavity do not depend on the position of the partially reflecting mirror (PRM), as opposed to linear cavities with a movable end mirror. The source of the optomechanical forces is thus not only due to radiation pressure, but also to dipole forces as in the case of atoms in a cavity field. As pointed out in [19], the phase fluctuations due to the linewidth of the driving laser, which result in optomechanical force fluctuations and thus in an additional Brownian noise for the oscillator, already question the possibility of ground state cooling of such macroscopic

devices. It is further mentioned that this problem can be circumvented by using a double-cavity, where under certain circumstances the phase noise would cancel. This should in principle also hold for a ring cavity, which would make it more advantageous. We will, however, not discuss the effect of pump laser phase fluctuations in this work.

In chapter 2 we will present the particular experimental setup under consideration in more detail and give some reference values, which will be used when making quantitative estimates. Chapter 3 briefly reviews the quantum mechanical description and the properties of a harmonic oscillator and the consequences of the coupling to a bosonic environment at temperature T, which lead to the so called *Langevin equation* of a dissipative harmonic oscillator. Moreover, the quantization of the electromagnetic field inside the ring cavity, at first omitting the PRM, is shortly presented. The influence of the PRM on the cavity fields and the coupling thereof is derived in chapter 4. There, we use a matrix formalism to obtain the eigenmodes and eigenfrequencies of the ring cavity and we then find the time evolution of the eigenmodes in terms of Langevin equations. At the end of this chapter, we investigate the steady-state solutions of the cavity fields. In chapter 5 the optomechanical force exerted on the micro-mechanical mirror by the cavity fields is derived by three different approaches. We look for the ability of trapping and cooling the PRM and estimate the limit temperature that can be achieved by using the present setup. Chapter 6 concludes the thesis.

Chapter 2

Experimental Setup

In this thesis, we will derive and analyze the optomechanical forces exerted on a movable partially reflecting micro-mechanical mirror (PRM) by the electromagnetic fields of a ring cavity. The experimental setup considered is sketched in figure 2.1. It consists of three massive, rigid mirrors, two of which are high-reflective end mirrors (M) and their motion can be completely neglected due to their huge mass. The third one is an in-out coupling mirror (CM) with a small, non-vanishing transmittivity T and is used to couple light into the ring cavity, as well as to obtain information about the radiation of the optical ring resonator and thereby also information about the PRM inside the resonator, since these two are coupled via optomechanical forces such as radiation pressure. The three massive mirrors are arranged to form a triangular ring cavity of circumference L, which is able to support different cavity modes, such as travelling plane wave modes or, alternatively, even and odd parity modes. We will, however, start our considerations with only two degenerate counterpropagating plane wave modes, which are driven by two external pump lasers at frequency ω_p whose radiation is coupled into the ring cavity through the CM. The restriction to only these two travelling plane wave modes is possible if the free spectral range of the cavity is much larger than the bandwidth κ of the considered modes, such that there is no coupling to other cavity modes. Moreover, the coupling to other modes by the PRM is also neglected.

The key feature of our experimental setup, however, is the micro-mechanical mirror placed into the beam line at the opposite position to the CM with its surface perpendicular to the propagation direction of the plane waves. It is fabricated to have a certain amplitude reflection coefficient $0 \leq |\rho| \leq 1$, which is one of the parameters of our system. This partially reflecting mirror (PRM) thereby couples the two counterpropagating waves due to the reflection thereof at the PRM's surface. We assume additionally that the mirror is conservative, such that we can neglect any absorption of the electromagnetic fields by the mirror. Moreover, the PRM is a movable object, that is, it may be displaced by a force acting on it, such as optomechanical forces. Micro-mechanical oscillators can be realized by single- and double-clamped cantilevers/beams [20] or membranes [17] made of some dielectric material. These devices can be considered as harmonic oscillators of effective mass m and resonance frequency Ω_m, where one usually restricts oneself onto the fundamental flexural mode of the device. Typically, the frequencies of mechanical oscillators are in the kHz do-

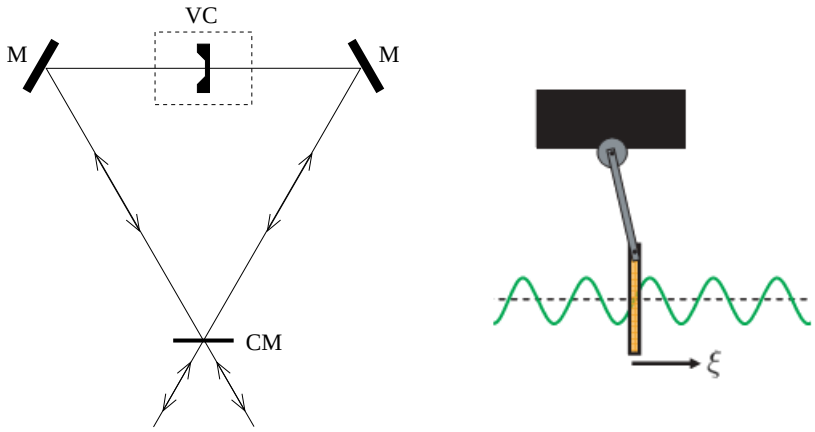

Figure 2.1: The left panel shows a schematic of the experimental setup under consideration, i.e. the ring cavity made by two massive, high-reflective mirrors (M) and an in-out coupling mirror (CM) to drive the cavity by external pump lasers. The partially reflecting micro-mechanical mirror resides in a vacuum chamber to minimize its coupling to the environment. The right panel illustrates the movable mirror in the electromagnetic cavity field. The optomechanical forces exerted on the mirror may induce a displacement ξ (from reference [17]).

main, but they can be raised up to GHz [20, 21]. As pointed out in ref. [22], it is possible to consider such macroscopic oscillators as a quantum oscillator, which we will do throughout this thesis. The setup can be realized in a way that we only have to consider the one-dimensional motion of the PRM along the coordinate of the beam line of the ring, say x. The PRM is put into a vacuum chamber as indicated in figure 2.1 in order to isolate it from the environment as far as possible, thereby increasing its quality. Furthermore, the thickness of the mechanical oscillator is assumed to be small compared to the wavelength of the cavity fields, such that we can neglect it and consider the PRM infinitely thin. Later, we will also see that the amplitude of the mirror displacement ξ is also much smaller than the wavelength of the cavity fields, i.e. $k\xi \ll 1$.

Reference parameters for the PRM In order to present quantitative results, we will assume a certain range of parameters concerning the micro-mechanical mirror under consideration. Throughout this thesis we will focus on thin oscillating dielectric membranes of certain reflectivity, whose properties have been examined by Thompson *et al* [17]. Figure 2.2 shows a photograph of such a membrane. The authors have placed the membrane into the middle of a Fabry-Perot cavity, such that it actually forms two separate linear cavities, which are coupled due to the non-vanishing membrane reflectivity. The membrane used in [17] has a resonance frequency of the lowest flexural mode of $\Omega_m \sim 10^5\,\mathrm{Hz}$, an effective mass $m \sim 10^{-11}\,\mathrm{kg}$ and a quality factor of $Q \sim 10^6$. Furthermore, the authors have successfully cooled such devices down to a temperature of $\sim 10^{-1}\,\mathrm{K}$. We will use these values as reference values when calculating the wanted quantities.

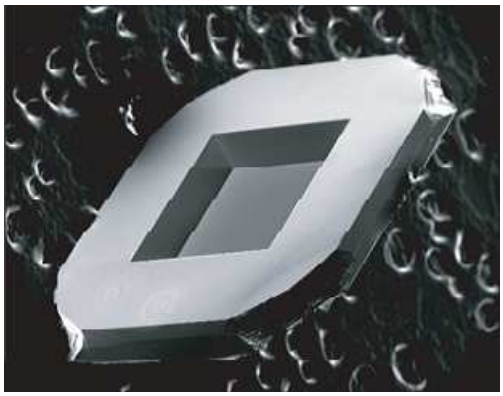

Figure 2.2: Photograph of a SiN membrane of dimensions $1\,\mathrm{mm}\times1\,\mathrm{mm}\times50\,\mathrm{nm}$ on a silicon chip (right panel from reference [17]).

The typical orders of magnitudes of the parameters used in this thesis are listed in table 2.1. As mentioned above, the parameters concerning the micro-mechanical oscillator are taken from [17].

	parameter	order of magnitude
micro-mech. osc.	m	$10^{-11}\,\mathrm{kg}$
	Ω_m	$10^{5}\,\mathrm{Hz}$
	Q_m	10^{6}
	T_0	$10^{-1}\,\mathrm{K}$
ring cavity	L	$10^{-2}\,\mathrm{m}$
	T	10^{-3}
	ω_p	$10^{15}\,\mathrm{Hz}$
implied parameters	$\tau = L/c$	$10^{-10}\,\mathrm{s}$
	$\kappa \approx T/\tau$	$10^{7}\,\mathrm{Hz}$

Table 2.1: Orders of magnitudes of the parameters used in this thesis

Distinct time scales and corresponding assumptions The setup under consideration possesses several typical time scales, which have different orders of magnitude and therefore allow for some approximation later on. The by far shortest time scale is given by the frequency of the cavity fields which is of the order of $\omega \sim 10^{15}\,\mathrm{Hz}$, since we will assume frequencies in the optical domain. This frequency marks a very fast time scale, which is very short compared to any time scale of the dynamics of the system. The next larger time scale is given by the cavity round trip time—the time needed for the radiation to circulate the ring once. This time is $\tau = L/c$ and is thus determined by the length of the cavity, which is typically of the order of $L \sim 10^{-2}\,\mathrm{m}$, although optical cavities of the order of $10\,\mu\mathrm{m}$ already exist [21]. For such small cavities, the round trip time scale is much shorter than the time scale of the mirror dynamics, $\Omega_m\tau \ll 1$, that is, the mirror is quasi-stationary during a single round trip of the radiation. This will be an important assumption when deriving the equations

of motion of the cavity fields in chapter 4, because these also depend on the mirror position and thus in general on its dynamics. A quite similar time scale to the round trip time τ will be the change of the eigenfrequencies of the cavity modes with the PRM reflectivity, which is alternatively described by the parameter $\theta \in [0, \pi/2]$. This change is found to be quantified by $\pm\theta/\tau$. The force, e.g. of a photon being reflected off the mirror's surface, is proportional to the actual frequency of the corresponding electromagnetic field. As the change of the eigenfrequencies is, however, much smaller than the optical frequencies of the cavity fields, we can neglect it when analyzing the optomechanical forces. Another time scale is set by the dynamics of the cavity fields itself, which is mainly determined by the dissipation rate of the cavity, κ. As we will see in chapter 4, for small incoupling mirror transmittivities $T \ll 1$ this rate can be approximated by $\kappa = T/\tau$ and typically using values of the order of $T \sim 10^{-3}$ renders the corresponding time scale much larger than the round trip time τ. This also corresponds to the requirement of the free spectral range ($\sim \tau^{-1}$) being much larger than the bandwidth of the cavity mode (κ) mentioned above. Finally, the resonance frequency of the micro-mechanical oscillator is assumed to be much smaller than the cavity bandwidth, i.e. $\Omega_m \ll \kappa$. This is also known as the *bad cavity limit*, which is obviously fulfilled if we apply the reference parameter given above. It implies that the mirror motion is still slow on the time scale of the field dynamics, which enables us to use certain approximations in the following calculations. Moreover, it prevents the mirror from scattering photons into other cavity modes than the considered one, since the mirror's oscillation frequency is also well below the free spectral range.

Chapter 3

Theoretical basis

3.1 Review of the quantum harmonic oscillator

As the harmonic oscillator is of central meaning to quantum mechanics in general and to this thesis in particular, we will give a short review of the main properties and briefly present possible states of the quantum mechanical oscillator. We then derive the Langevin equations describing the dissipative dynamics of a driven harmonic oscillator coupled to a bosonic heat bath, as those will form the basis of our analysis of the cavity fields.

3.1.1 Basic description and states

The time evolution of a general quantum mechanical system is governed by the Schrödinger equation

$$i\hbar|\dot{\psi}\rangle = H|\psi\rangle \tag{3.1}$$

where $H : \mathcal{H} \to \mathcal{H}$ is the system's Hamilton operator (Hamiltonian) and $|\psi\rangle \in \mathcal{H}$ is an element of the system's Hilbert space $\mathcal{H}$ and represents the state of the corresponding system. In this so called *Schrödinger picture* the operators representing physical observables are kept constant and the states of the system evolve in time according to the Schrödinger equation (3.1).

Another possible way of considering time evolution is the use of the *Heisenberg picture* where the state $|\psi\rangle$ is kept constant but now the operators are time-dependent. The dynamics of an operator $\mathcal{O}$ is then determined by Heisenberg's equation of motion

$$\dot{\mathcal{O}} = \frac{i}{\hbar}[H, \mathcal{O}] \tag{3.2}$$

In both cases, it is the Hamiltonian that generates the time evolution of a quantum mechanical system. Thus, we will first take a look at the particular Hamiltonian of a harmonic oscillator and then briefly review some of the most important states the oscillator can be in and which will be used in this thesis.

The Hamiltonian of the harmonic oscillator

As noted above, the quantum description of the harmonic oscillator of frequency ω is based on its Hamiltonian, which is—if expressed in terms of the position operator

q and its canonical conjugate, the momentum operator p—given by

$$H_{\text{osc}} = \frac{p^2}{2m} + \frac{1}{2}m\omega^2 q^2 = \frac{m\omega^2}{2}\left(q + i\frac{p}{m\omega}\right)\left(q - i\frac{p}{m\omega}\right) - \frac{\hbar\omega}{2} \tag{3.3}$$

where the Hermitian operators q and p satisfy the canonical commutation relation

$$[q, p] := qp - pq = i\hbar\,\mathbb{1} \tag{3.4}$$

and $\mathbb{1}$ is the identity operator. As suggested by the second formulation of (3.3), one can define a new pair of operators, which are a linear combination of q and p given by

$$a := \sqrt{\frac{m\omega}{2\hbar}}\left(q + i\frac{p}{m\omega}\right) \tag{3.5}$$

and its hermitian conjugate

$$a^\dagger := \sqrt{\frac{m\omega}{2\hbar}}\left(q - i\frac{p}{m\omega}\right) \tag{3.6}$$

It is easy to check that these operators obey the (bosonic) commutation relation

$$[a, a^\dagger] = \mathbb{1} \tag{3.7}$$

Then, the oscillator's Hamiltonian takes the well-known form

$$H_{\text{osc}} = \hbar\omega\left(aa^\dagger - \frac{1}{2}\right) = \hbar\omega\left(a^\dagger a + \frac{1}{2}\right) \tag{3.8}$$

Fock states

As can be seen in (3.8), the eigenbasis of H_{osc} is identical to the eigenbasis of the number operator $n := a^\dagger a$. The eigenstates of the operator n are the so called *number states* or *Fock states*

$$a^\dagger a|n\rangle = n|n\rangle \tag{3.9}$$

Thus, we have

$$H|n\rangle = \hbar\omega\left(n + \frac{1}{2}\right)|n\rangle =: E_n|n\rangle \tag{3.10}$$

where one can see the structure of energy levels of a harmonic oscillator. Hence, the number $n \in \mathbb{N}^0$ labels the energy levels and is therefore also a number of excitations of the oscillator. The effect of a and $a^\dagger$ onto these states is described by

$$a|n\rangle = \sqrt{n}|n-1\rangle \tag{3.11}$$

$$a^\dagger|n\rangle = \sqrt{n+1}|n+1\rangle \tag{3.12}$$

which is the reason that these operators are called *ladder operators* or *annihilation and creation operator*, respectively. The ground state of the oscillator, i.e. the state of minimum energy, corresponds to $n = 0$ and is also called *vacuum state*. As already indicated, the set of Fock states $\{|n\rangle\}_{n\in\mathbb{N}^0}$ forms an orthonormal basis of the oscillator's associated Hilbert space, i.e. $\langle n|m\rangle = \delta_{nm}$, and therefore a general state $|\psi\rangle$ of the harmonic oscillator can be expressed as a superposition of Fock states

$$|\psi\rangle = \sum_{n=0}^{\infty} c_n|n\rangle \tag{3.13}$$

Coherent states

A class of states of particular importance consists of the eigenstates of the annihilation or lowering operator with eigenvalue α

$$a|\alpha\rangle = \alpha|\alpha\rangle \tag{3.14}$$

These eigenstates are specified by the complex number α and are called *coherent states*. They were introduced by Glauber [23] and Sudarshan [24]. In the Fock basis, they take the form

$$|\alpha\rangle = e^{-|\alpha|^2/2} \sum_{n=0}^{\infty} \frac{\alpha^n}{\sqrt{n!}} |n\rangle \tag{3.15}$$

and alternatively they can also be described in terms of *Glauber's displacement operator* D_α

$$|\alpha\rangle = D_\alpha|0\rangle, \qquad \text{where} \quad D_\alpha = \exp(\alpha a^\dagger - \alpha^* a) \tag{3.16}$$

which expresses that the coherent state is just a displaced vacuum state, hence the name of the operator. Coherent states are normalized, $\langle\alpha|\alpha\rangle = 1$, but not orthogonal, $|\langle\alpha|\beta\rangle|^2 = \exp(-|\alpha - \beta|^2)$.

In case of the harmonic oscillator with a Hamiltonian as in (3.8), the time evolution of the annihilation operator in the Heisenberg picture is governed by the Heisenberg equation

$$\dot{a} = \frac{i}{\hbar}[H_{\text{osc}}, a] = -i\omega a \tag{3.17}$$

and if we take a look at the expectation value of a in a coherent state $\langle a\rangle_\alpha = \langle\alpha|a|\alpha\rangle = \alpha$ we find that $\alpha(t) = \alpha(0)e^{-i\omega t}$. The expectation value of the oscillator's position operator $q = q_0(a + a^\dagger)$ then behaves like

$$\langle q(t)\rangle_\alpha = q_0\big[\alpha(t) + \alpha^*(t)\big] = 2q_0|\alpha(0)|\cos(\omega t - \varphi_\alpha) \tag{3.18}$$

where $q_0 = \Delta q = \sqrt{\hbar/2m\omega}$ is the zero-point fluctuation of position and $\alpha(0) = |\alpha(0)|e^{i\varphi_\alpha}$. Here, one sees that the mean position of an oscillator in a coherent state fulfills a classical oscillation. Furthermore, one can show that $\Delta q \cdot \Delta p = \hbar/2$ holds for any coherent state, i.e. irrespective of the complex number α the coherent state is a minimum uncertainty state, which is not hard to understand as a coherent state is nothing else than a displaced vacuum (cf. (3.16)). These two facts show that a quantum oscillator being in a coherent state is the closest analog to a classical oscillator.

Thermal state

If the oscillator is in contact with an environment in thermal equilibrium at temperature T, it will be excited to a so called *thermal state*. However, the thermal state is actually not a pure state like $|\psi\rangle \in \mathcal{H}$, which implies perfect knowledge of the state of the system, but rather a mixed state, where we know the state of the system only

probabilistically. In that case, one has to use the language of the density operator. Written in terms of the Fock basis, for a mixed state it has the form

$$\rho_T = \sum_{n=0}^{\infty} p_n(T)|n\rangle\langle n| \tag{3.19}$$

where the normalized probability distribution $p_n(T)$ of the energy levels $E_n = \hbar\omega(n+1/2)$ is given by the usual Boltzmann factor

$$p_n(T) = \frac{\exp(E_n/k_BT)}{\sum_n \exp(E_n/k_BT)} = e^{-n\frac{\hbar\omega}{k_BT}}\left(1 - e^{-\frac{\hbar\omega}{k_BT}}\right) \tag{3.20}$$

and depends on the frequency of the oscillator ω and the temperature T. Here, k_B is Boltzmann's constant. The meaning of $p_n(T)$ is that it gives the probability of finding the oscillator in the state $|n\rangle$.

In general, the kth moment of an operator $\mathcal{O}$, with respect to the state of the system specified by a density matrix ρ, is defined by

$$\langle\mathcal{O}^k\rangle = \mathrm{tr}(\rho\mathcal{O}^k) = \sum_{n=0}^{\infty}\langle n|\rho\mathcal{O}^k|n\rangle \tag{3.21}$$

where the latter equation corresponds to an expansion into a Fock basis. The mean and variance of an operator $\mathcal{O}$ are defined as $\langle\mathcal{O}\rangle$ and $(\Delta\mathcal{O})^2 := \langle\mathcal{O}^2\rangle - \langle\mathcal{O}\rangle^2$, respectively.

Applying this to the oscillator's position and momentum operator given by

$$q = \sqrt{\frac{\hbar}{2m\omega}}(a^\dagger + a) \tag{3.22}$$

$$p = i\sqrt{\frac{\hbar m\omega}{2}}(a^\dagger - a) \tag{3.23}$$

and assuming a thermal state ρ_T, one finds

$$\langle q\rangle_T = \langle p\rangle_T = 0 \tag{3.24}$$

where we used of the orthonormality of the Fock basis and the particular action of a and $a^\dagger$ onto Fock states mentioned in (3.11) and (3.12). The non-vanishing variances are given by

$$(\Delta q)^2 = \langle q^2\rangle_T = q_0^2\big(2\bar{n}_T + 1\big), \qquad q_0 = \sqrt{\frac{\hbar}{2m\omega}} \tag{3.25}$$

$$(\Delta p)^2 = \langle p^2\rangle_T = p_0^2\big(2\bar{n}_T + 1\big), \qquad p_0 = \sqrt{\frac{\hbar m\omega}{2}} \tag{3.26}$$

where q_0 and p_0 are the zero-point position and momentum uncertainties, respectively. We also made use of the well-known Bose-Einstein distribution

$$\bar{n}_T = \langle a^\dagger a\rangle_T = \sum_n n p_n(T) = \frac{1}{\exp(\hbar\omega/k_BT) - 1} \tag{3.27}$$

giving the average number of excitation of the oscillator, which is no longer zero (ground state) at finite temperature T. Equation (3.25) reveals that the position uncertainty is minimized to q_0 as $T \to 0$, which corresponds to the oscillator being in its ground state, i.e. $\bar{n}_T = 0$.

Using the results above, the mean energy of the oscillator in a thermal state is found to be

$$\langle H \rangle_T = \frac{\langle p^2 \rangle_T}{2m} + \frac{1}{2} m\omega^2 \langle q^2 \rangle_T \tag{3.28}$$

$$= \frac{\hbar\omega}{2}\left(\bar{n}_T + \frac{1}{2}\right) + \frac{\hbar\omega}{2}\left(\bar{n}_T + \frac{1}{2}\right) \tag{3.29}$$

$$= \hbar\omega\left(\bar{n}_T + \frac{1}{2}\right) \tag{3.30}$$

$$= \frac{\hbar\omega}{2}\coth\left(\frac{\hbar\omega}{2k_B T}\right) \tag{3.31}$$

The equivalence of (3.28) and (3.30) is obvious by the two representations of the oscillator's Hamiltonian given in (3.3) and (3.8).

Equation (3.29) displays that the mean kinetic and potential energy of an oscillator contribute equal amounts to the mean total energy. This is nothing else than the famous equipartition theorem, which is an implication of the fact that the oscillator is assumed to be in thermal equilibrium. At high temperatures, i.e. $\hbar\omega \ll k_B T$, one can apply the relation

$$\coth\left(\frac{\beta}{2}\right) = \frac{e^{\beta}+1}{e^{\beta}-1} \approx \frac{1}{\beta} \tag{3.32}$$

whereby the mean energy (3.31) turns into the usual high-temperature equipartition theorem,

$$\langle H \rangle_T = k_B T \qquad (\hbar\omega \ll k_B T) \tag{3.33}$$

Application to the micro-mechanical mirror As mentioned above, we will treat the mechanical oscillator inside the ring cavity as a quantum oscillator and we will in particular assume it to be in a thermal state at the initial temperature $T_0 \sim 10^{-1}\,\mathrm{K}$. The other reference parameters of the mechanical oscillator are given in table 2.1. In order to observe quantum effects of such an oscillator, the following relation has to be fulfilled [22]

$$k_B T \lesssim \frac{\hbar\Omega_m}{2} \tag{3.34}$$

which ensures that the thermal fluctuations induced by the environment are smaller than the zero-point energy of a harmonic oscillator. Applying our reference parameters, this calls for temperatures $T \lesssim 10^{-6}\,\mathrm{K}$, which is, to the best of our knowledge, far away from being realized in experiments. This, however, motivates the task to optically cool such micro-mechanical devices by coupling it to electromechanical cavity fields, as is done with the current setup.

Moreover, we find the following orders of magnitude for the position and momentum uncertainties ξ_0 and p_0 of our mechanical oscillator, respectively,

$$\xi_0 = \sqrt{\frac{\hbar}{2m\Omega_m}} \sim 10^{-14}\,\mathrm{m} \tag{3.35}$$

$$p_0 = \sqrt{\frac{\hbar m\Omega_m}{2}} \sim 10^{-20}\,\mathrm{kg}\frac{\mathrm{m}}{\mathrm{s}} \tag{3.36}$$

We therefore work in the *Lamb-Dicke limit* as the Lamb-Dicke parameter $k\xi_0 \sim 10^{-7} \ll 1$ is much smaller than unity. In particular, the variances of the dimensionless mirror displacement $k\xi$ and the scaled mirror velocity kv are

$$k\Delta\xi = k\xi_0\sqrt{2\bar{n}_{T_0}+1} \sim 10^{-5} \ll 1 \tag{3.37}$$

$$\frac{k\Delta v}{\kappa} = \frac{kp_0}{m\kappa}\sqrt{2\bar{n}_{T_0}+1} \sim 10^{-7} \ll 1 \tag{3.38}$$

That is, the typical mirror displacement is much smaller than the wavelength of the cavity fields and the mirror moves much less than a wavelength on the time scale of the field dynamics. This enables us to use certain approximations later on. We also find that the mirror momentum is several orders of magnitudes larger than the typical photon momentum, i.e.

$$\frac{\Delta p}{\hbar k} \sim 10^9 \tag{3.39}$$

which will be exploited in section 5.1.3.

3.1.2 Coupling to a bosonic environment and Langevin equations

In the previous section, we reviewed some of the fundamental properties of the isolated quantum harmonic oscillator and of an oscillator in a thermal state. In reality, a system is never really isolated due to the coupling to the environment or to a reservoir (or heat bath). These couplings of course change the behaviour of the system and lead to different Heisenberg equations. However, the external variables can be eliminated leading to Langevin equations for the system variables including noise operators which will form the basis of our analysis. The considerations made in this section follow the standard derivation of the Langevin equation for the oscillator's annihilation operator. Further details can be found for instance in [25, 26, 27].

In the following, we consider the coupling of the harmonic oscillator (system) to a reservoir consisting of a large number of harmonic oscillators with closely spaced frequencies ω_k and annihilation (and creation) operators b_k (and $b_k^\dagger$) satisfying the bosonic commutation relations $[b_k, b_{k'}^\dagger] = \delta_{kk'}$. The total system is then described by the Hamiltonian

$$H = H_{\mathrm{osc}} + H_{\mathrm{bath}} + H_{\mathrm{int}} \tag{3.40}$$

$$= \hbar\omega a^\dagger a + \sum_k \hbar\omega_k b_k^\dagger b_k + \hbar\sum_k g_k(a^\dagger b_k + a b_k^\dagger) \tag{3.41}$$

The terms in H account for the energy of the system's oscillator, the energy of the reservoir's oscillators and the interaction energy between the system and the reservoir, respectively. Here, a very general type of system-reservoir coupling of the form qq_k is used where q (q_k) is the position of the system's (reservoir's) oscillator(s). This product contains terms like $a^\dagger b_k$, $ab_k^\dagger$, $a^\dagger b_k^\dagger$ and ab_k. If we recall from the previous section the time-dependence of annihilation and creation operators in the Heisenberg picture, we see that the two former terms oscillate at the frequency difference $\omega - \omega_k$ and the latter ones at the sum of frequencies $\omega + \omega_k$. We then apply the often used *rotating-wave approximation* and drop the terms oscillating at the frequency sum. There are two arguments justifying this procedure which is a good approximation in most of the cases. First, the latter two terms are oscillating so fast that on any time scale of interest—typically much larger than $1/\omega_{(k)}$—their average is zero. Second, the products $a^\dagger b_k^\dagger$ and ab_k do not conserve the total energy. The term $a^\dagger b_k^\dagger$ corresponds to the simultaneous creation of one excitation of both interacting oscillators and induces a change in total energy of $\approx 2\hbar\omega$, whereas the term ab_k destroys one excitation of each oscillator, hence the change in total energy of $\approx -2\hbar\omega$. Only the terms $a^\dagger b_k$ and $ab_k^\dagger$ describe energy conserving processes like creation (annihilation) of one quantum of energy of the system's oscillator combined with an annihilation (creation) of one quantum of energy of the corresponding reservoir's oscillator.

Using the Hamiltonian (3.41), the Heisenberg equations of motion for the operators a and b_k are

$$\dot{a} = -i\omega a - i\sum_k g_k b_k \tag{3.42}$$

$$\dot{b}_k = -i\omega_k b_k - i g_k a \tag{3.43}$$

the second of which may be formally integrated to yield

$$b_k(t) = b_k(0)e^{-i\omega_k t} - i g_k \int_0^t dt'\, a(t') e^{-i\omega_k (t-t')} \tag{3.44}$$

Inserting this expression into (3.42), we find

$$\dot{a} = -i\omega a - \sum_k g_k^2 \int_0^t dt'\, a(t') e^{-i\omega_k (t-t')} + f(t) \tag{3.45}$$

$$f(t) = -i\sum_k g_k b_k(0) e^{-i\omega_k t} \tag{3.46}$$

and written in a frame rotating at frequency ω, i.e. $a(t) = \tilde{a}(t)e^{-i\omega t}$ for which $[\tilde{a}, \tilde{a}^\dagger] = \infty$ holds, the equation of motion for the slowly varying operator $\tilde{a}$ reads

$$\dot{\tilde{a}} = -\sum_k g_k^2 \int_0^t dt'\, \tilde{a}(t') e^{-i(\omega_k - \omega)(t-t')} + F(t) \tag{3.47}$$

where $F(t) = f(t)e^{i\omega t}$. Since we are dealing with a quasi-continuum of oscillator modes in the reservoir, we may apply the replacement $\sum_k \to \int D(\omega_k) d\omega_k$ in (3.47) where $D(\omega_k)$ is the density of states. Given that $\tilde{a}$ is a slowly varying operator, we

see that the time integral in (3.47) only contributes if $\omega_k \approx \omega$. Moreover, $g(\omega_k)^2$ and $D(\omega_k)$ do not vary significantly around the characteristic frequency ω, such that we can also replace $g(\omega_k)^2 \to g(\omega)^2$ and $D(\omega_k) \to D(\omega)$. The integration over frequency then yields a $\delta(t-t')$ which makes the time integration trivial. Altogether we find

$$\sum_k g_k^2 \int_0^t dt'\, \tilde{a}(t') e^{-i(\omega_k-\omega)(t-t')} \approx \frac{1}{2}\kappa\tilde{a}(t) \tag{3.48}$$

with a damping coefficient

$$\kappa = 2\pi g(\omega)^2 D(\omega) \tag{3.49}$$

Thus, we now have the Langevin equation

$$\dot{\tilde{a}} = -\frac{1}{2}\kappa\tilde{a} + F(t) \tag{3.50}$$

where $F(t)$ is a noise operator only depending on reservoir variables, as can be seen from (3.46). This equation describes a damped harmonic oscillator subject to fluctuations from the reservoir. It shows that the consequence of the coupling to the environment is that it induces dissipation to the formerly undamped oscillator. Therefore, the system will dissipate its energy into the reservoir, but due to the remaining fluctuations it will on average not completely reach its ground state.

For instance, assume a heat bath in thermal equilibrium at temperature T. That is, all the harmonic oscillators of the reservoir are in a thermal state. Thus, also making use of section 3.1.1, we have to use the following relations for the mode operators of the bath:

$$\langle b_k(0)\rangle = \langle b_k^\dagger(0)\rangle = 0 \tag{3.51}$$

$$\langle b_k(0) b_{k'}^\dagger(0)\rangle = \langle b_{k'}^\dagger(0) b_k(0)\rangle + \delta_{kk'} = (\bar{n}_{T,k}+1)\delta_{kk'} \tag{3.52}$$

$$\langle b_k(0) b_{k'}(0)\rangle = \langle b_k^\dagger(0) b_{k'}^\dagger(0)\rangle = 0 \tag{3.53}$$

where $\bar{n}_{T,k} = [\exp(\hbar\omega_k/k_BT)-1]^{-1}$ is the mean excitation number of the oscillator with resonance frequency ω_k in thermal equilibrium at temperature T. These properties can be used to determine the average and the correlation function of $F(t)$

$$\langle F(t)\rangle = 0 \tag{3.54}$$

$$\langle F(t) F^\dagger(t')\rangle = \kappa\big[\bar{n}_T(\omega)+1\big]\delta(t-t') \tag{3.55}$$

where we used assumptions similar to the ones made in the derivation of (3.48). That is, these particular assumptions lead to a zero-mean Markovian Gaussian white noise. In the limit $T \to 0$, for which $\bar{n}_T(\omega) \to 0$, the noise $F(t)$ is due only to the vacuum fluctuations of the environment's oscillators. For instance, for optical frequencies $\omega \sim 10^{15}\,\mathrm{Hz}$ at room temperature, which implies $\hbar\omega \gg k_BT$, this limit is applicable. That is, the optical electromagnetic field in thermal equilibrium at room temperature exhibits only vacuum fluctuations to a good approximation.

Interestingly, the presence of the noise operator $F(t)$ is necessary to preserve the commutation relation of a (or $\tilde{a}$) at all times. If we had naïvely guessed the equation of motion of the damped harmonic oscillator to be

$$\dot{\tilde{a}} = -\frac{1}{2}\kappa \tag{3.56}$$

which implies the solution

$$\tilde{a}(t) = \tilde{a}(0)e^{-\kappa t/2} \tag{3.57}$$

we would find

$$[\tilde{a}(t), \tilde{a}^\dagger(t)] = e^{-\kappa t} \tag{3.58}$$

which is of course not compatible to quantum mechanics. However, the appearance of the noise term with the appropriate correlation properties keeps the commutator equal to unity at all times. This means that damping is always accompanied by fluctuations, which is a manifestation of the *fluctuation-dissipation theorem* of statistical mechanics.

As we will see below, the quantized electromagnetic field is nothing else than a collection of harmonic oscillators and if one deals with a lossy cavity, i.e. one of the cavity mirrors is not perfect, the associated oscillator is coupled to the electromagnetic modes of the outside world, which play the role of the bosonic environment. Consequently, the corresponding cavity mode will be subject to dissipation and fluctuations which is the reason that Langevin equations of the type as in (3.50) will be central to our analysis.

3.1.3 Pumping of the oscillator

Since the coupling of the oscillator to the environment induces dissipation, one has to feed energy back into the oscillator in order to keep the system "alive". This can formally be achieved by adding a pump term to the total Hamiltonian which has the form

$$H_{\text{pump}} = i\hbar E(e^{-i\omega_0 t}a^\dagger - e^{i\omega_0 t}a) \tag{3.59}$$

where we have E chosen to be real. This corresponds to a classical driving of the oscillator by a force oscillating at ω_0. The pump Hamiltonian is obviously closely related to Glauber's displacement operator given in (3.16) which creates a coherent state from the vacuum – a kind of instantaneous pumping. The consequence is an extra term in the equation of motion of the oscillator

$$\dot{a} = -\left(i\omega + \frac{\kappa}{2}\right)a + Ee^{-i\omega_0 t} + f(t) \tag{3.60}$$

At this point it is convenient to go to a frame rotating at the pump frequency ω_0 in order to remove the time-dependence of the pump term, i.e. $a(t) = \tilde{a}(t)e^{-i\omega_0 t}$, resulting in

$$\dot{\tilde{a}} = -\left(i\Delta + \frac{\kappa}{2}\right)\tilde{a} + E + F(t) \tag{3.61}$$

where we defined the detuning of the pump laser from the cavity resonance frequency, $\Delta = \omega - \omega_0$. This is the general Langevin equation for the annihilation operator of

a damped oscillator driven by a classical force E oscillating at frequency ω_0 and fluctuations $F(t)$. The equation for the creation operator $a^\dagger$ is redundant since it is obtained simply by hermitian conjugation of (3.61). As indicated above, the properties of the fluctuating force $F(t)$ depend on the particular environment the oscillator is coupled to.

3.2 Quantization of the electromagnetic field

As we want to include the quantum nature of the electromagnetic field into our considerations, such as quantum fluctuations, we will in this section give a short review of the quantization of the electromagnetic field within the ring cavity, where we first omit the presence of the movable mirror inside the ring resonator. Thereby we obtain an expression for the electromagnetic field operator which will be used throughout this thesis. The derivations mainly follow the ones made in nearly any textbook on quantum mechanics. Finally, we adapt the field operators to the particular setup under consideration and apply some simplifications.

3.2.1 General quantization

The starting point for the quantization of the electromagnetic field is of course the famous Maxwell equations. In our case, it is sufficient to restrict ourselves to the source-free version (SI units)

$$\nabla \cdot \mathbf{B} = 0 \tag{3.62}$$

$$\nabla \times \mathbf{E} = -\frac{\partial \mathbf{B}}{\partial t} \tag{3.63}$$

$$\nabla \cdot \mathbf{D} = 0 \tag{3.64}$$

$$\nabla \times \mathbf{H} = \frac{\partial \mathbf{D}}{\partial t} \tag{3.65}$$

together with

$$\mathbf{D} = \varepsilon_0 \mathbf{E} \tag{3.66}$$

$$\mathbf{B} = \mu_0 \mathbf{H} \tag{3.67}$$

where ε_0 and μ_0 are the electric permittivity and magnetic permeability of free space which obey $\varepsilon_0 \mu_0 = c^{-2}$. We define the usual vector potential $\mathbf{A}$ and scalar potential ϕ, in terms of which the fields are given by

$$\mathbf{E} = -\nabla\phi - \frac{\partial \mathbf{A}}{\partial t} \tag{3.68}$$

$$\mathbf{B} = \nabla \times \mathbf{A} \tag{3.69}$$

As is known from classical electrodynamics, the potentials $\mathbf{A}$ and ϕ are not uniquely defined, since a *gauge transformation*

$$\mathbf{A}' = \mathbf{A} + \nabla\chi \tag{3.70}$$

$$\phi' = \phi - \frac{\partial \chi}{\partial t} \tag{3.71}$$

with an arbitrary scalar function χ does not change the measurable fields $\mathbf{E}$ and $\mathbf{B}$. Here, we will make use of the gauge most commonly used in quantum optics, the *Coulomb gauge*, given by the choice $\phi = 0$ and $\nabla \cdot \mathbf{A} = 0$. With the particular definitions (3.68) and (3.69), the Maxwell equations (3.62) and (3.63) are automatically satisfied and by applying the Coulomb gauge $\nabla \cdot \mathbf{A} = 0$, eq. (3.64) is also always fulfilled. The remaining Maxwell equation then turns into the standard wave equation for the vector potential

$$\nabla^2 \mathbf{A}(\mathbf{r}, t) = \frac{1}{c^2} \frac{\partial^2 \mathbf{A}(\mathbf{r}, t)}{\partial t^2} \tag{3.72}$$

To solve this differential equation, we perform the standard separation of variables

$$\mathbf{A}(\mathbf{r}, t) = \sum_k \left(\frac{\hbar}{2\omega_k \varepsilon_0} \right)^{\frac{1}{2}} \left[a_k(t) \mathbf{u}_k(\mathbf{r}) + a_k^\dagger(t) \mathbf{u}_k^*(\mathbf{r}) \right] \tag{3.73}$$

and the substitution of this ansatz into (3.72) results in

$$\left(\nabla^2 + \frac{\omega_k^2}{c^2} \right) \mathbf{u}_k(\mathbf{r}) = 0 \tag{3.74}$$

$$\frac{\partial^2 a_k}{\partial t^2} + \omega_k^2 a_k = 0 \tag{3.75}$$

where ω_k^2/c^2 is the separation constant. Eq. (3.74) is known as *Helmholtz equation* and together with the boundary conditions of the quantization volume it defines the *mode functions* $\mathbf{u}_k(\mathbf{r})$. Eq. (3.75) is of course the equation of motion of a harmonic oscillator with solutions

$$a_k(t) = a_k e^{-i\omega_k t} \tag{3.76}$$

$$a_k^\dagger(t) = a_k^\dagger e^{i\omega_k t} \tag{3.77}$$

where the amplitudes a_k and $a_k^\dagger$ are, for the time being, a pair of complex conjugate numbers. When quantizing the system, these amplitudes will be identified as the annihilation and creation operator of the kth mode, respectively.

The particular choice of mode functions depends on the system and its boundary conditions. For example, in case of a linear cavity, it is convenient to choose sinusoidal mode functions. However, we consider a ring cavity, which suggests plane waves with periodic boundary conditions as mode functions. Hence, we set

$$\mathbf{u}_{k,\lambda}(\mathbf{r}) = \sqrt{\frac{1}{V}} \boldsymbol{\epsilon}_\lambda \exp(i\mathbf{k} \cdot \mathbf{r}) \tag{3.78}$$

where $\boldsymbol{\epsilon}_\lambda$ are unit polarization vectors and V is the volume of quantization. We see that $\mathbf{u}_{k,\lambda}$ is indeed a solution of (3.74) and $\mathbf{k}^2 = \omega_k^2/c^2$. The Coulomb gauge $\nabla \cdot \mathbf{A} = 0$ implies

$$\nabla \cdot \mathbf{u}_{k,\lambda} = 0 \tag{3.79}$$

and that leads to the restriction $\mathbf{k} \cdot \boldsymbol{\epsilon}_\lambda = 0$. That is, the polarization vectors are required to be orthogonal to the wave vector $\mathbf{k}$, meaning that the electromagnetic

waves in the Coulomb gauge are *transverse* fields. In three-dimensional space, this leaves only two independent polarization vectors, i.e. $\lambda \in \{1, 2\}$, which we choose to be mutually orthogonal. We thus have the conditions

$$\mathbf{k} \cdot \boldsymbol{\epsilon}_\lambda = 0, \qquad \boldsymbol{\epsilon}_\lambda \cdot \boldsymbol{\epsilon}_{\lambda'} = \delta_{\lambda\lambda'} \tag{3.80}$$

Moreover, the mode functions $\mathbf{u}_{k,\lambda}(\mathbf{r})$ form an orthonormal set, i.e.

$$\int \mathbf{u}^*_{k,\lambda}(\mathbf{r}) \mathbf{u}_{k',\lambda'}(\mathbf{r})\, d^3\mathbf{r} = \delta_{kk'}\delta_{\lambda\lambda'} \tag{3.81}$$

The finite volume of quantization in combination with periodic boundary conditions leads to a discrete set of eigenmodes which is the reason that we assumed discretized wave vectors $\mathbf{k}$ from the beginning (cf. (3.73)). Explicitly, periodic boundary conditions restrict the wave vector in the following form

$$k_i = \frac{2\pi n_i}{L_i}, \qquad n_i \in \mathbb{Z} \tag{3.82}$$

where $i \in \{x, y, z\}$ and L_i is the length of the quantization volume in the i-direction such that $V = L_x L_y L_z$. The corresponding discrete mode spectrum is then given via the dispersion relation $\omega_k^2 = c^2\mathbf{k}^2$.

Using (3.73) for the vector potential, the total energy of the multimode radiation field is

$$\begin{aligned} H &= \frac{1}{2} \int \left(\varepsilon_0 \mathbf{E}^2 + \mu_0^{-1} \mathbf{B}^2\right) d^3\mathbf{r} && (3.83)\\ &= \frac{1}{2} \int \left[\varepsilon_0 \left(\frac{\partial \mathbf{A}}{\partial t}\right)^2 + \mu_0^{-1} \big(\nabla \times \mathbf{A}\big)^2\right] d^3\mathbf{r} && (3.84)\\ &= \frac{1}{2} \sum_{k,\lambda} \hbar\omega_k (a_{k,\lambda} a^\dagger_{k,\lambda} + a^\dagger_{k,\lambda} a_{k,\lambda}) && (3.85)\\ &= \sum_{k,\lambda} H_{k,\lambda} && (3.86) \end{aligned}$$

where we used properties (3.79) and (3.81) to obtain (3.85). As indicated by (3.86), this is equivalent to a set of independent harmonic oscillators, each one associated with one mode k and one polarization λ. Thus, since the $a_{k,\lambda}$ also obey the same differential equation as a harmonic oscillator (cf. (3.75)), the quantization of the radiation field is accomplished by promoting the amplitudes $a_{k,\lambda}$ and $a^\dagger_{k,\lambda}$ to be mutually adjoint operators subjected to the canonical commutation relations

$$[a_{k,\lambda}, a^\dagger_{k',\lambda'}] = \delta_{kk'}\delta_{\lambda\lambda'}, \qquad [a_{k,\lambda}, a_{k',\lambda'}] = [a^\dagger_{k,\lambda}, a^\dagger_{k',\lambda'}] = 0 \tag{3.87}$$

Then, H represents the Hamiltonian of the radiation field, which may of course be recast in the standard form

$$H = \sum_{k,\lambda} \hbar\omega_k \left(a^\dagger_{k,\lambda} a_{k,\lambda} + \frac{1}{2}\right) \tag{3.88}$$

and we see that this is also nothing else than the sum of the number of photons in each mode multiplied by the respective energy of one photon in that mode, including the zero-point energy of each of the oscillators.

Using Heisenberg's equation of motion with the Hamiltonian of (3.88), one can easily check the time evolution of the operators $a_{k,\lambda}$ and $a^\dagger_{k,\lambda}$ to be as shown in (3.76) and (3.77).

Thus, the final form of the vector potential operator is

$$\mathbf{A}(\mathbf{r},t) = \sum_{k,\lambda} \left(\frac{\hbar}{2\omega_k \varepsilon_0 V}\right)^{\frac{1}{2}} \left[\boldsymbol{\epsilon}_\lambda a_{k,\lambda}\, e^{i(\mathbf{k}\cdot\mathbf{r}-\omega_k t)} + \boldsymbol{\epsilon}^*_\lambda a^\dagger_{k,\lambda}\, e^{-i(\mathbf{k}\cdot\mathbf{r}-\omega_k t)}\right] \tag{3.89}$$

and this implies the electric field operator

$$\mathbf{E}(\mathbf{r},t) = -\frac{\partial \mathbf{A}(\mathbf{r},t)}{\partial t} \tag{3.90}$$

$$= i\sum_{k,\lambda} \left(\frac{\hbar\omega_k}{2\varepsilon_0 V}\right)^{\frac{1}{2}} \left[\boldsymbol{\epsilon}_\lambda a_{k,\lambda}\, e^{i(\mathbf{k}\cdot\mathbf{r}-\omega_k t)} - \boldsymbol{\epsilon}^*_\lambda a^\dagger_{k,\lambda}\, e^{-i(\mathbf{k}\cdot\mathbf{r}-\omega_k t)}\right] \tag{3.91}$$

and the magnetic field operator

$$\mathbf{B}(\mathbf{r},t) = \nabla \times \mathbf{A}(\mathbf{r},t) \tag{3.92}$$

$$= i\sum_{k,\lambda} \left(\frac{\hbar}{2\omega_k \varepsilon_0 V}\right)^{\frac{1}{2}} \left[(\mathbf{k}\times\boldsymbol{\epsilon}_\lambda) a_{k,\lambda}\, e^{i(\mathbf{k}\cdot\mathbf{r}-\omega_k t)} - (\mathbf{k}\times\boldsymbol{\epsilon}^*_\lambda) a^\dagger_{k,\lambda}\, e^{-i(\mathbf{k}\cdot\mathbf{r}-\omega_k t)}\right] \tag{3.93}$$

Throughout this thesis we will only work with the electric and magnetic field operators and therefore it is convenient to get rid of the factor i in those expressions. This can simply be done if we define new raising and lowering operators $\tilde{a}_{k,\lambda} := i a_{k,\lambda}$. As this is a simple unitary transformation, it does not affect the commutation relations, hence $[\tilde{a}_{k,\lambda}, \tilde{a}^\dagger_{k',\lambda'}] = [a_{k,\lambda}, a^\dagger_{k',\lambda'}] = \delta_{kk'}\delta_{\lambda\lambda'}$. For the sake of simplicity, we will however drop the tilde for the new operators and we thus will use

$$\mathbf{E}(\mathbf{r},t) = \sum_{k,\lambda} \left(\frac{\hbar\omega_k}{2\varepsilon_0 V}\right)^{\frac{1}{2}} \left[\boldsymbol{\epsilon}_\lambda a_{k,\lambda}\, e^{i(\mathbf{k}\cdot\mathbf{r}-\omega_k t)} + \boldsymbol{\epsilon}^*_\lambda a^\dagger_{k,\lambda}\, e^{-i(\mathbf{k}\cdot\mathbf{r}-\omega_k t)}\right] \tag{3.94}$$

$$\mathbf{B}(\mathbf{r},t) = \sum_{k,\lambda} \left(\frac{\hbar}{2\omega_k \varepsilon_0 V}\right)^{\frac{1}{2}} \left[(\mathbf{k}\times\boldsymbol{\epsilon}_\lambda) a_{k,\lambda}\, e^{i(\mathbf{k}\cdot\mathbf{r}-\omega_k t)} + (\mathbf{k}\times\boldsymbol{\epsilon}^*_\lambda) a^\dagger_{k,\lambda}\, e^{-i(\mathbf{k}\cdot\mathbf{r}-\omega_k t)}\right] \tag{3.95}$$

3.2.2 Application to the current setup

In the previous section we performed the quantization of the electromagnetic field in three-dimensional space and obtained an expression for the vector potential operator from which we were able to derive the electric and magnetic field operator. However, as we want to describe light beams circulating in a ring cavity, it is possible to reduce

the degrees of freedom by defining a ring coordinate, say $0 \leq x \leq L$, where L is the circumference of the ring, along which the light propagates. Thereby, the wave vector for light travelling along this coordinate reduces to $\mathbf{k} = (k, 0, 0)^T$ and we choose the two polarization vectors to be $\boldsymbol{\epsilon}_1 \equiv \boldsymbol{\epsilon}_y = (0, 1, 0)^T$ and $\boldsymbol{\epsilon}_2 \equiv \boldsymbol{\epsilon}_z = (0, 0, 1)^T$ so that the conditions (3.80) hold. The wave number k will then be discretized in the form

$$k_n = \frac{2\pi n}{L}, \qquad n \in \mathbb{Z} \tag{3.96}$$

and the corresponding eigenfrequencies are given by

$$\omega_n = \frac{2\pi c n}{L}, \qquad n \in \mathbb{N}^0 \tag{3.97}$$

which are equidistant mode frequencies separated by the free spectral range (FSR) $\Delta\omega = 2\pi c/L$. For each frequency $\omega_k = c|k|$ there exist two wave numbers of opposite sign, that is, for each frequency ω_k one has a mode travelling in the positive x-direction ($k > 0$, clockwise propagation, index R) and one mode propagating in the negative x-direction ($k < 0$, counterclockwise propagation, index L). In the following, we will only deal with one pair of such degenerate modes. Furthermore, we will focus on isotropic optical elements in the ring cavity, that is, these elements do not couple the two different polarizations and we therefore restrict ourselves, for example, to an electric field which is linearly polarized in the y-direction. The consequence is that $\mathbf{k} \times \boldsymbol{\epsilon}_y = k\boldsymbol{\epsilon}_z = \mathrm{sgn}(k)\,\omega_k \boldsymbol{\epsilon}_z/c$ and the magnetic field is thus linearly polarized in the z-direction, as one would expect. One can also see that the sign of the polarization of the magnetic field depends on the sign of the wave number k, i.e. on the direction of propagation.

Applying all these assumptions, the only non-vanishing terms will be

$$\begin{aligned} E(x,t) \equiv E_y(x,t) = \sqrt{\frac{\hbar\omega_k}{2\varepsilon_0 V}} \Big[& a_R\, e^{i(kx-\omega_k t)} + a_R^\dagger\, e^{-i(kx-\omega_k t)} \\ & + a_L\, e^{-i(kx+\omega_k t)} + a_L^\dagger\, e^{i(kx+\omega_k t)} \Big] \end{aligned} \tag{3.98}$$

$$\begin{aligned} B(x,t) \equiv B_z(x,t) = \frac{1}{c}\sqrt{\frac{\hbar\omega_k}{2\varepsilon_0 V}} \Big[& a_R\, e^{i(kx-\omega_k t)} + a_R^\dagger\, e^{-i(kx-\omega_k t)} \\ & - a_L\, e^{-i(kx+\omega_k t)} - a_L^\dagger\, e^{i(kx+\omega_k t)} \Big] \end{aligned} \tag{3.99}$$

As mentioned above, the minus signs in the expression for the B-field are due to the dependence of the polarization on the sign of k.

Chapter 4

Fields in a ring cavity with a PRM

In order to investigate the optomechanical forces on the partial reflecting mirror (PRM) inside the ring cavity, we first take a look at the electromagnetic fields in the ring resonator and the effect of the presence of the PRM on them. In this chapter we derive the equations of motion of the cavity fields using a transfer matrix description for their propagation along the ring and the scattering by the PRM. We first describe the evolution of the fields in steps of the round trip time $\tau = L/c$ and subsequently find equations of motion for the field operators on larger time scales. We also discuss the eigenfrequencies and eigenmodes of the ring resonator for arbitrary reflectivities of the PRM. At the end of the present chapter, we analyze the steady-state solutions of the fields, the fluctuations around them and their correlations, since the magnitude and the fluctuations of the force acting on the PRM will depend on these.

4.1 Matrix description of field propagation

The starting point of our considerations is the knowledge of the scattering amplitudes of electromagnetic plane waves by a beam splitter or partial reflecting mirror, which are most easily expressed in terms of a scattering matrix containing reflection and transmission coefficients. Therefore, in this section we formulate the propagation of the electromagnetic field inside the ring cavity and the effects of optical elements using a matrix formulation. Each element the light comes across—in the present case these will only be mirrors of certain reflectivity—is represented by a square matrix, and the effect it causes on the field corresponds to the application of this matrix to a vector containing the field amplitudes or operators. One then combines these matrices according to the particular setup under consideration to find an expression for the evolution of the field operators after one round trip. The idea behind this is that during one round trip one scattering process takes place at the mirror, whereby the electromagnetic energy stored in the two resonator modes is redistributed.

As already mentioned in section 3.2.2, we consider two degenerate, counterpropagating electromagnetic plane waves of frequency $\omega = ck$ coupled into the ring cavity of length L—one travelling clockwise (index R) and one travelling counterclockwise

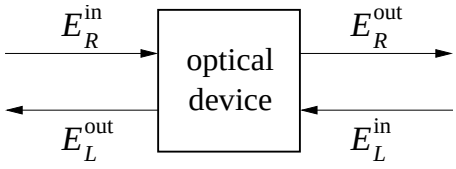

Figure 4.1: Schematic drawing of a four-port device.

(index L). The corresponding electric fields are

$$E_R(x,t) = \sqrt{\frac{\hbar\omega_k}{2\varepsilon_0 V}}\left[a_R\, e^{i(kx-\omega t)} + a_R^\dagger\, e^{-i(kx-\omega t)}\right] \tag{4.1}$$

$$E_L(x,t) = \sqrt{\frac{\hbar\omega_k}{2\varepsilon_0 V}}\left[a_L\, e^{-i(kx+\omega t)} + a_L^\dagger\, e^{i(kx+\omega t)}\right] \tag{4.2}$$

For the time being, the a_i are simply the complex amplitudes of the plane waves which will later be associated with annihilation operators. We need not explicitly distinguish between amplitudes and operators, since we do not have to consider any commutations of the operators throughout this section.

Each optical element as well as the propagation of the light along the x-direction can be viewed as a linear four-port device [29]. As depicted in figure 4.1, the electric fields E_R^{in} and E_L^{in} enter the "instrument", get mixed and, in general, different fields E_R^{out} and E_L^{out} leave it. Depending on the type of the optical device, these four electric fields are related in a certain way. Neglecting any non-linear optical effects, these relations can be expressed in terms of 2×2 matrices connecting two of the four components to the two remaining ones. One now has two different possibilities to formulate the relations between the four ports. Either one uses a scattering matrix formalism, which connects the incoming parts with the outgoing ones

$$\begin{pmatrix} E_R^{\text{out}} \\ E_L^{\text{out}} \end{pmatrix} = \mathbb{S} \begin{pmatrix} E_R^{\text{in}} \\ E_L^{\text{in}} \end{pmatrix} \tag{4.3}$$

and the wave propagation outside the device is well defined. Alternatively, one may employ a transfer matrix formalism[1], which transforms the components on one side of the device into the ones on the other side

$$\begin{pmatrix} E_R^{\text{out}} \\ E_L^{\text{in}} \end{pmatrix} = \mathbb{T} \begin{pmatrix} E_R^{\text{in}} \\ E_L^{\text{out}} \end{pmatrix} \tag{4.4}$$

Here, we choose the direction of transfer to match the positive direction of the space coordinate, i.e. we follow the R-mode. Equation (4.4) is an equivalent formulation, which is simply obtained by rearranging the equations (4.3)[2].

[1] This is of course only possible since we consider a one-dimensional beam line configuration. In general, one cannot use a transfer matrix description for multi-dimensional scattering problems.

[2] Given a scattering matrix $\mathbb{S}$, the corresponding general transfer matrix reads

$$\mathbb{T} = \begin{pmatrix} \mathbb{S}_{11} - \frac{\mathbb{S}_{12}\mathbb{S}_{21}}{\mathbb{S}_{22}} & \frac{\mathbb{S}_{12}}{\mathbb{S}_{22}} \\ -\frac{\mathbb{S}_{21}}{\mathbb{S}_{22}} & \frac{1}{\mathbb{S}_{22}} \end{pmatrix} \tag{4.5}$$

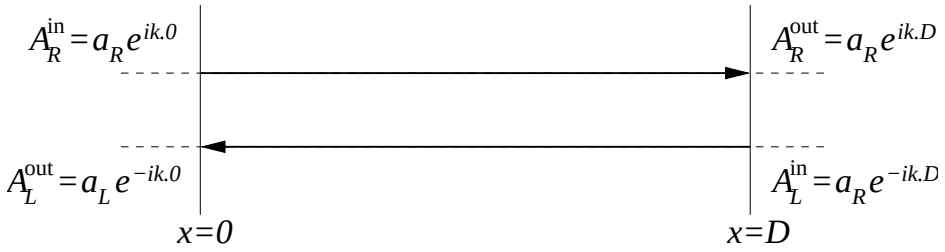

Figure 4.2: Electric fields at two different positions separated by the distance D in order to illustrate the effect of the transfer matrix $\mathbb{T}^L_{\text{prop}}$.

The linear transformations $\mathbb{S}$ and $\mathbb{T}$ also imply that we do not have to use the complete expressions for the electric fields (4.1) and (4.2), but it is sufficient to consider their dimensionless positive frequency part $A_R = a_R e^{ikx}$ and $A_L = a_L e^{-ikx}$, respectively, which we will do from now on.

In the following sections we present the scattering and transfer matrices needed for our calculations.

4.1.1 Matrix representation for basic optical elements

Isotropic propagation

In order to obtain a transfer matrix corresponding to a shift in space along a path length D, one can imagine that this path is also a linear four-port "device", which is entered and left by the components $A^{\text{in}}_{R/L}$ and $A^{\text{out}}_{R/L}$, respectively. This situation is shown in figure 4.2. The application of the transfer matrix $\mathbb{T}^D_{\text{prop}}$ corresponds to a spatial transformation $x \mapsto x + D$, i.e.

$$\begin{pmatrix} A_R(x+D) \\ A_L(x+D) \end{pmatrix} = \mathbb{T}^D_{\text{prop}} \begin{pmatrix} A_R(x) \\ A_L(x) \end{pmatrix} \tag{4.6}$$

where $\mathbb{T}^D_{\text{prop}}$ is determined by the x-dependence of the two plane waves, such that

$$\mathbb{T}^D_{\text{prop}} = \begin{pmatrix} e^{ikD} & 0 \\ 0 & e^{-ikD} \end{pmatrix} \tag{4.7}$$

The minus sign in the exponent of the lower right entry of the transfer matrix reflects the fact that the spatial shift is opposed to the direction of propagation of the L-mode whereas it happens into the same direction as the wave of the R-mode is travelling.

According to (4.5) and the additional comment, the corresponding scattering matrix is

$$\mathbb{S}^D_{\text{prop}} = \begin{pmatrix} e^{ikD} & 0 \\ 0 & e^{ikD} \end{pmatrix} \tag{4.8}$$

If one starts with a transfer matrix $\mathbb{T}$, the corresponding scattering matrix $\mathbb{S}$ is also given by the above equation with $\mathbb{T}$ and $\mathbb{S}$ interchanged.

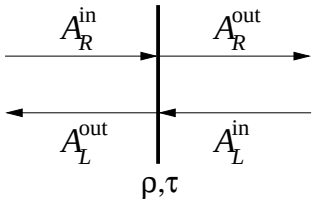

Figure 4.3: Sketch of the PRM including the incoming and outgoing plane waves. ρ and τ are the complex amplitude reflection and transmission coefficients, respectively.

Partially reflecting mirror

The key feature of our experimental setup is the mobile partially reflecting mirror (PRM) inside the ring cavity. Referring to figure 4.3, the scattering matrix for this optical device may be written as

$$\mathbb{S}_{\text{prm}} = \begin{pmatrix} \tau & \rho \\ \rho & \tau \end{pmatrix} \tag{4.9}$$

where $\rho = re^{i\varphi_\rho}$ and $\tau = te^{i\varphi_\tau}$ are the complex reflection and transmission coefficients for the amplitudes, respectively. Moreover, $|\rho| = r = \sqrt{R_{\text{prm}}}$ and $|\tau| = t = \sqrt{T_{\text{prm}}}$, R_{prm} and T_{prm} denoting the intensity reflection and transmission coefficients of the PRM, respectively. Here, we chose the PRM to be symmetric, i.e. invariant under reflection of space at the mirror's position $(x - x_m) \mapsto -(x - x_m)$, which results in the fact that the complex reflection and transmission coefficients for the left and right-hand side are equal. At this point, the phases $\varphi_{\rho/\tau}$ are undetermined.

In order to preserve the commutation relations of the field operators, i.e.

$$[a^{\text{out}}_{R/L}, (a^{\text{out}}_{R/L})^\dagger] \stackrel{!}{=} [a^{\text{in}}_{R/L}, (a^{\text{in}}_{R/L})^\dagger] = 1 \tag{4.10}$$

one requires $\mathbb{S}_{\text{prm}}$ to be unitary. Hence, ρ and τ are subject to the conditions

$$|\rho|^2 + |\tau|^2 = 1 \tag{4.11}$$
$$\rho\tau^* + \rho^*\tau = 0 \tag{4.12}$$

the first of which is a manifestation of energy conservation meaning that unitary beam splitters are conservative. It transforms into

$$r^2 + t^2 = 1 \tag{4.13}$$

if ρ and τ are substituted by their representations in polar coordinates given above. Equation (4.12) implies $\varphi_\rho - \varphi_\tau = \pm\pi/2$ and without loss of generality we pick

$$\varphi_\rho = \varphi_\tau + \pi/2 \tag{4.14}$$

By this choice, we see that

$$\mathbb{S}_{\text{prm}} = e^{i\varphi_\tau} \begin{pmatrix} t & ir \\ ir & t \end{pmatrix} \tag{4.15}$$

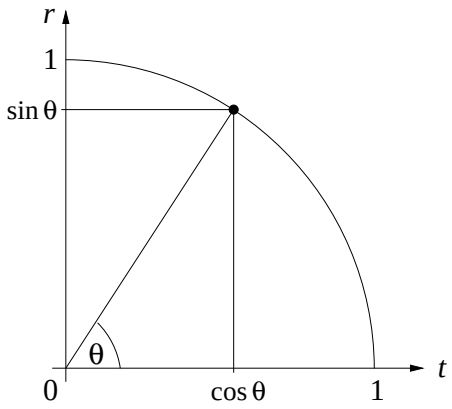

Figure 4.4: Eigenvalue $e^{i\theta}$ of $\mathbb{S}_{\mathrm{prm}}$ in the complex plane.

the eigenvalues of which are easily found to be

$$\lambda_{\pm} = (t \pm ir)e^{i\varphi_\tau} =: e^{i\theta_\pm}e^{i\varphi_\tau} \tag{4.16}$$

Employing relation (4.13), we find $|\lambda_\pm|^2 = 1$ as it should be for a unitary matrix, and one can therefore recast $(t \pm ir)$ as a pure phase factor. Additionally, it holds that

$$\det \mathbb{S} = \lambda_+\lambda_- = e^{2i\varphi_\tau} = e^{i(\theta_+ + \theta_-)}e^{2i\varphi_\tau} \tag{4.17}$$

thus leading to the relation $\theta := \theta_+ = -\theta_-$, as can also be seen from the very definition of $\theta_\pm$ bearing in mind $r, t \in \mathbb{R}$. Figure 4.4 shows the eigenvalue $e^{i\theta}$ in the complex plane and also depicts the properties

$$\cos\theta = t \tag{4.18}$$

$$\sin\theta = r \tag{4.19}$$

$$\tan\theta = \frac{r}{t} \tag{4.20}$$

The introduction of θ thus allows us to describe r and t by a single parameter. We will, however, use both notations interchangeably. Note that one could have also started from the relations (4.18) and (4.19), as suggested by (4.13), which then would have implied the second part of (4.16) automatically.

Using (4.5), the transfer matrix representing the PRM is

$$\mathbb{T}_{\mathrm{prm}} = \frac{1}{t}\begin{pmatrix} e^{i\varphi_\tau} & ir \\ -ir & e^{-i\varphi_\tau} \end{pmatrix} \tag{4.21}$$

As mentioned in section 3.2.2, we consider an isotropic mirror, that is a mirror which does not couple different polarizations of the modes. If $r \neq 0$, it does however couple the R- and L-modes due to the reflections at the PRM. This fact is also reflected in the non-vanishing off-diagonal elements of $\mathbb{S}_{\mathrm{prm}}$ and $\mathbb{T}_{\mathrm{prm}}$.

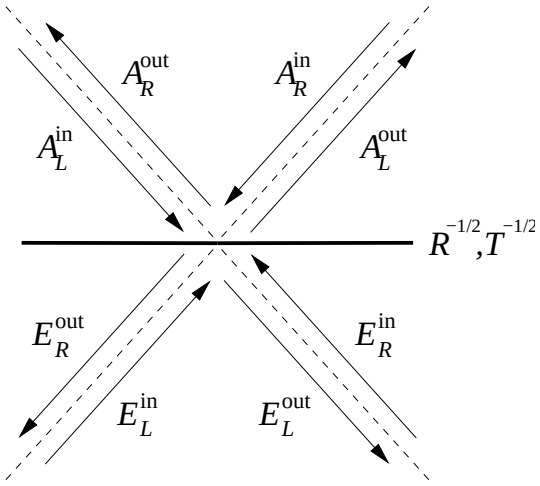

Figure 4.5: Schematic drawing of the incoupling mirror (CM). R and T are the intensity reflection and transmission coefficients, respectively.

Incoupling mirror of the ring cavity

The ring resonator also contains a partial reflecting mirror to couple light into and out of the cavity. This incoupling mirror (CM)[3] is actually an eight-port device, as can be seen in figure 4.5, which obeys the scattering matrix formulation

$$\begin{pmatrix} A_R^{\text{out}} \\ A_L^{\text{out}} \\ \mathcal{E}_R^{\text{out}} \\ \mathcal{E}_L^{\text{out}} \end{pmatrix} = \Sigma_{\text{cm}} \begin{pmatrix} A_R^{\text{in}} \\ A_L^{\text{in}} \\ \mathcal{E}_R^{\text{in}} \\ \mathcal{E}_L^{\text{in}} \end{pmatrix} \tag{4.22}$$

where the 4×4 scattering matrix Σ_{cm} is given by

$$\Sigma_{\text{cm}} = \begin{pmatrix} \sqrt{R} & 0 & -i\sqrt{T} & 0 \\ 0 & \sqrt{R} & 0 & -i\sqrt{T} \\ -i\sqrt{T} & 0 & \sqrt{R} & 0 \\ 0 & -i\sqrt{T} & 0 & \sqrt{R} \end{pmatrix} \tag{4.23}$$

Here, $\mathcal{E}_{R/L}^{\text{in/out}}$ are the field amplitudes pumped into and leaking out of the R- and L-modes, respectively. Moreover, R and T are the intensity reflection and transmission coefficients of the CM. Since the CM is also assumed to be a conservative mirror, the Σ_{cm} is unitary, which leads to the relation $R + T = 1$. As opposed to the scattering matrix for the PRM, we chose a slightly different phase convention for Σ_{cm}. The phase difference between the complex reflection and transmission coefficients for the fields is again $\pi/2$, as in the previous section about the PRM, however, the global phase is chosen such that the reflected parts do not experience a phase shift. As

[3]Usually, such mirrors are called "coupling mirror", as they couple the cavity fields to the fields of the outside world, and the common abbreviation is CM. Throughout this thesis, we will use the term "*in*coupling mirror" to distinguish it from the PRM, which technically is a coupling mirror, too, as it couples the R- and L-modes of the cavity. We will, however, also use the short notation CM, because there is no danger to mix it up with the abbreviation PRM.

we will see below, a non-vanishing reflection (transmission) phase shift at the CM (PRM) would simply induce a global shift of the eigenfrequencies of the cavity, but the physics would not be altered.

Actually, we are looking for a relation between the in and out components of the resonator fields at the CM, which suggests to restrict our focus onto the upper two equations of (4.22), which read

$$\begin{pmatrix} A_R^{\mathrm{out}} \\ A_L^{\mathrm{out}} \end{pmatrix} = \mathbb{S}_{\mathrm{cm}} \begin{pmatrix} A_R^{\mathrm{in}} \\ A_L^{\mathrm{in}} \end{pmatrix} + \mathbb{S}_{\mathrm{in}} \begin{pmatrix} \mathcal{E}_R^{\mathrm{in}} \\ \mathcal{E}_L^{\mathrm{in}} \end{pmatrix} \tag{4.24}$$

with

$$\mathbb{S}_{\mathrm{cm}} = \begin{pmatrix} \sqrt{R} & 0 \\ 0 & \sqrt{R} \end{pmatrix}, \qquad \mathbb{S}_{\mathrm{in}} = \begin{pmatrix} \sqrt{T} & 0 \\ 0 & \sqrt{T} \end{pmatrix} \tag{4.25}$$

where we hid the transmission phase factor in $\mathcal{E}_{R/L}^{\mathrm{in}} \equiv \mathcal{E}_{R/L}$, for the sake of simplicity. Again, it is not a hard task to derive the corresponding transfer matrix relation

$$\begin{pmatrix} A_R^{\mathrm{out}} \\ A_L^{\mathrm{in}} \end{pmatrix} = \mathbb{T}_{\mathrm{cm}} \begin{pmatrix} A_R^{\mathrm{in}} \\ A_L^{\mathrm{out}} \end{pmatrix} + \mathbb{T}_{\mathrm{in}} \begin{pmatrix} \mathcal{E}_R \\ \mathcal{E}_L \end{pmatrix} \tag{4.26}$$

where

$$\mathbb{T}_{\mathrm{cm}} = \begin{pmatrix} \sqrt{R} & 0 \\ 0 & 1/\sqrt{R} \end{pmatrix}, \qquad \mathbb{T}_{\mathrm{in}} = \begin{pmatrix} \sqrt{T} & 0 \\ 0 & -\sqrt{T}/\sqrt{R} \end{pmatrix} \tag{4.27}$$

The lower right entries can also be verified bearing in mind the backward translation of the L-mode within the transfer matrix description. Therefore this mode is "amplified" by the factor $1/\sqrt{R}$ and the input light is subtracted with a suitable prefactor rather than added. The non-existent off-diagonal terms in $\mathbb{S}_{\mathrm{cm}}$ and $\mathbb{T}_{\mathrm{cm}}$ show that the R- and L-modes are not coupled at the incoupling mirror.

4.1.2 One complete round trip and eigenfrequencies

Now we have collected all the tools we need to compute the evolution of the field over a complete round trip. In the following, we will deal with a symmetric geometry, that is the path length from the incoupling mirror to the movable mirror's rest position ($\xi = 0$) is exactly $L/2$. For now, imagine the ring to be bent open to a straight line of coordinate x starting at the point $x = 0$ just at the surface of the incoupling mirror. The power of the transfer matrix description is that one can easily describe the evolution of the light waves along a beam line incorporating different linear optical elements simply by multiplying the transfer matrices in the order the corresponding devices are arranged along the beam line. The reason for that is that the "output" of one transfer matrix is the "input" of the adjacent one. The situation in the present case is sketched in figure 4.6. Moreover, the transfer matrix formulation is more convenient, e.g. for calculating the eigenfrequencies of the closed beam line, especially if one has to consider several optical elements.

The advantage of the scattering matrix description for the present setup is that we treat the R and L-modes symmetrically, which will be more convenient for evaluating the optomechanical force on the PRM, whereas in the transfer matrix picture one mode is followed backwards.

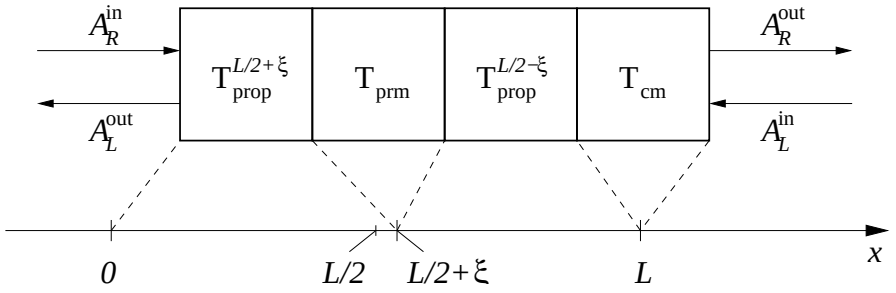

Figure 4.6: Schematic drawing of the beam line including the PRM and the CM. The transfer matrices corresponding to each part of the beam line are also indicated. Here, the PRM position is $L/2 + \xi$ where the value for ξ is exaggerated for the sake of better visibility.

Transfer matrix formalism

Successive application of the transfer matrix relations of chapter 4.1.1 for all optical elements being encountered by the light as it travels around the ring including the transfer matrices for propagation yields

$$\begin{pmatrix} A_R^T \\ A_L^T \end{pmatrix}_L = \mathbb{T}_1 \begin{pmatrix} A_R^T \\ A_L^T \end{pmatrix}_0 + \mathbb{T}_{\text{in}} \begin{pmatrix} \mathcal{E}_R \\ \mathcal{E}_L \end{pmatrix} \tag{4.28}$$

where

$$\mathbb{T}_1 := \mathbb{T}_{\text{cm}} \mathbb{T}_{\text{prop}}^{L/2-\xi} \mathbb{T}_{\text{prm}} \mathbb{T}_{\text{prop}}^{L/2+\xi} = \frac{1}{t} \begin{pmatrix} \sqrt{R}\, e^{i(kL+\varphi_\tau)} & ir\sqrt{R}\, e^{-2ik\xi} \\ -\frac{ir}{\sqrt{R}} e^{2ik\xi} & \frac{1}{\sqrt{R}} e^{-i(kL+\varphi_\tau)} \end{pmatrix} \tag{4.29}$$

and $\mathbb{T}_{\text{in}}$ was defined in (4.27). The superscript T denotes that these are the amplitudes in the transfer matrix picture which differ somewhat from the ones used in the scattering matrix picture, as can be seen in (4.43) and figure 4.7. At this point, the PRM displacement ξ enters the calculation, since the propagation distance between the incoupling mirror and the PRM, $L/2 \pm \xi$, depends on the particular position of the PRM, as is indicated by the upper index of $\mathbb{T}_{\text{prop}}$. Later we will see that one obtains equivalent results if one formally puts the PRM in the middle position $x = L/2$—whereby the formal propagation length from the incoupling mirror to the PRM then also becomes $L/2$—and uses a position dependent phase of the reflection coefficient instead, namely $\rho_R = ire^{2ik\xi}$ and $\rho_L = ire^{-2ik\xi}$. Note that these are already visible in the off-diagonal elements of $\mathbb{T}_1$ in (4.29).

The steady state of the fields is then defined by the requirement

$$\begin{pmatrix} A_R^T \\ A_L^T \end{pmatrix}_L \stackrel{!}{=} \begin{pmatrix} A_R^T \\ A_L^T \end{pmatrix}_0 =: \begin{pmatrix} a_R^T \\ a_L^T \end{pmatrix}_{\text{ss}} \tag{4.30}$$

or in other words, one requires that the field should not have changed after one complete round trip. The solution thereof is given by

$$\begin{pmatrix} a_R^T \\ a_L^T \end{pmatrix}_{\text{ss}} = (\mathbb{1} - \mathbb{T}_1)^{-1} \mathbb{T}_{\text{in}} \begin{pmatrix} \mathcal{E}_R \\ \mathcal{E}_L \end{pmatrix} =: \mathbb{T}_{\text{ss}} \begin{pmatrix} \mathcal{E}_R \\ \mathcal{E}_L \end{pmatrix} \tag{4.31}$$

with

$$\mathbb{T}_{\mathrm{ss}} = \left[2 - \frac{1}{t}\left(\sqrt{R}\, e^{i(kL+\varphi_\tau)} + \frac{1}{\sqrt{R}} e^{-i(kL+\varphi_\tau)}\right)\right]^{-1} \times \begin{pmatrix} \sqrt{T}\left(1 - \frac{1}{t\sqrt{R}} e^{-i(kL+\varphi_\tau)}\right) & \frac{ir\sqrt{T}}{t} e^{-2ik\xi} \\ \frac{ir\sqrt{T}}{t\sqrt{R}} e^{2ik\xi} & -\frac{\sqrt{T}}{\sqrt{R}}\left(1 - \frac{\sqrt{R}}{t} e^{i(kL+\varphi_\tau)}\right) \end{pmatrix} \tag{4.32}$$

and $\mathbb{1}$ is the identity matrix.

The eigenfrequencies $\omega = ck$ of the ring resonator are given by the poles of the prefactor in (4.32) because then the field amplitude inside the cavity will become large. Thus we look for the solutions of

$$2 - \frac{1}{t}\left(\sqrt{R}\, e^{i(kL+\varphi_\tau)} + \frac{1}{\sqrt{R}} e^{-i(kL+\varphi_\tau)}\right) = 0 \tag{4.33}$$

which are

$$k_\pm L + \varphi_\tau = 2\pi n \mp \theta + i \ln\sqrt{R}, \qquad n \in \mathbb{Z} \tag{4.34}$$

$$= k_n^{(0)} L \mp \theta + i \ln\sqrt{R} \tag{4.35}$$

where $k_n^{(0)}$ is the nth eigenfrequency of the ring resonator without the PRM as in (3.96) and θ was defined by $t = \cos\theta$ (also cf. (4.16)). Not surprisingly, the eigenfrequencies are in general complex frequencies and their imaginary part corresponds to dissipation induced by the incoupling mirror ($R < 1$). In case of a perfect "incoupling" mirror, i.e. $R = 1$ ($T = 0$), the imaginary part vanishes and condition (4.34) turns into

$$\cos(kL + \varphi_\tau) = t, \qquad (R = 1) \tag{4.36}$$

That is, a different choice for the phase of the complex transmission coefficient τ simply produces a global shift in the spectrum of eigenfrequencies of the resonator. Later, we will see that this is the only place where the particular choice of φ_τ becomes relevant. For example, it will not affect the expression for the optomechanical force we will use for further calculations, so we will choose $\varphi_\tau = 0$. However, for the sake of consistency, we will keep φ_τ throughout the current section. A more detailed discussion of the mode spectrum will be given in section 4.2 where the peculiar sign convention of (4.34) will also become clear.

Scattering matrix formalism

The situation in the scattering matrix picture is actually quite similar to the one depicted in figure 4.6, of course, using scattering matrices instead of transfer matrices. The major difference, however, is that one cannot simply multiply the matrices to get an expression for one round trip as in the transfer matrix picture. Instead, the equations for each of the sections of the beam line have to be rearranged and combined with each other until one finally arrives at the relation

$$\begin{pmatrix} A_R^S \\ A_L^S \end{pmatrix}_{\pm L} = \sqrt{R}\, \tilde{\mathbb{S}}_1 \begin{pmatrix} A_R^S \\ A_L^S \end{pmatrix}_0 + \sqrt{T} \begin{pmatrix} \mathcal{E}_R \\ \mathcal{E}_L \end{pmatrix} \tag{4.37}$$

where

$$\tilde{\mathbb{S}}_1 := e^{ikL}e^{i\varphi_\tau}\begin{pmatrix} t & ire^{-2ik\xi} \\ ire^{2ik\xi} & t \end{pmatrix} \tag{4.38}$$

Here, $\tilde{\mathbb{S}}_1$ represents the scattering matrix of one round trip including the reflection at the PRM. It does however not include the action of the incoupling mirror as this simply produces the factor $\sqrt{R}$ and the additional term on the right-hand side of (4.37). Again, equation (4.38) exhibits the equivalence to the use of position-dependent reflection coefficients $\rho_{R/L}$ mentioned above. The propagation along the ring adds up to a global phase factor $\exp(ikL)$, irrespective of using the actual distances $L/2 \pm \xi$ or the formal ones $L/2$, and the off-diagonal elements contain $\rho_{R/L}$, anyway. Similar to the previous section, the superscript S indicates that we are dealing with the field amplitudes in the scattering matrix picture. The conceptual difference to the transfer matrix formulation, which was already explained in the beginning of section 4.1.1, is reflected in the index $\pm L$.

Again, the steady state of the fields can be found by requiring

$$\begin{pmatrix} A_R^S \\ A_L^S \end{pmatrix}_{\pm L} \stackrel{!}{=} \begin{pmatrix} A_R^S \\ A_L^S \end{pmatrix}_0 =: \begin{pmatrix} a_R^S \\ a_L^S \end{pmatrix}_{\mathrm{ss}} \tag{4.39}$$

which yields

$$\begin{pmatrix} a_R^S \\ a_L^S \end{pmatrix}_{\mathrm{ss}} = \sqrt{T}\left(\mathbb{1} - \sqrt{R}\tilde{\mathbb{S}}_1\right)^{-1}\begin{pmatrix} \mathcal{E}_R \\ \mathcal{E}_L \end{pmatrix} =: \tilde{\mathbb{S}}_{\mathrm{ss}}\begin{pmatrix} \mathcal{E}_R \\ \mathcal{E}_L \end{pmatrix} \tag{4.40}$$

where

$$\tilde{\mathbb{S}}_{\mathrm{ss}} = \frac{\sqrt{T}}{1 - 2t\sqrt{R}e^{i(kL+\varphi_\tau)} + Re^{2i(kL+\varphi_\tau)}} \tag{4.41}$$

$$\times \begin{pmatrix} 1 - t\sqrt{R}e^{i(kL+\varphi_\tau)} & ir\sqrt{R}e^{i(kL+\varphi_\tau)}e^{-2ik\xi} \\ ir\sqrt{R}e^{i(kL+\varphi_\tau)}e^{2ik\xi} & 1 - t\sqrt{R}e^{i(kL+\varphi_\tau)} \end{pmatrix} \tag{4.42}$$

The eigenfrequencies are also given by the poles of the prefactor in (4.42) which are the same as in (4.34). Thus, all the properties concerning the mode spectrum that have been mentioned above can also be derived from the scattering matrix formulation.

As an additional note, the steady states of the two different matrix descriptions are connected by the relations

$$a_L^T = \frac{1}{\sqrt{R}}(a_L^S - \sqrt{T}\mathcal{E}_L), \qquad a_R^T = a_R^S \tag{4.43}$$

which are visualized in figure 4.7.

4.2 Eigenmodes of ring cavity and mode spectrum

In the following, we look for the eigenmodes of the ring cavity including the PRM which are related to the eigenvectors of the scattering matrix $\tilde{\mathbb{S}}_1$. We already took

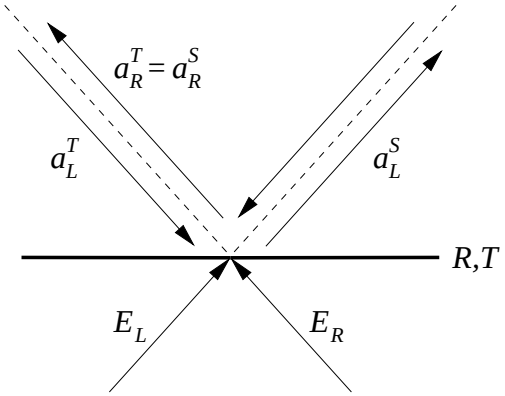

Figure 4.7: Relation of steady-state amplitudes of the transfer and scattering matrix description at the surface of the CM as given in eq. (4.43)

a short look at the eigenvalues of almost the same matrix in section 4.1.1. Here, we will go a little more into detail by deriving the annihilation operators of the cavity eigenmodes and discussing their frequency spectrum.

Eigenmodes of the cavity Similar to the considerations made in section 4.1.1, the eigenvalues of $\tilde{\mathbb{S}}_1$ as given in (4.38) are

$$\lambda_\pm = (t \pm ir)e^{ikL} = e^{\pm i\theta}e^{ikL}, \qquad \theta \in [0, \pi/2] \tag{4.44}$$

and the corresponding normalized eigenvectors are

$$\mathbf{v}_\pm = \frac{1}{\sqrt{2}} \begin{pmatrix} e^{-ik\xi} \\ \pm e^{ik\xi} \end{pmatrix} \tag{4.45}$$

Note that we have set $\varphi_\tau = 0$, which we will retain from now on. We observe that the eigenvectors are orthogonal with respect to the usual complex scalar product, i.e. $\mathbf{v}_\pm^* \cdot \mathbf{v}_\mp = 0$. The transition from the R/L basis to the $\pm$ basis is described by the unitary transformation matrices

$$\mathcal{V} = \frac{1}{\sqrt{2}} \begin{pmatrix} e^{ik\xi} & e^{-ik\xi} \\ e^{ik\xi} & -e^{-ik\xi} \end{pmatrix} \qquad \mathcal{V}^{-1} = \mathcal{V}^\dagger = \frac{1}{\sqrt{2}} \begin{pmatrix} e^{-ik\xi} & e^{-ik\xi} \\ e^{ik\xi} & -e^{ik\xi} \end{pmatrix} \tag{4.46}$$

such that

$$\tilde{\mathbb{S}}_1^{(\pm)} = \mathcal{V}\tilde{\mathbb{S}}_1\mathcal{V}^{-1} = e^{ikL} \begin{pmatrix} e^{i\theta} & 0 \\ 0 & e^{-i\theta} \end{pmatrix} \tag{4.47}$$

The field operators of the eigenmodes of the cavity are then simply the expansion coefficients in the eigenbasis, i.e.

$$\begin{pmatrix} a_R \\ a_L \end{pmatrix} = \sum_{j=\pm} a_j \mathbf{v}_j \tag{4.48}$$

We can solve (4.48) for $a_\pm$ by applying $\mathcal{V}$ to (4.48), which yields

$$\begin{pmatrix} a_+ \\ a_- \end{pmatrix} = \mathcal{V} \begin{pmatrix} a_R \\ a_L \end{pmatrix} = \frac{1}{\sqrt{2}} \begin{pmatrix} a_R e^{ik\xi} + a_L e^{-ik\xi} \\ a_R e^{ik\xi} - a_L e^{-ik\xi} \end{pmatrix} \tag{4.49}$$

where we exploited $\mathcal{V}\mathbf{v}_+ = (1,0)^T$ and $\mathcal{V}\mathbf{v}_- = (0,1)^T$. If one now replaces $a_{R/L}$ in the expression for electric field given by (4.1) and (4.2), the mode functions $u_\pm(x)$ corresponding to the $\pm$ modes become visible

$$a_R e^{ikx} + a_L e^{-ikx} = a_+ u_+(x) + a_- u_-(x) \tag{4.50}$$

where

$$u_+(x) = \sqrt{2}\,\cos[k(x-\xi)], \qquad u_-(x) = i\sqrt{2}\,\sin[k(x-\xi)] \tag{4.51}$$

Obviously, the $+$ $(-)$ mode function is an even (odd) function with respect to the mirror position and has an antinode (node) at the mirror.

Eigenfrequencies of the cavity In section 4.1.2 we already derived the cavity eigenfrequencies using both the scattering and the transfer matrix formalism. In the following, we recover them by another argument and discuss their dependence on the PRM's reflectivity.

We first consider a lossless cavity, i.e. $R = 1$. According to (4.37) the amplitudes after one spatial round trip are given by

$$\begin{pmatrix} a_R \\ a_L \end{pmatrix}_{\mathrm{1RT}} = \tilde{\mathbb{S}}_1 \begin{pmatrix} a_R \\ a_L \end{pmatrix} \tag{4.52}$$

and written in the $\pm$ basis this becomes

$$\begin{pmatrix} a_+ \\ a_- \end{pmatrix}_{\mathrm{1RT}} = \tilde{\mathbb{S}}_1^{(\pm)} \begin{pmatrix} a_+ \\ a_- \end{pmatrix} = e^{ikL} \begin{pmatrix} e^{i\theta} & 0 \\ 0 & e^{-i\theta} \end{pmatrix} \begin{pmatrix} a_+ \\ a_- \end{pmatrix} \tag{4.53}$$

Observe that the $+$ mode remains unchanged after one round trip if $e^{ikL}e^{i\theta} = 1$, whereas the $-$ mode stays unaffected if $e^{ikL}e^{-i\theta} = 1$. This gives rise to the eigenfrequency condition

$$k_\pm L = \omega_\pm \tau = 2\pi n \mp \theta = k_n^{(0)} L \mp \theta \tag{4.54}$$

which may also be formulated as

$$\cos(kL) = t, \qquad (R = 1) \tag{4.55}$$

The eigenfrequencies are just the same as found in section 4.1.2. The mode spectrum (4.55) with its dependence on the magnitude of the PRM's amplitude transmittivity t is shown in figure 4.8. From (4.54), we see that in case of the completely transparent "mirror", i.e. $\cos\theta = t = 1$, one recovers the eigenfrequencies of an empty ring resonator of length L, $\omega_n^{(0)} = ck_n^{(0)}$, being separated by $2\pi c/L$ in frequency. In that case, the two eigenmodes are degenerate, as we assumed initially. If one now allows for $t \neq 1$ $(\theta \neq 0)$, the two eigenmodes get coupled via the PRM which lifts the degeneracy and splits ω_+ and ω_- apart. Here, the low-frequency mode is the $+$ mode which has an antinode at the mirror, whereas the high-frequent $-$ mode shows a node at the mirror. This suggests an interpretation of the frequency difference as a difference in dielectric polarization energy [30], which is also the case in photonic crystals. These exhibit a band structure of the electromagnetic field basically consisting of a "dielectric band" and an "air band". The mode function—and thereby also the

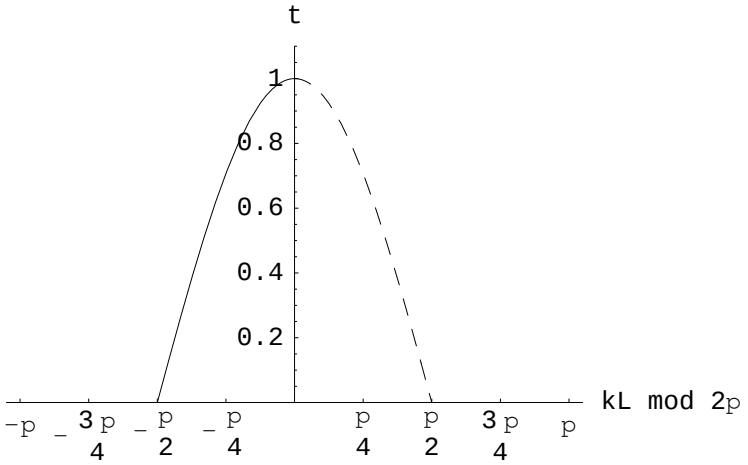

Figure 4.8: Plot of the cavity eigenfrequencies to show their dependence on PRM transmittivity t. The left/dashed (right/solid) branch corresponds to an eigenfrequency of the + (−) mode. The mode spectrum is only shown in the interval $[-\pi, \pi]$, since it is 2π-periodic.

electric field—of the latter is mainly localized in vacuum ($\varepsilon = \varepsilon_0$), whereas the mode function for fields in the dielectric band is mainly localized in the dielectric material the photonic crystal is made of ($\varepsilon > \varepsilon_0$). Thus, the average polarization energy

$$\bar{E}_{\text{pol}} = \int dx\, \varepsilon(x) E^2(x) \tag{4.56}$$

is smaller for air band modes, which results in a larger eigenfrequency. In case of the ring cavity with a PRM, the mode having a high electric field inside the dielectric, i.e. the PRM, is also the low-frequency mode.

For perfect reflectivity, i.e. $\cos\theta = t = 0$, one finds the frequency spectrum of standing waves where two adjacent modes are separated by $\pi c/L$ in frequency. This is not surprising, since if the PRM is a perfect mirror, the light is always reflected back and forth and the cavity then is identical to a linear cavity of length L.

Hamiltonian for the fields As the basis transformation $\mathcal{V}$ is unitary, the Hamiltonian governing the time evolution of the eigenmodes in the $\pm$ basis is simply given by $H^{\pm}_{\text{light}} = \hbar\omega_+ a_+^\dagger a_+ + \hbar\omega_- a_-^\dagger a_-$, which is of course diagonal in that basis. Substituting $a_\pm$ by $a_{R/L}$ according to (4.49) and inserting (4.54) for the eigenfrequencies then gives

$$H_{\text{light}} = \hbar\omega_n^{(0)} \left(a_R^\dagger a_R + a_L^\dagger a_L \right) - \hbar\frac{\theta}{\tau} \left(a_R^\dagger a_L e^{-2ik\xi} + a_L^\dagger a_R e^{2ik\xi} \right) \tag{4.57}$$

The coupling terms are proportional to the reflection parameter θ, that is, for zero reflection ($\theta = 0$) the mode coupling vanishes, whereas it is maximal for a perfect reflecting mirror ($\theta = \pi/2$), just as it should be.

We only want to mention the field Hamiltonian here, but later we will see that it is indeed responsible for the time evolution of the fields. Interestingly, this Hamiltonian does not generate the correct dynamics of the position and momentum operator of the PRM, as we will see below.

4.3 Time evolution of the cavity fields

4.3.1 Discrete time evolution of field amplitudes

So far, we have only dealt with stationary scattering states and derived formulae which relate the field amplitudes before and after a complete spatial round trip. We will now give some arguments that allow us to translate the spatial transformation in the scattering matrix picture into a temporal one. This equation then describes how the field amplitudes have changed after the time $\tau = L/c$ the light needs to circulate the ring once.

Consider the positive frequency part of the electric fields

$$E_R(x,t) \propto e^{i(kx-\omega t)} \tag{4.58}$$

$$E_L(x,t) \propto e^{-i(kx+\omega t)} \tag{4.59}$$

If we now introduce the spatial shifts of one round trip in the scattering matrix description, i.e. $x \mapsto x+L$ for the R-mode and $x \mapsto x-L$ for the L-mode, we see that both expressions gain a phase factor $\exp(ikL)$

$$E_R(x+L,t) \propto e^{ikL}e^{i(kx-\omega t)} = e^{i[kx-\omega(t-\tau)]} \propto E_R(x,t-\tau) \tag{4.60}$$

$$E_L(x-L,t) \propto e^{ikL}e^{-i(kx+\omega t)} = e^{-i[kx+\omega(t-\tau)]} \propto E_L(x,t-\tau) \tag{4.61}$$

and, moreover, that this is equivalent to a temporal shift of τ into the past. On the other hand, if one waits for the time τ to pass, one finds that a phase factor $\exp(-i\omega\tau)$ appears in both cases

$$E_R(x,t+\tau) \propto e^{-i\omega\tau}e^{i(kx-\omega t)} = e^{i[k(x-L)-\omega t]} \propto E_R(x-L,t) \tag{4.62}$$

$$E_L(x,t+\tau) \propto e^{-i\omega\tau}e^{-i(kx+\omega t)} = e^{-i[k(x+L)-\omega t]} \propto E_R(x+L,t) \tag{4.63}$$

This illustrates that in case of plane waves the transition from the spatial description (4.37) to a temporal formulation is formally done by replacement $\exp(ikL) \mapsto \exp(-i\omega\tau)$. We thereby obtain the discrete time evolution of the field amplitudes in steps of the round trip time τ.

$$\begin{pmatrix} a_R \\ a_L \end{pmatrix}_{t_0+\tau} = \sqrt{R}\mathbb{S}_1 \begin{pmatrix} a_R \\ a_L \end{pmatrix}_{t_0} + \sqrt{T} \begin{pmatrix} \mathcal{E}_R \\ \mathcal{E}_L \end{pmatrix} \tag{4.64}$$

where $\mathbb{S}_1$ has the form

$$\mathbb{S}_1 = e^{-i\omega\tau} \begin{pmatrix} t & ire^{-2ik\xi} \\ ire^{2ik\xi} & t \end{pmatrix} \tag{4.65}$$

Now, the phase factor in (4.65) is what one would actually expect from a time evolution because the annihilation operator for a harmonic oscillator evolves in time as $a(t) = a\exp(-i\omega t)$.

The results above are valid only under the assumption that the mirror position ξ does not change significantly during one round trip of the light, that is $\Omega_m\tau \ll 1$, where Ω_m is the oscillation frequency of the PRM. As explained in section 2, this

assumption implies that one has to minimize the length of the ring resonator L as far as possible and that Ω_m must not be too large. Considering our reference values, this assumption is applicable to the present setup and we can thus treat ξ as being constant over one round trip time τ.

4.3.2 Transition to Langevin equations

In section 3.1.3, we derived the equation of motion for the annihilation operator of a damped harmonic oscillator subject to an oscillating, classical driving force. As each of the resonator modes is represented by such a harmonic oscillator, we expect the free time evolution of each of the corresponding annihilators to obey a Langevin equation as in (3.60). Additionally, the two modes under consideration are coupled by the PRM inside the ring cavity. We therefore expect the following type of Langevin equation for the field operators of the R- and L-mode

$$\dot{\mathbf{a}} = M\mathbf{a} - \frac{\kappa}{2}\mathbf{a} + \mathbf{E} + \sqrt{\kappa}\,\mathbf{a}^{\text{in}} =: \tilde{M}\mathbf{a} + \mathbf{E} + \sqrt{\kappa}\,\mathbf{a}^{\text{in}} \tag{4.66}$$

where we defined the column vector notation $\mathbf{a} := (a_R, a_L)^T$. Furthermore, $\mathbf{a}^{\text{in}} := (a_R^{\text{in}}, a_L^{\text{in}})^T$ contains the input noise operators, $\mathbf{E} := (E_R, E_L)^T$ represents the driving due to external laser fields, $\tilde{M} := M - \kappa/2$ is a 2×2 matrix and κ is the intensity damping rate of the modes. Note, that all the vectors $\mathbf{a}$, $\mathbf{E}$ and $\mathbf{a}^{\text{in}}$ are time-dependent in this picture. The diagonal elements of $\tilde{M}$ contain the oscillation and damping terms for the R- and L-mode, respectively, and the off-diagonal elements account for the coupling due to the PRM. As the PRM position ξ is in general time-dependent, we expect the coupling to vary on the time scale Ω_m^{-1}, which means that also $\tilde{M}$ is a function of time. Therefore, the formal solution of (4.66) is given by

$$\mathbf{a}(t) = e^{I(t)}\mathbf{a}(0) + e^{I(t)} \int_0^t dt'\, e^{-I(t')} \left[\mathbf{E}(t') + \sqrt{\kappa}\,\mathbf{a}^{\text{in}}(t')\right] \tag{4.67}$$

where

$$I(t) = \int_0^t dt'\, \tilde{M}(t') \tag{4.68}$$

Due to the fact that $\Omega_m \tau \ll 1$, i.e. the PRM position roughly does not change over one round trip time τ, we can apply the approximation $I(\tau) \approx \tilde{M}\tau$. Adopting our result for the evolution of the cavity fields after one round trip time τ given by (4.64), we then require

$$\mathbf{a}(\tau) = e^{\tilde{M}\tau}\mathbf{a}(0) + e^{\tilde{M}\tau} \int_0^\tau dt'\, e^{-\tilde{M}t'} \left[\mathbf{E}(t') + \sqrt{\kappa}\,\mathbf{a}^{\text{in}}(t')\right] \tag{4.69}$$

$$\stackrel{!}{=} \sqrt{R}\mathbb{S}_1\mathbf{a}(0) + \sqrt{T}\mathcal{E} \tag{4.70}$$

where $\mathcal{E} := (\mathcal{E}_R, \mathcal{E}_L)^T$. Thus, we identify $\mathbb{S}_1 = e^{M\tau}$ and $\sqrt{R} = e^{-\kappa\tau/2}$, the latter relation leading to

$$\kappa = -\frac{c \ln R}{L} \stackrel{R \ll 1}{\approx} \frac{T}{\tau} \tag{4.71}$$

which is exactly the damping rate one would expect for one reflection at a mirror of intensity reflectivity R during one round trip. The other equation implies $M = \ln \mathbb{S}_1/\tau$, but what is the logarithm of $\mathbb{S}_1$?
The answer to this question is actually not that difficult using our knowledge of the eigenbasis of $\mathbb{S}_1$ gained in section 4.2. Written in its eigenbasis, $\mathbb{S}_1^{(\pm)} = \mathcal{V}\mathbb{S}_1\mathcal{V}^{-1} = \mathrm{diag}(\lambda_+, \lambda_-)$ is diagonal and therefore the logarithm thereof is simply given by

$$\ln \mathbb{S}_1^{(\pm)} = \begin{pmatrix} \ln \lambda_+ & 0 \\ 0 & \ln \lambda_- \end{pmatrix} = \begin{pmatrix} -i\omega\tau + i\theta & 0 \\ 0 & -i\omega\tau - i\theta \end{pmatrix} \tag{4.72}$$

where we neglected the fact that the logarithm is actually only determined up to a factor $2\pi i n$, which again corresponds to the free spectral range of the eigenmodes of the empty ring cavity. The logarithm of $\mathbb{S}_1$ can now be found by transforming (4.72) back into the R/L basis. Altogether, one finds

$$M = \frac{1}{\tau}(\mathcal{V}^{-1} \ln \mathbb{S}_1^{(\pm)} \mathcal{V}) = \begin{pmatrix} -i\omega & \frac{i\theta}{\tau} e^{-2ik\xi} \\ \frac{i\theta}{\tau} e^{2ik\xi} & -i\omega \end{pmatrix} \tag{4.73}$$

Alternatively, we observe that $\mathbb{S}_1$ can be rewritten in the following way

$$e^{i\omega\tau}\mathbb{S}_1 = \begin{pmatrix} t & ire^{-2ik\xi} \\ ire^{2ik\xi} & t \end{pmatrix} \tag{4.74}$$

$$= \mathbb{1}\cos\theta + i\sigma_\xi \sin\theta \tag{4.75}$$

$$= \exp(i\theta\sigma_\xi) \tag{4.76}$$

where

$$\sigma_\xi = \begin{pmatrix} 0 & e^{-2ik\xi} \\ e^{2ik\xi} & 0 \end{pmatrix} \tag{4.77}$$

having a property similar to the Pauli matrices, namely $\sigma_\xi^2 = 1$, which was used to obtain (4.76). Thus, we find

$$\mathbb{S}_1 = \exp\big(-i\omega\tau\mathbb{1} + i\theta\sigma_\xi\big) = \exp\left[\begin{pmatrix} -i\omega\tau & i\theta e^{-2ik\xi} \\ i\theta e^{2ik\xi} & -i\omega\tau \end{pmatrix}\right] \tag{4.78}$$

whose logarithm is obvious and leads to the same M as found above. These considerations are closely related to the fact that $e^{i\omega\tau}\mathbb{S}_1 \in SU(2)$.

As expected, the diagonal elements of M produce the oscillation of the field operators at frequency ω while the off-diagonal elements of M describe the coupling of the two modes. The latter are proportional to θ, that is the coupling is maximal for a perfect mirror ($\theta = \pi/2$) and vanishes for zero reflectivity ($\theta = 0$), as required. Moreover, the PRM position ξ enters through the position-dependent phase factor for the reflection at the PRM. Therefore, $\tilde{M}$ is time-dependent on a time scale of the PRM motion. In the following, we restrict ourselves to cases where $\Omega_m \ll \kappa$, that is the PRM motion is also slow on the time scale of the field dynamics, which may also be considered as a "bad cavity limit". Hence, for times not too long compared to κ^{-1}, one can view ξ to be effectively constant which renders $\tilde{M}$ time-independent on the time scale of the field dynamics.

In case of a lossless cavity without pumping, i.e. $\kappa = 0$ and $\mathbf{E} = 0$, one has the equations of motion

$$\begin{pmatrix} \dot{a}_R \\ \dot{a}_L \end{pmatrix} = \begin{pmatrix} -i\omega & \frac{i\theta}{\tau} e^{-2ik\xi} \\ \frac{i\theta}{\tau} e^{2ik\xi} & -i\omega \end{pmatrix} \begin{pmatrix} a_R \\ a_L \end{pmatrix} \equiv \frac{i}{\hbar} \left[H_{\text{light}}, \begin{pmatrix} a_R \\ a_L \end{pmatrix} \right] \tag{4.79}$$

where

$$H_{\text{light}} = \hbar\omega \left(a_R^\dagger a_R + a_L^\dagger a_L \right) - \hbar \frac{\theta}{\tau} \left(a_R^\dagger a_L e^{-2ikx_m} + a_L^\dagger a_R e^{2ikx_m} \right) \tag{4.80}$$

That is, the Hamiltonian found at the end of section 4.2 indeed generates the equations of motion of the field operators derived above via Heisenberg's general equation of motion.

Finally, we look for the equations of motion for $a_\pm$ which are easily obtained by transforming (4.66) into the $\pm$ basis using $\mathcal{V}$ and $\mathcal{V}^{-1}$. Of course, $\tilde{M}$ is also diagonal in this basis and it reveals the eigenvalues

$$\tilde{\lambda}_\pm = -i \left(\omega \mp \frac{\theta}{\tau} \right) - \frac{\kappa}{2} = -i\omega_\pm - \frac{\kappa}{2} \tag{4.81}$$

and one thus gets

$$\dot{a}_+ = \left(-i\omega_+ - \frac{\kappa}{2} \right) a_+ + E_+ + \sqrt{\kappa}\, a_+^{\text{in}} \tag{4.82}$$

$$\dot{a}_- = \left(-i\omega_- - \frac{\kappa}{2} \right) a_- + E_- + \sqrt{\kappa}\, a_-^{\text{in}} \tag{4.83}$$

where $(E_+, E_-)^T = \mathcal{V}(E_R, E_L)^T$ and $(a_+^{\text{in}}, a_-^{\text{in}})^T = \mathcal{V}(a_R^{\text{in}}, a_L^{\text{in}})^T$. Not surprisingly, in this new basis the equations of motion are uncoupled. As the basis transformation matrices $\mathcal{V}$ and $\mathcal{V}^{-1}$ also depend on ξ which was supposed to be only slowly varying with time, the equations of motion in the $\pm$ basis actually contain a PRM velocity-dependent term which stems from the time derivative of the phase factors $\exp(\pm ik\xi)$. However, the mirror velocity $\dot{\xi}$ is so small – more precisely $k\dot{\xi} \ll \kappa$ – that we neglect those terms for the time being. In chapter 5, we will come back to the effect of the PRM velocity on the cavity variables in order to investigate the velocity-dependence of the optomechanical force, which leads to a friction force.

4.4 Scattered mode functions

Until now, we used the mode functions suggested by the empty ring cavity, namely, circulating plane waves $u_{R/L}(x) \propto e^{\pm ikx}$. One might now raise the objection that the plane wave mode functions are only suitable for the empty ring cavity and for small couplings, that is for small PRM reflectivities $r \ll 1$ ($\theta \ll 1$). To counter this objection, we introduce another set of mode functions—the scattered modes—and compare the results to the ones gained above.

If an electromagnetic plane wave impinges upon the PRM it is divided into a transmitted and reflected part. As an alternative choice, we now consider a "composite mode function" mad from the incoming part and the corresponding scattered

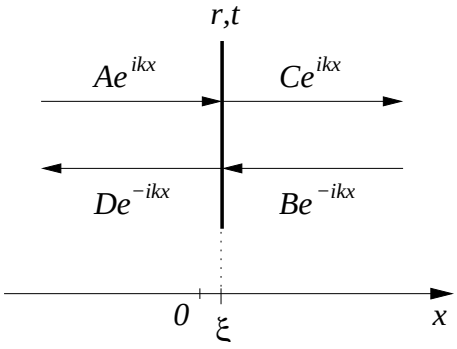

Figure 4.9: General solution of the Helmholtz eq. (3.74) using plane waves. The PRM is sited at position ξ. On either side of the PRM, there exist plane waves travelling to the left and right, respectively, with arbitrary amplitudes A, B, C and D.

parts. One of the two mode functions then corresponds to a plane wave coming from the left and being scattered at the PRM, $u_r(x)$, and the second one describes a plane wave impinging from the right and the scattered parts thereof, $u_l(x)$.

The general solution of the Helmholtz equation (3.74) in terms of plane waves is depicted in figure 4.9. It consists of simple plane waves on either side of the PRM, each of which has components travelling in the positive and negative x-direction with arbitrary amplitudes, respectively. Hence,

$$u_{\text{gen}}(x) = \begin{cases} Ae^{ikx} + De^{-ikx} & x < \xi \\ Ce^{ikx} + Be^{-ikx} & x > \xi \end{cases} \tag{4.84}$$

What is known additionally, is the relation of incoming and outgoing parts at the mirror position via a scattering matrix ($\varphi_\tau = 0$)

$$\begin{pmatrix} Ce^{ik\xi} \\ De^{-ik\xi} \end{pmatrix} = \begin{pmatrix} t & ir \\ ir & t \end{pmatrix} \begin{pmatrix} Ae^{ik\xi} \\ Be^{-ik\xi} \end{pmatrix} \tag{4.85}$$

which is easily seen to be equivalent to

$$\begin{pmatrix} C \\ D \end{pmatrix} = \begin{pmatrix} t & ire^{-2ik\xi} \\ ire^{2ik\xi} & t \end{pmatrix} \begin{pmatrix} A \\ B \end{pmatrix} \tag{4.86}$$

Note that this is equivalent to (4.38), which we obtained from the matrix description of the field propagation. The mode function describing light of unit amplitude coming from the left is then selected by the amplitude vector $(A, B)^T = (1, 0)^T$ and is therefore given by

$$u_r(x) = \begin{cases} e^{ikx} + ir_\xi e^{-ikx} & x < \xi \\ te^{ikx} & x > \xi \end{cases} \tag{4.87}$$

and the one representing the similar case with light approaching from the right, i.e. $(A, B)^T = (0, 1)^T$, reads

$$u_l(x) = \begin{cases} te^{-ikx} & x < \xi \\ e^{-ikx} + ir_\xi^* e^{ikx} & x > \xi \end{cases} \tag{4.88}$$

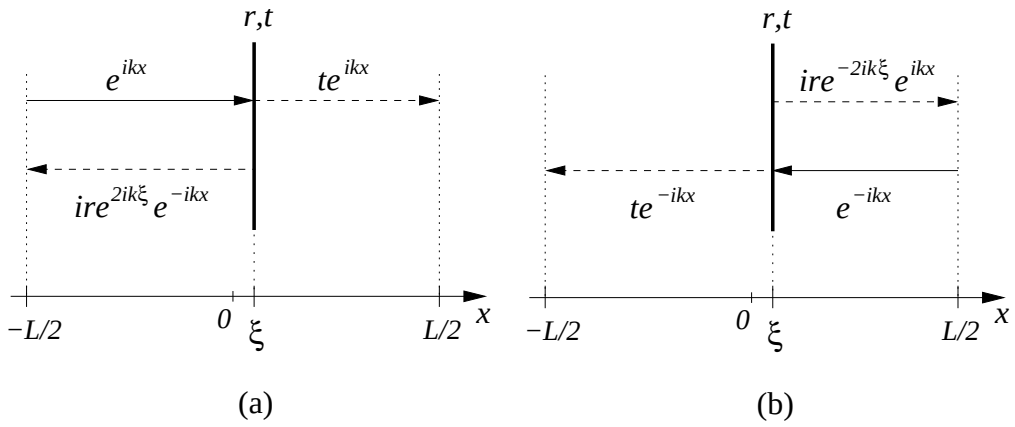

Figure 4.10: Scattered mode functions: panel (a) shows mode function $u_r(x)$ with a plane wave approaching from the left (solid arrow) and its transmitted and reflected parts (dashed arrows); panel (b) depicts the opposite case $u_l(x)$.

where we introduced the complex position-dependent reflection coefficient $r_\xi := re^{2ik\xi}$. Figure 4.10 illustrates the scattered mode functions $u_{r/l}(x)$. In order to find the proper normalization, we observe

$$\int_{-L/2}^{L/2} dx|u_{r/l}(x)|^2 = L - 2\frac{r}{k}\sin^2\left[k(L/2 \pm \xi)\right] \pm 2\xi r^2 \approx L \tag{4.89}$$

where the upper (lower) signs corresponds to the $r(l)$-mode. In the last step, we made use of the relations $\xi \ll k^{-1} \ll L$. Thus, the mode functions are normalized by the factor $1/\sqrt{L}$ to a good approximation and we can continue to use the normalization $\mathcal{N} := \sqrt{\hbar\omega/2\varepsilon_0 V}$ for the electric field operator

$$E^{(+)}(x,t) = \mathcal{N}\left[a_r u_r(x) + a_l u_l(x)\right] \tag{4.90}$$

$$= \mathcal{N} \cdot \begin{cases} \left(e^{ikx} + ir_\xi e^{-ikx}\right) a_r + te^{-ikx} a_l & x < \xi \\ te^{ikx} a_r + \left(e^{-ikx} + ir_\xi^* e^{ikx}\right) a_l & x > \xi \end{cases} \tag{4.91}$$

which is the positive frequency part of the real-valued electric field $E = E^{(+)} + E^{(-)}$. For the sake of short notation, we will however drop the superscript $(+)$, as the following will be true for both E and $E^{(+)}$.

Due to the ring geometry of the setup under consideration, one has to require additional boundary conditions, namely, continuity of the electric field and its first x-derivative at $x = \pm L/2$

$$E(-L/2,t) \stackrel{!}{=} E(L/2,t) \tag{4.92}$$

$$\partial_x E(-L/2,t) \stackrel{!}{=} \partial_x E(L/2,t) \tag{4.93}$$

That is, we glue together the ends of the interval $[-L/2, L/2]$. Inserting the expression for the electric field given above, we find the matrix relation

$$\begin{pmatrix} e^{-ikL} + ir_\xi - t & -e^{-ikL} - ir_\xi^* + t \\ e^{-ikL} - ir_\xi - t & e^{-ikL} - ir_\xi^* - t \end{pmatrix} \begin{pmatrix} a_r \\ a_l \end{pmatrix} \stackrel{!}{=} 0 \tag{4.94}$$

which can only hold for non-trivial solutions if the determinant of the matrix vanishes, implying the condition

$$k_\pm L = 2\pi n \mp \theta, \qquad n \in \mathbb{Z} \tag{4.95}$$

and, again, the same the same eigenfrequency relation as in (4.34) and (4.54) shows up. To find the eigenvectors, we sum up the two equations (4.94), insert the eigenfrequencies and find

$$a_l^{(\pm)} = \pm e^{2ik\xi} a_r^{(\pm)} \tag{4.96}$$

from which the orthonormal basis vectors

$$\tilde{\mathbf{v}}_\pm = \frac{1}{\sqrt{2}} \begin{pmatrix} e^{-ik\xi} \\ \pm e^{ik\xi} \end{pmatrix} \tag{4.97}$$

can be read off. Note that these are exactly the same as in (4.45). By defining the field operators of the eigenmodes $\tilde{a}_\pm := a_r^{(\pm)}$, we get the transformation relation

$$\begin{pmatrix} a_r \\ a_l \end{pmatrix} = \tilde{a}_+ \tilde{\mathbf{v}}_+ + \tilde{a}_- \tilde{\mathbf{v}}_- = \mathcal{V}^{-1} \begin{pmatrix} \tilde{a}_+ \\ \tilde{a}_- \end{pmatrix} \tag{4.98}$$

where $\mathcal{V}^{-1}$ is the same basis transformation used in the previous sections

$$\mathcal{V}^{-1} = \frac{1}{\sqrt{2}} \begin{pmatrix} e^{-ik\xi} & e^{-ik\xi} \\ e^{ik\xi} & -e^{ik\xi} \end{pmatrix} \tag{4.99}$$

In order to find the mode functions corresponding to the $\pm$ modes above, we replace the r/l-mode operators in (4.90) and (4.91) according to relation (4.98), leading to

$$E(x,t) = \mathcal{N}\big[\tilde{a}_+ \tilde{u}_+(x) + \tilde{a}_- \tilde{u}_-(x)\big] \tag{4.100}$$

where

$$\tilde{u}_+ = \sqrt{2}\, e^{i\theta/2} \cos\big[k|x-\xi| + \theta/2\big] \tag{4.101}$$

$$\tilde{u}_- = i\sqrt{2}\, e^{-i\theta/2} \sin\big[k(x-\xi) - (\theta/2)\,\mathrm{sgn}(x-\xi)\big] \tag{4.102}$$

$$= i\sqrt{2}\, e^{-i\theta/2} \begin{cases} -\sin\big[k|x-\xi| - \theta/2\big] & x < \xi \\ \sin\big[k|x-\xi| - \theta/2\big] & x > \xi \end{cases} \tag{4.103}$$

and we see that $\tilde{u}_+$ ($\tilde{u}_-$) is an even (odd) function with respect to the mirror position ξ. These mode functions are shown in figure 4.11 for different values of θ and there we also see the reason for the particular θ-dependence of the eigenfrequencies. As θ increases, i.e. the PRM becomes more and more reflective, the + (−) mode is "attracted" to ("repelled" from) the PRM, thereby increasing (decreasing) the wavelength due to the boundary condition and thus the corresponding eigenfrequency becomes smaller (larger), as indicated by (4.95)[4].

[4]Barton *et al* [31] treat the PRM as a δ-potential for the electric fields. The corresponding matching condition then implies transmission and reflection coefficients of the form $\tau = \cos\theta\, e^{i\theta}$ and $\rho = i\sin\theta\, e^{i\theta}$, respectively. The only difference to our convention is the phase factor $e^{i\theta}$, which results in the fact that the odd mode function as well as its eigenfrequency do not depend on θ at all, whereas the even mode experiences twice the change as it does with our convention. In that case, one avoids the discontinuity of $\tilde{u}_-$ at the mirror, however, as we already mentioned above, the optomechanical force we will derive in section 5 does not depend on the particular phase convention.

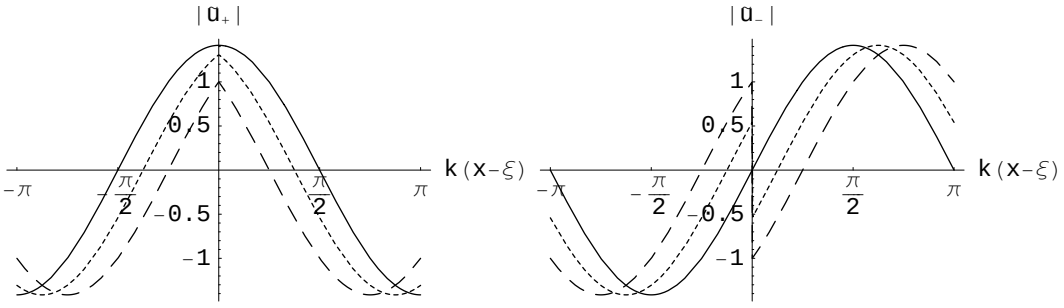

Figure 4.11: Plots of the mode functions $|\tilde{u}_+(x)|$ (left panel) and $|\tilde{u}_-(x)|$ (right panel) for $\theta = 0$ (solid line), $\theta = \pi/4$ (short dashed line) and $\theta = \pi/2$ (long dashed line)

We also would like to find a connection between the R/L-modes and the r/l-modes, each of which gives a possibility to represent the electric field operator

$$E(x,t)/\mathcal{N} = a_R u_R(x) + a_L u_L(x) = a_r u_r(x) + a_l u_l(x) \tag{4.104}$$

Due to the orthonormal nature of the mode functions, the field operators $a_{R/L}$ are then given by the projection of $E(x,t)$ written in the r/l basis onto the mode functions $u_{R/L}(x)$, respectively, i.e.

$$a_{R/L} = \frac{1}{\mathcal{N}}\frac{1}{L}\int_{-L/2}^{L/2} dx\, u^*_{R/L}(x) E(x,t) \tag{4.105}$$

which then leads to

$$\begin{pmatrix} a_R \\ a_L \end{pmatrix} = \mathcal{W}^{-1} \begin{pmatrix} a_r \\ a_l \end{pmatrix} \tag{4.106}$$

where

$$\mathcal{W}^{-1} = \begin{pmatrix} \sqrt{\frac{1+t}{2}} & \frac{ir^*_\xi}{\sqrt{2(1+t)}} \\ \frac{ir_\xi}{\sqrt{2(1+t)}} & \sqrt{\frac{1+t}{2}} \end{pmatrix} = \begin{pmatrix} \cos(\theta/2) & i\sin(\theta/2)e^{-2ik\xi} \\ i\sin(\theta/2)e^{2ik\xi} & \cos(\theta/2) \end{pmatrix} \tag{4.107}$$

where we have normalized $\mathcal{W}^{-1}$ in order to be unitary and hence preserve the commutation relations. Observe, that if $r \to 0$ ($\theta \to 0$), i.e. the PRM gets completely transparent, then $\mathcal{W}^{-1} \to \mathbb{1}$. The reason for that is the vanishing reflected part in $u_{r/l}(x)$ and therefore only the plane waves described by $u_{R/L}(x)$ remain. One may therefore tend to think that the R/L-basis is only suitable for small or vanishing PRM reflectivities, as mentioned in the beginning of this section.

If one puts together the results collected above, namely,

$$\begin{pmatrix} \tilde{a}_+ \\ \tilde{a}_- \end{pmatrix} = \mathcal{V}\mathcal{W} \begin{pmatrix} a_R \\ a_L \end{pmatrix} \tag{4.108}$$

one can now derive an equation of motion for $a_{R/L}$ or, alternatively, an equation describing the discrete time evolution thereof, since both have a simple form in the eigenbasis. Starting from the discrete stationary time evolution of the eigenmodes expressed by

$$\begin{pmatrix}\tilde{a}_+(t+\tau)\\ \tilde{a}_-(t+\tau)\end{pmatrix} = \mathbb{S}_1^{(\pm)}\begin{pmatrix}\tilde{a}_+(t)\\ \tilde{a}_-(t)\end{pmatrix}, \qquad \mathbb{S}_1^{(\pm)} := \begin{pmatrix}e^{-i\omega_+\tau} & 0\\ 0 & e^{-i\omega_-\tau}\end{pmatrix} \tag{4.109}$$

where $\omega_\pm\tau = \omega_n^{(0)} \mp \theta$ are the eigenfrequencies, one finds

$$\begin{pmatrix}a_R(t+\tau)\\ a_L(t+\tau)\end{pmatrix} = \mathcal{W}^{-1}\mathcal{V}^{-1}\mathbb{S}_1^{(\pm)}\mathcal{V}\mathcal{W}\begin{pmatrix}a_R(t)\\ a_L(t)\end{pmatrix} =: \Lambda\begin{pmatrix}a_R(t)\\ a_L(t)\end{pmatrix} \tag{4.110}$$

If we insert $\mathbb{1} = \mathcal{V}^{-1}\mathcal{V}$ on either side of Λ and define $\tilde{\mathcal{W}} = \mathcal{V}\mathcal{W}\mathcal{V}^{-1}$, we observe

$$\Lambda = \mathcal{V}^{-1}\mathcal{V}\Lambda\mathcal{V}^{-1}\mathcal{V} = \mathcal{V}^{-1}\tilde{\mathcal{W}}^{-1}\mathbb{S}_1^{(\pm)}\tilde{\mathcal{W}}\mathcal{V} = \mathcal{V}^{-1}\mathbb{S}_1^{(\pm)}\mathcal{V} = \begin{pmatrix}t & ire^{-2ik\xi}\\ ire^{2ik\xi} & t\end{pmatrix} \tag{4.111}$$

For the middle step consider the following argument. The matrix $\mathcal{W}$ is an element of the same subgroup as $e^{i\omega\tau}\mathbb{S}_1 \in SU(2)$, which was mentioned in section 4.3.2. Actually, it is almost the same matrix using the angle $\theta/2$ instead of θ. This implies that it is diagonalized by $\mathcal{V}$, too, and since diagonal matrices always commute, $[\mathbb{S}_1^{(\pm)}, \tilde{\mathcal{W}}] = 0$ holds.

Surprisingly, the matrix generating the time step τ in the r/l-basis, $\mathcal{V}^{-1}\mathbb{S}_1^{(\pm)}\mathcal{V}$, is exactly the same as the one for the R/L-basis, Λ, and, moreover, both are equal to $\mathbb{S}_1$ matching the results found above. Thus, it makes no difference whether we use the R/L- or the r/l-basis, although the latter one seems to be the proper one at first sight. Note, that the phase factor of (4.65) does not show up here as it equals 1 due to the fact that $\omega_n^{(0)}\tau = 2\pi n$ holds.

Towards the equations of motion, we start from the known dynamics in the $\pm$ basis

$$\begin{pmatrix}\dot{\tilde{a}}_+\\ \dot{\tilde{a}}_-\end{pmatrix} = M^{(\pm)}\begin{pmatrix}\tilde{a}_+\\ \tilde{a}_-\end{pmatrix}, \qquad M^{(\pm)} := \begin{pmatrix}-i\omega_+ & 0\\ 0 & -i\omega_-\end{pmatrix} \tag{4.112}$$

which turns into

$$\begin{pmatrix}\dot{a}_R\\ \dot{a}_L\end{pmatrix} = \mathcal{W}^{-1}\mathcal{V}^{-1}M^{(\pm)}\mathcal{V}\mathcal{W}\begin{pmatrix}a_R\\ a_L\end{pmatrix} = M\begin{pmatrix}a_R\\ a_L\end{pmatrix} \tag{4.113}$$

where we applied the same arguments as above to find

$$M = \begin{pmatrix}-i\omega_n^{(0)} & i\frac{\theta}{\tau}e^{-2ik\xi}\\ i\frac{\theta}{\tau}e^{2ik\xi} & -i\omega_n^{(0)}\end{pmatrix} \tag{4.114}$$

Again, the equations are identical for the R/L- and r/l-basis, respectively, and we also recover the results found in section 4.3.2.

Therefore, we will continue to use the R/L-basis since the description in terms of these is equivalent to one using the r/l-basis, as we have seen above. Furthermore, the R/L-basis gives an intuitive way of including the pumping and also of deriving the force on the PRM as we will see in chapter 5.

4.5 Steady-state and fluctuations of the fields

In the present section, we will take a closer look at the properties of the resonator fields and their dependence on the pumping. This will help us to understand the optomechanical forces being developed in chapter 5. The groundwork for our analysis is given by the equations of motion for the field operators $a_\pm$ since this is the proper basis for arbitrary PRM reflectivities. Recall the corresponding Langevin equations

$$\dot{a}_+ = \left(-i\omega_+ - \frac{\kappa}{2}\right) a_+ + E_+ e^{-i\omega_p t} + \sqrt{\kappa}\, a_+^{\text{in}} \tag{4.115}$$

$$\dot{a}_- = \left(-i\omega_- - \frac{\kappa}{2}\right) a_- + E_- e^{-i\omega_p t} + \sqrt{\kappa}\, a_-^{\text{in}} \tag{4.116}$$

where $(E_+, E_-)^T = \mathcal{V}(E_R, E_L)^T$ are the pump parameters and $(a_+^{\text{in}}, a_-^{\text{in}})^T = \mathcal{V}(a_R^{\text{in}}, a_L^{\text{in}})^T$ are the input noise operators. The eigenfrequencies were given by $\omega_\pm = \omega_0 \mp \theta/\tau$ where ω_0 is an eigenfrequency of the ring resonator without the PRM. The pump parameters $E_{R/L}$ represent the coherent driving of the clockwise/counterclockwise travelling plane wave modes by external laser fields at frequency ω_p and will be discussed in detail in the subsequent section.

For the sake of convenience, we rewrite the equations of motion in a frame rotating at the pump frequency ω_p by the replacement $a_\pm \to a_\pm e^{-i\omega_p t}$ and obtain

$$\dot{a}_+ = \left(-i\Delta_0 + i\frac{\theta}{\tau} - \frac{\kappa}{2}\right) a_+ + E_+ + \sqrt{\kappa}\, a_+^{\text{in}} \tag{4.117}$$

$$\dot{a}_- = \left(-i\Delta_0 - i\frac{\theta}{\tau} - \frac{\kappa}{2}\right) a_- + E_- + \sqrt{\kappa}\, a_-^{\text{in}} \tag{4.118}$$

where we introduced the detuning of the pump laser from the resonance frequency of the empty cavity, $\Delta_0 = \omega_0 - \omega_p$. Note, that we did not choose a different notation for the rotating frame operators since we retain this description from now on, keeping in mind that we are working in a rotating frame. Moreover, most of the physical quantities under consideration do not change if we go into a frame rotating at a different frequency due to the fact that they are bilinear in the creation and annihilation operators.

The coherent pumping suggests that the time evolution of the resonator modes is also given by small fluctuations around a steady-state value [6], [7], i.e.

$$a_\pm(t) = \alpha_\pm + \delta a_\pm(t) \tag{4.119}$$

where we require $\langle a_\pm \rangle = \alpha_\pm$ and $\langle \delta a_\pm \rangle = 0$. Inserting this ansatz into (4.117) and (4.118) splits each of the equations into a relation for the the steady-state amplitudes

$$\alpha_+ = \frac{E_+}{i\Delta_0 - i\frac{\theta}{\tau} + \frac{\kappa}{2}} \tag{4.120}$$

$$\alpha_- = \frac{E_-}{i\Delta_0 + i\frac{\theta}{\tau} + \frac{\kappa}{2}} \tag{4.121}$$

and an equation of motion for the field fluctuations

$$\dot{\delta a}_+ = \left(-i\Delta_0 + i\frac{\theta}{\tau} - \frac{\kappa}{2}\right)\delta a_+ + \sqrt{\kappa}\, a_+^{\text{in}} \tag{4.122}$$

$$\dot{\delta a}_- = \left(-i\Delta_0 - i\frac{\theta}{\tau} - \frac{\kappa}{2}\right)\delta a_- + \sqrt{\kappa}\, a_-^{\text{in}} \tag{4.123}$$

The properties of these will be discussed in the following sections. But first we want to present the pumping scheme under consideration and its implications on the pump parameters.

4.5.1 General and symmetric pumping scheme

As mentioned above, the driving of the R- and L-mode of the cavity is represented by the two pump parameters $E_{R/L}$, respectively, and is realized by two independent external pump lasers. In such case, they have the form

$$E_R = E_R^0 e^{i\varphi_R}, \qquad E_L = E_L^0 e^{-i\varphi_L} \tag{4.124}$$

and the magnitudes are given by

$$E_{R/L}^0 = \sqrt{\frac{\kappa P_{R/L}}{\hbar\omega_p}} \tag{4.125}$$

where $P_{R/L}$ is the power of the external pump laser for the R/L-mode, respectively. The intensity damping rate of the cavity field $\kappa \approx T/\tau$ also enters and it plays the role of a coupling efficiency between the pump laser and the cavity fields. The fact that $\left|E_{R/L}\right| \propto \sqrt{\kappa} \propto \sqrt{T}$ simply originates from the attenuation of the pump laser amplitude at the transmission through the CM. All this corresponds to a semi-classical treatment of the pump laser field where the cavity is driven by a classical oscillating field $E_{R/L}e^{-i\omega_p t}$ plus the vacuum fluctuations from the outside modes. Alternatively, one may imagine that one of the "outside world modes", namely one of frequency ω_p, is a pumping mode being in a coherent state which we know to have exactly the properties just mentioned (cf. section 3.1.1).

Throughout this thesis we assume the input noise to be Markovian, Gaussian white noise with zero-mean, i.e.

$$\langle a_i^{\text{in}} \rangle = 0, \qquad \left\langle a_i^{\text{in}}(t) a_j^{\text{in}\dagger}(t') \right\rangle = \delta_{ij}\delta(t-t'), \qquad i,j \in \{R,L\} \tag{4.126}$$

which corresponds to a zero-temperature field (cf. section 3.1.2) and no laser noise. Furthermore, the driving lasers are not cross-correlated as indicated by δ_{ij}. Due to the unitarity of the basis transformation $\mathcal{V}$, which connects the $\pm$ and the R/L-basis, we find these facts to hold for the noise operators in the $\pm$ basis, too. That is, equation (4.126) is also true for $i,j \in \{+,-\}$.

The pump parameters of the $\pm$ and the R/L-basis are of course also connected by $\mathcal{V}$, hence

$$E_\pm = \frac{1}{\sqrt{2}}\left(E_R e^{ik\xi} \pm E_L e^{-ik\xi}\right) \tag{4.127}$$

and the corresponding "intensities" are given by

$$|E_\pm|^2 = \frac{1}{2}\left[(E_R^0)^2 + (E_L^0)^2 \pm 2E_R^0 E_L^0 \cos(2k\xi + \phi)\right] \tag{4.128}$$

$$\approx \begin{cases} (E_R^0 \pm E_L^0)^2 & \phi = 0 \\ \frac{1}{2}\left[(E_R^0)^2 + (E_L^0)^2\right] \mp 2E_R^0 E_L^0 \cdot k\xi & \phi = \pi/2 \\ (E_R^0 \mp E_L^0)^2 & \phi = \pi \end{cases} \tag{4.129}$$

where we neglected all powers of $k\xi$ larger than $n = 1$ in the last step, since $k\xi \ll 1$. Obviously, the choice of the phase difference of the pump lasers, $\phi = \varphi_R + \varphi_L$, determines the particular pumping of the $\pm$ modes, since the steady-state amplitudes (4.120) and (4.121) are proportional to $E_\pm$. If $\phi = 0$, the pump parameter for the $+\,(-)$ mode is roughly the sum (difference) of the pump parameters for the R/L-modes and vice versa if $\phi = \pi$. If $\phi = \pi/2$, both modes are more or less equally driven. Moreover, we find

$$E_+^* E_- = \frac{1}{2}\left[(E_R^0)^2 - (E_L^0)^2 + 2iE_R^0 E_L^0 \sin(2k\xi + \phi)\right] \tag{4.130}$$

$$\approx \frac{1}{2}\left[(E_R^0)^2 - (E_L^0)^2\right] + iE_R^0 E_L^0 \begin{cases} 2k\xi & \phi = 0 \\ 1 & \phi = \pi/2 \\ -2k\xi & \phi = \pi \end{cases} \tag{4.131}$$

which will be important in section 5 when investigating the steady-state average of the optomechanical force on the PRM.

Equation (4.124) shows the most general pumping scheme we will consider. As we will see in section 5, the case of asymmetric magnitude pumping, i.e. $E_R^0 \neq E_L^0$, produces a constant term in the steady-state value of the optomechanical force, which then leads to a static displacement of the PRM on average. Actually, this constant term is already visible in (4.130), as it will originate from the difference of the pumping intensities. For the sake of simplicity, we will, however, mostly consider symmetric magnitude pumping, i.e. $E_R^0 = E_L^0 = E_0$, which may be realized as depicted in figure 4.12. A laser beam is sent to a 50:50 beam splitter (BS) and the two product beams of equal amplitude are then coupled into the ring resonator in order to drive the R/L mode, respectively. Moreover, we also choose the phase of $E_{R/L}$ in a symmetric manner, such that

$$E_R = E_0 e^{i\varphi}, \qquad E_L = E_0 e^{-i\varphi} \tag{4.132}$$

which yields

$$E_\pm = \frac{E_0}{\sqrt{2}}\left(e^{i(k\xi+\varphi)} \pm e^{-i(k\xi+\varphi)}\right) = \sqrt{2}\,E_0 \begin{cases} \cos(k\xi + \varphi) & +\text{ mode} \\ i\sin(k\xi + \varphi) & -\text{ mode} \end{cases} \tag{4.133}$$

As the mirror displacement is very small compared to the wavelength, i.e. $k\xi \ll 1$, the choice of the phase φ determines which one of the $\pm$ modes is pumped. If $\varphi = 0$, mainly the $+$ mode is excited and if one wants to drive the $-$ mode, one has to choose $\varphi = \pi/2$. The choice $\varphi = \pi/4$ leads roughly to equal excitement of both modes with only small variations by the PRM displacement $k\xi$. These three cases

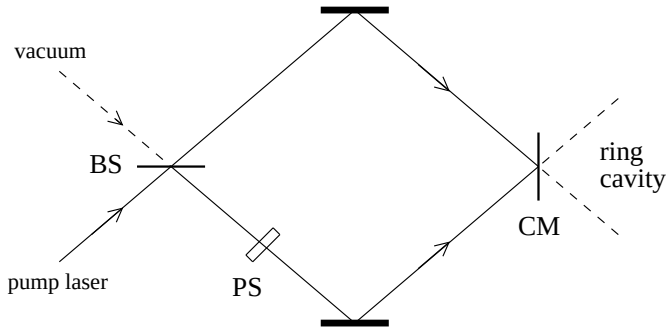

Figure 4.12: Setup to realize amplitude-symmetric pumping. A laser beam hits the 50:50 beam splitter (BS) where it is split into two beams of equal amplitude. The phase shifter (PS) is to correct the phase difference of the lower beam due to the reflection at the BS and the beams are coupled into the ring through the incoupling mirror (CM).

are also suggested by (4.129) for amplitude-symmetric pumping, which makes clear why we selected $\phi = 2\varphi = 0, \pi/2, \pi$ in (4.129).

Thus, in addition to the choice of the pump frequency $\omega_p \approx \omega_+$ or $\omega_p \approx \omega_-$, the phase φ is thus a second parameter to control the driving of only one of the $\pm$ modes.

4.5.2 Steady-state amplitudes

Obviously, the steady-state amplitudes

$$\alpha_\pm = \frac{E_\pm}{i\Delta_0 \mp i\frac{\theta}{\tau} + \frac{\kappa}{2}} \tag{4.134}$$

are proportional to the pumping parameters $E_\pm$ discussed above and equation (4.119) implies that the average photon number of each mode is given by

$$\langle a_\pm^\dagger a_\pm \rangle = |\alpha_\pm|^2 \tag{4.135}$$

which is plotted in figure 4.13. These plots nicely illustrate the properties mentioned in the previous section. First, as $\varphi = 0$ selects the $+$ mode to be mainly pumped, the intensity of that mode is relatively high, whereas the $-$ mode has very little intensities. Second, the intensity of the $+$ mode is very robust against a displacement of the mirror, as opposed to the $-$ mode which contains on average no photons if the mirror resides at its rest position $\xi = 0$. If the mirror, however, is displaced, the symmetry of the setup is broken and the $-$ mode is slightly excited, too. Third, in the direction of detuning, the plots exhibit a Lorentzian profile as one would expect for damped harmonic oscillators. One can also see that the bandwidth (FWHM) is given by κ. From this fact we deduce that the $\pm$ modes are well separated if $2\theta/\tau \gg \kappa$ implying $\theta \gg T/2$. That is, for PRM reflectivities much larger than the incoupling mirror transmittivity the degeneracy of the modes is completely lifted and the proper basis then is the $\pm$ basis – a behaviour similar to the dressed states of an atom in a linear cavity. For instance, using a transmittivity of about $T = 10^{-3}$ immediately suggests the use of the $\pm$ basis all the time.

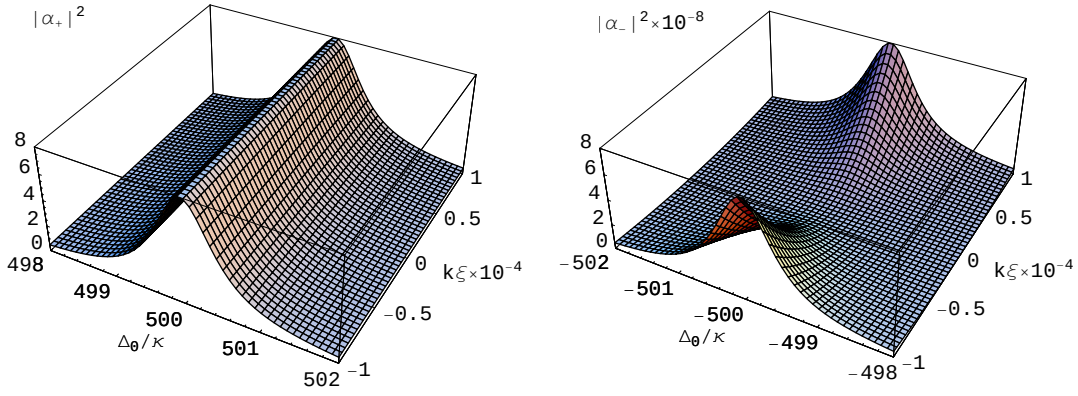

Figure 4.13: Average photon number of the + mode (left panel) and the − mode (right panel) for $\theta = 0.5$, $T = 10^{-3}$, $E_0 = \kappa$ and $\varphi = 0$.

Finally, note the particular detunings required to excite the modes. The offset of the eigenfrequencies from the resonance frequency ω_0 normalized by κ is $\mp\theta/(\kappa\tau) = \mp\theta/T$, where we applied low incoupling mirror transmittivity T as in (4.71). Given the values of the parameters used in figure 4.13, one can thus verify the required detunings for each mode.

4.5.3 Fluctuations

In order to investigate the fluctuations of the fields we first take a look at the averages and correlations of the input noise, given the pumping setup sketched in figure 4.12. Initially, we have the mixing of two modes at the BS, one is the actual pumping laser, a_p, and the other one is just the vacuum, a_0, i.e.

$$a_p = \alpha_p + a_p^{\text{in}} \tag{4.136}$$

$$a_0 = a_0^{\text{in}} \tag{4.137}$$

where the noise operators satisfy the properties mentioned in (4.126) By making use of the scattering matrix of a 50:50 BS—equation (4.9) with $r = t = 1/\sqrt{2}$ and of course $\varphi_\tau = 0$—we find the field amplitudes impinging upon the incoupling mirror to be

$$a_R^p = \frac{1}{\sqrt{2}}\left(\alpha_p + a_p^{\text{in}} - i a_0^{\text{in}}\right) =: \frac{\alpha_p}{\sqrt{2}} + a_R^{\text{in}} \tag{4.138}$$

$$a_L^p = \frac{1}{\sqrt{2}}\left(\alpha_p + a_p^{\text{in}} + i a_0^{\text{in}}\right) =: \frac{\alpha_p}{\sqrt{2}} + a_L^{\text{in}} \tag{4.139}$$

where we already took into account the phase correction of the PS and identified the input noise operators $a_{R/L}^{\text{in}}$. Their mean and correlations are also found to be the same as in (4.126). That is, this particular pumping setup also realizes Markovian, Gaussian white noise at the input of the R- and L-modes, which is not cross-correlated. Again, due to the unitarity of $\mathcal{V}$, this also holds for the noise operators in the $\pm$ basis.

After we derived the properties of the input noise operators, we now want to find the correlations of the field fluctuations which are governed by the equations of motion (4.122) and (4.123). As we are interested in steady-state solutions, we consider the equations in the frequency domain, since transients are neglected there. For the Fourier transformation we use the convention

$$f(\omega) = \frac{1}{\sqrt{2}\pi} \int dt\, e^{i\omega t} f(t) \tag{4.140}$$

implying that when going into the frequency domain one uses the replacement $d/dt \to -i\omega$ and one thus obtains the solutions

$$\delta a_+(\omega) = \frac{\sqrt{\kappa}\, a_+^{\mathrm{in}}(\omega)}{-i\omega + i\Delta_+ + \frac{\kappa}{2}} \tag{4.141}$$

$$\delta a_-(\omega) = \frac{\sqrt{\kappa}\, a_-^{\mathrm{in}}(\omega)}{-i\omega + i\Delta_- + \frac{\kappa}{2}} \tag{4.142}$$

where we defined the detunings from the eigenfrequencies $\omega_\pm$ by $\Delta_\pm := \omega_\pm - \omega_p = \Delta_0 \mp \theta/\tau$, which are related by $\Delta_+ = \Delta_- - 2\theta/\tau$. The correlations of $a_\pm^{\mathrm{in}}$ in the frequency domain are simply $\langle a_i^{\mathrm{in}}(\omega) a_j^{\mathrm{in}\dagger}(\omega')\rangle = \delta_{ij}\delta(\omega - \omega')$, hence

$$\left\langle \delta a_\pm(\omega) \delta a_\pm^\dagger(\omega') \right\rangle = \frac{\kappa\, \delta(\omega - \omega')}{\left| -i\omega + i\Delta_\pm + \frac{\kappa}{2} \right|^2} \tag{4.143}$$

and, again, the cross-correlations vanish. One now simply has to transform this expression back into the time domain which yields

$$\left\langle \delta a_\pm(t) \delta a_\pm^\dagger(t') \right\rangle = \int d\omega\, e^{-i\omega(t-t')} \left[\frac{1}{\pi} \frac{\frac{\kappa}{2}}{\left(\frac{\kappa}{2}\right)^2 + (\omega - \Delta_\pm)^2} \right] \tag{4.144}$$

$$= \exp\left[-i\Delta_\pm (t - t') \right] \exp\left(\frac{\kappa}{2} |t - t'| \right) \tag{4.145}$$

As the correlation function only depends on the time difference $t - t'$ the field noise is still stationary, just as the input noise. However, the field fluctuations are now coloured, that is, the spectrum of the fluctuations is non-uniform. This can be seen from (4.144), since the Fourier transform of a stationary correlation function gives the power spectral density of that process, as is stated by the Wiener-Khintchine theorem [32]. One thus finds a Lorentzian spectrum for the field noise of bandwidth (FWHM) κ. This "filtering" of the white input noise is due to the typical response of a damped harmonic oscillator to different driving frequencies. In other words, the frequencies of the input noise far away from the resonance frequency of the electromagnetic field mode(s) do not create a significant response of the mode under consideration. Only fluctuations at frequencies near the resonance frequency $\omega_\pm$ induce significant fluctuations of the field. By the way, this fact is also responsible for the Lorentz-shaped detuning dependence visible in figure 4.13. In the "bad cavity limit" the time scale of interest is much larger than the typical time scale on which the field dynamics takes place, κ, and one can thus approximate correlation functions like (4.145) with a delta correlation, as we will do in section 5.

Chapter 5

Optomechanical force on the PRM

In the present chapter we will present different approaches to obtain an expression for the optomechanical force exerted on the PRM due to the presence of electromagnetic fields inside the ring cavity. First, we use Maxwell's stress tensor, which describes optomechanical forces acting on dielectric surfaces. We compute its values on either side of the PRM and the net force is then proportional to the difference of these values. Second, we evaluate the change of linear momentum of the electromagnetic field after one scattering process at the PRM. Given that we consider a lossless (unitary) PRM, this change of field momentum is then proportional to the force acting on the micro-mechanical mirror. As a third method, we will derive a unitary operator generating the discrete time evolution of the fields in steps of the round trip time τ, which we found in chapter 4. The application of this unitary operator to the momentum operator of the PRM also produces a change of momentum, which then can be translated into a force.

The second part of this chapter deals with the analysis of this optomechanical force, especially its dependence on the detuning of the pump lasers from the cavity eigenfrequencies, $\Delta_{\pm}$, the pump amplitudes, $E^0_{R/L}$, and the PRM reflectivity and displacement, θ and ξ, respectively.

5.1 Three ways to the force operator

5.1.1 Maxwell stress tensor

The Maxwell stress tensor is the stress tensor of an electromagnetic field and is generally given by

$$\sigma_{ij} = \varepsilon_0 E_i E_j + \frac{1}{\mu_0} B_i B_j - \frac{1}{2}\left(\varepsilon_0 \mathbf{E}^2 + \frac{1}{\mu_0}\mathbf{B}^2\right)\delta_{ij}, \qquad i,j \in \{x,y,z\} \tag{5.1}$$

where $\mathbf{E} = (E_x, E_y, E_z)^T$ and $\mathbf{B} = (B_x, B_y, B_z)^T$ are general electric and magnetic fields, respectively. The ijth element of the tensor can be interpreted as a force parallel to the i-axis suffered by a surface element of unit area perpendicular to the j-axis. In other words, the iith element gives the pressure onto the surface normal to the i-axis. Since we only consider fields travelling along the x-direction, we only

need to consider σ_{xx} on either side of the PRM. Under the circumstances described in section 3.2.2, Maxwell's stress tensor thus boils down to

$$\sigma \equiv \sigma_{xx} = -\frac{1}{2}\left(\varepsilon_0 E^2 + \frac{1}{\mu_0} B^2\right) \tag{5.2}$$

where

$$E(x,t) \equiv E_y(x,t) = \sqrt{\frac{\hbar\omega_k}{2\varepsilon_0 V}}\Big[a_R\, e^{ikx} + a_L\, e^{-ikx} + h.c.\Big] \tag{5.3}$$

$$B(x,t) \equiv B_z(x,t) = \frac{1}{c}\sqrt{\frac{\hbar\omega_k}{2\varepsilon_0 V}}\Big[a_R\, e^{ikx} - a_L\, e^{-ikx} + h.c.\Big] \tag{5.4}$$

and *h.c.* denotes the hermitian conjugate of the preceding terms. Also keep in mind that the annihilation operators are actually time-dependent as we are working in the Heisenberg picture. Due to the meaning of the diagonal elements of Maxwell's stress tensor mentioned above, the total force acting on the PRM is then given by

$$F = A\big(\sigma^{\mathrm{rhs}} - \sigma^{\mathrm{lhs}}\big) \tag{5.5}$$

where σ^{rhs} and σ^{lhs} denote the optomechanical pressure σ evaluated at the surface on the right-hand side of the PRM, ξ^+, and on its left-hand side, ξ^-, respectively. Here, A is the area of illumination of the PRM's surface which is assumed to be equal to the cross section of the cavity modes, i.e. $A = V/L$. As one can see from (5.2) and (5.5), the force is actually proportional to the difference of the energy densities of the electromagnetic field on either side of the PRM.

As we have already mentioned, the electromagnetic fields on either side of the PRM are not mutually independent, but the field amplitudes are related via the PRM's scattering matrix

$$\begin{pmatrix} a_R' \\ a_L' \end{pmatrix} = \mathbb{S}_{\mathrm{prm}} \begin{pmatrix} a_R \\ a_L \end{pmatrix}, \qquad \mathbb{S}_{\mathrm{prm}} = \begin{pmatrix} \tau & \rho e^{-2ik\xi} \\ \rho e^{2ik\xi} & \tau \end{pmatrix} \tag{5.6}$$

where the primed variables represent the outgoing amplitudes and ξ is the PRM displacement. The schematic setup of this situation was already depicted in figure 4.3, however, using a slightly different notation. In (5.6), we choose to employ the complex transmission and reflection coefficients $\tau = te^{i\varphi_\tau}$ and $\rho = ire^{i\varphi_\tau}$, respectively, where $t, r \geq 0$, since we want to verify that the force F does indeed not depend on the particular choice of the transmission phase φ_τ, as claimed in section 4.1.2. Recall that we chose $t, r \geq 0$ and, moreover, $t = \cos\theta$ and $r = \sin\theta$, such that $\theta \in [0, \pi/2]$.

Hence, the electric field on the left-hand side of the PRM is

$$E_{\mathrm{lhs}} = \sqrt{\frac{\hbar\omega}{2\varepsilon_0 V}}\left(a_R e^{ik\xi} + a_L' e^{-ik\xi} + h.c.\right) \tag{5.7}$$

$$= \sqrt{\frac{\hbar\omega}{2\varepsilon_0 V}}\left[(1+\rho) a_R e^{ik\xi} + \tau a_L e^{-ik\xi} + h.c.\right] \tag{5.8}$$

and the magnetic field becomes

$$B_{\rm lhs} = \frac{1}{c}\sqrt{\frac{\hbar\omega}{2\varepsilon_0 V}}\left(a_R e^{ik\xi} - a'_L e^{-ik\xi} + h.c.\right) \tag{5.9}$$

$$= \frac{1}{c}\sqrt{\frac{\hbar\omega}{2\varepsilon_0 V}}\left[(1-\rho)a_R e^{ik\xi} - \tau a_L e^{-ik\xi} + h.c.\right] \tag{5.10}$$

implying a left-hand side optomechanical pressure

$$\begin{aligned}\sigma^{\rm lhs} = &-\frac{\hbar\omega}{2V}\Big\{\big(1+|\rho|^2\big)\big(1+2a_R^\dagger a_R\big) + |\tau|^2\big(1+2a_L^\dagger a_L\big)\\ &+2\Big[\tau\rho\, a_R a_L + \tau\rho^* a_R^\dagger a_L e^{-2ik\xi} + h.c.\Big]\\ &+\Big[\big(1+\rho^2\big)a_R^2 e^{2ik\xi} + \tau^2 a_L^2 e^{-2ik\xi} + h.c.\Big]\Big\}\end{aligned} \tag{5.11}$$

The appearance of "1+" in front of the photon number operators $a^\dagger_{R/L}a_{R/L}$ is due to the bosonic commutation relation of the creation and annihilation operators and represents the force resulting from the vacuum fluctuations, i.e. the Casimir force.

Similarly, for the right-hand side we obtain the electric field

$$E_{\rm rhs} = \sqrt{\frac{\hbar\omega}{2\varepsilon_0 V}}\left(a'_R e^{ik\xi} + a_L e^{-ik\xi} + h.c.\right) \tag{5.12}$$

$$= \sqrt{\frac{\hbar\omega}{2\varepsilon_0 V}}\left[\tau a_R e^{ik\xi} + (1+\rho)a_L e^{-ik\xi} + h.c.\right] \tag{5.13}$$

the magnetic field

$$B_{\rm rhs} = \frac{1}{c}\sqrt{\frac{\hbar\omega}{2\varepsilon_0 V}}\left(a'_R e^{ik\xi} - a_L e^{-ik\xi} + h.c.\right) \tag{5.14}$$

$$= \frac{1}{c}\sqrt{\frac{\hbar\omega}{2\varepsilon_0 V}}\left[\tau a_R e^{ik\xi} - (1-\rho)a_L e^{-ik\xi} + h.c.\right] \tag{5.15}$$

and the optomechanical pressure on the right-hand side thus is

$$\begin{aligned}\sigma^{\rm rhs} = &-\frac{\hbar\omega}{2V}\Big\{|\tau|^2\big(1+2a_R^\dagger a_R\big) + \big(1+|\rho|^2\big)\big(1+2a_L^\dagger a_L\big)\\ &+2\Big[\tau\rho\, a_R a_L + \tau^*\rho\, a_R^\dagger a_L e^{-2ik\xi} + h.c.\Big]\\ &+\Big[\tau^2 a_R^2 e^{2ik\xi} + \big(1+\rho^2\big)a_L^2 e^{-2ik\xi} + h.c.\Big]\Big\}\end{aligned} \tag{5.16}$$

The net force suffered by the mirror then turns out to be

$$\begin{aligned}F = &-\frac{\hbar\omega}{L}\Big\{2|\rho|^2\big(a_L^\dagger a_L - a_R^\dagger a_R\big) + \Big[\big(\tau^*\rho - \tau\rho^*\big)a_R^\dagger a_L e^{-2ik\xi} + h.c.\Big]\\ &+\Big[\big(\tau^2 - \rho^2 - 1\big)\big(a_R^2 e^{2ik\xi} - a_L^2 e^{-2ik\xi}\big) + h.c.\Big]\Big\}\end{aligned} \tag{5.17}$$

Observe that the vacuum (Casimir) forces from either side have cancelled each other. If we now insert the polar representations of ρ and τ given above, we discover the factors

$$|\rho|^2 = r^2 \tag{5.18}$$

$$\tau^*\rho - \tau\rho^* = 2irt \tag{5.19}$$

$$\tau^2 - \rho^2 - 1 = e^{2i\varphi_\tau} - 1 \tag{5.20}$$

Thus, we see that the only terms depending on the choice of φ_τ are the ones proportional to squared field operators. Since the time evolution of those is roughly of the form $a(t) = a\, e^{i\omega t}$, the squared expressions represent a component of the force oscillating at about twice the optical frequency, which is simply too fast for the relatively inert PRM to react and we can therefore drop these terms due to physical irrelevance. Besides this physical argument, it is also possible to consider a time average of the force over one round trip time $\tau' = L/c$, which is still very short compared to the time scale of the mirror motion ($\Omega_m\tau' \ll 1$), as explained in section 2, whereby the fast oscillating terms cancel out as well. The terms containing the product of one creation and one annihilation operator, however, will survive such an average as those are at most slowly varying with time. Altogether, we see that if suitably averaged, F effectively does not depend on the choice of the transmission phase φ_τ and the total optomechanical force acting on the PRM is thus given by

$$F = -\frac{2\hbar\omega}{L}\Big[r^2\big(a_L^\dagger a_L - a_R^\dagger a_R\big) - irt\big(a_L^\dagger a_R e^{2ik\xi} - a_R^\dagger a_L e^{-2ik\xi}\big)\Big] \tag{5.21}$$

To understand this expression consider the following. The R/L-mode contains $n_{R/L} = a_{R/L}^\dagger a_{R/L}$ photons which require the round trip time τ' to circulate the ring cavity once. The factor r^2 quantifies the relative part of photons being reflected at the PRM's surface, each of which induces a transfer of momentum of magnitude $2\hbar k$ onto the PRM. The forces thereby produced are thus given by $2\hbar k r^2 n_{R/L}/\tau'$ and since the photons of the two modes impinge onto the PRM from opposite sides, the total force is proportional to the photon number difference. Finally, the identity $\hbar\omega/L = \hbar k/\tau'$ shows that the first part in (5.21), which is also independent of the PRM displacement ξ, accounts for the *radiation pressure* due to photon reflection. The correct sign of the radiation pressure terms can also be verified easily. For example, if one only has photons in the R-mode, i.e. $n_L = 0$, the remaining radiation pressure term is positive, that is the force points into the positive x-direction, as one would expect in that case, since photons are reflected off the PRM back into the negative x-direction.

The remaining ξ-dependent part of the force (5.21) can be interpreted as a *dipole force* similar to the one encountered in the case of atoms in a field of standing waves. It involves the phase relation between a_R and a_L, which is determined by the phase relation of the pump lasers. The ξ-dependence is due to the position dependence of the field distribution and thus allows for an interpretation of the dipole force in terms of the induced dielectric polarization of the PRM, as already mentioned in the end of section 4.2.

5.1.2 Change of linear field momentum

Another way of deriving the force on the PRM due to the light is to consider the change of the linear field momentum of the electromagnetic field after one scattering process has taken place. In general, electromagnetic fields carry a momentum, which can be described by the field momentum density [33]

$$\boldsymbol{\mathcal{P}} = \frac{\mathbf{S}}{c^2} = \varepsilon_0 \, \mathbf{E} \times \mathbf{B} \tag{5.22}$$

where $\mathbf{S} = \mathbf{E} \times \mathbf{H}$ is the Poynting vector. Thus, the total linear field momentum is given by

$$\boldsymbol{\pi} = \varepsilon_0 \int_V d^3x \, \mathbf{E} \times \mathbf{B} = \varepsilon_0 A \int_0^L dx \, E_y B_z \mathbf{e}_x =: \pi \, \mathbf{e}_x \tag{5.23}$$

where we specialized to the one-dimensional situation and E_y and B_z can be seen from (5.3) and (5.4), respectively. Not surprisingly, the only non-vanishing component of the total field momentum is the x-component, as this is the direction of propagation of the electromagnetic field. Eq. (5.23) thus states that the field momentum is proportional to

$$E_y B_z = \frac{\hbar\omega}{2c\varepsilon_0 V} \left[\left(a_R^2 - {a_L^\dagger}^2\right) e^{2ikx} + \left({a_R^\dagger}^2 - a_L^2\right) e^{-2ikx} + 2a_R^\dagger a_R - 2a_L^\dagger a_L \right] \tag{5.24}$$

integrated over the whole cavity of length L. Additionally, we know from previous sections how the field operators have evolved after one round trip time $\tau = L/c$, namely,

$$\begin{pmatrix} a_R' \\ a_L' \end{pmatrix} = \mathbb{S}_1 \begin{pmatrix} a_R \\ a_L \end{pmatrix} = e^{-i\omega\tau} \begin{pmatrix} t & ire^{-2ik\xi} \\ ire^{2ik\xi} & t \end{pmatrix} \begin{pmatrix} a_R \\ a_L \end{pmatrix} \tag{5.25}$$

where we assumed an ideal ring cavity without dissipation and driving and, moreover, we returned to our choice of the transmission phase, $\varphi_\tau = 0$. After one round trip, the field momentum will in general be different from the one before due to the coupling to the PRM which redistributes the field amplitudes. One then has a field momentum π', which now contains the primed field operators instead. Figure 5.1 schematically shows the field distribution before and after a scattering process.

The fact that we deal with a conservative, i.e. lossless, PRM implies that the total momentum of the whole system should remain unchanged, that is, the change of the field momentum is equal in magnitude to the change of the PRM momentum, however, they have opposite signs. Altogether, this leads to a force acting on the PRM which is given by

$$F = -\frac{\Delta\pi}{\tau} = \frac{\pi - \pi'}{\tau} = \frac{c\varepsilon_0 A}{L} \int_0^L dx \, (E_y B_z - E_y' B_z') \tag{5.26}$$

In the following, we will again neglect the squared terms $\left(a_{R/L}^{(\dagger)}\right)^2$ of (5.24) since the spatial integral of the fast oscillating terms $e^{\pm 2ikx}$ scales like $k^{-1} \ll L$ and is thus

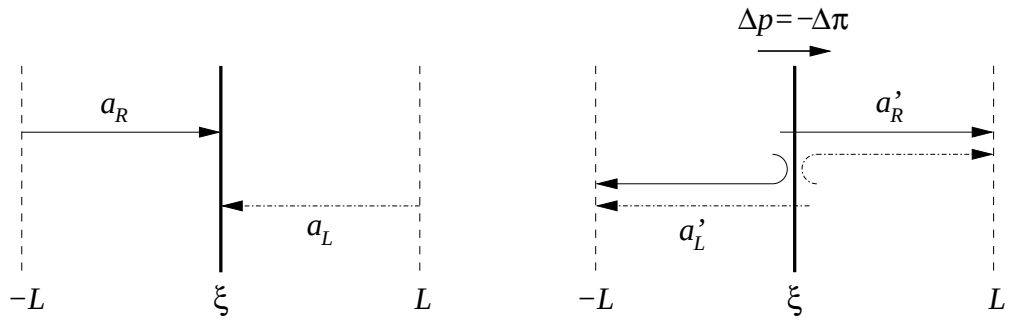

Figure 5.1: Schematic picture of the field distribution before (left panel) and after (right panel) a scattering process. The pictures correspond to times t_0 and $t_0+\tau$, respectively. The arrows represent the plane waves of the R/L-mode which extent over the whole ring cavity, but for the sake of clarity only the part of the R/L-mode which will hit the PRM during the round trip time τ is drawn. The change of PRM momentum Δp due to the interaction with the electromagnetic field is also indicated.

only a small correction to the ξ-independent terms. Hence, we find the expression

$$F = \frac{\hbar\omega}{L}\left(a_R^\dagger a_R - a_L^\dagger a_L - a_R'^\dagger a_R' + a_L'^\dagger a_L'\right) \tag{5.27}$$

$$= \frac{\hbar\omega}{L}\Big[\underbrace{(1-t^2+r^2)}_{=2r^2}\left(a_R^\dagger a_R - a_L^\dagger a_L\right) + 2irt\left(a_L^\dagger a_R e^{2ik\xi} - a_R^\dagger a_L e^{-2ik\xi}\right)\Big] \tag{5.28}$$

$$= -\frac{2\hbar\omega}{L}\Big[r^2\left(a_L^\dagger a_L - a_R^\dagger a_R\right) - irt\left(a_L^\dagger a_R e^{2ik\xi} - a_R^\dagger a_L e^{-2ik\xi}\right)\Big] \tag{5.29}$$

which is obviously exactly the same force as found in the previous section using Maxwell's stress tensor.

5.1.3 Unitary operator for one round trip

As a third approach to the optomechanical force we will now construct the unitary operator $\mathcal{U}_1$ which generates the time evolution of the system in steps of the round trip time of the light, $\tau = L/c$. The application of $\mathcal{U}_1$ to the PRM's momentum operator p then reveals how it has changed after the time τ has passed, thereby giving the possibility of deriving the force corresponding to that momentum change.

The starting point is given by the discrete time evolution of the field operators in terms of a S-matrix description as in (5.25), where we neglected cavity losses and driving (those can be added by hand later on at the level of Langevin equations). As we already know, eq. (5.25) describes how the field operators have evolved up to the time $t+\tau$, given the corresponding field operators at time t. We would now like to derive a unitary operator, $\mathcal{U}_1$, which exactly generates this discrete time evolution, however, in the fashion normally used in quantum mechanics, i.e.

$$\begin{pmatrix} a_R(t+\tau) \\ a_L(t+\tau) \end{pmatrix} = \mathbb{S}_1 \begin{pmatrix} a_R(t) \\ a_L(t) \end{pmatrix} \stackrel{!}{=} \mathcal{U}_1^\dagger \begin{pmatrix} a_R(t) \\ a_L(t) \end{pmatrix} \mathcal{U}_1 \tag{5.30}$$

At this point, we again make use of the eigenbasis of the cavity to define the unitary time evolution operator $\mathcal{U}_1$ to be

$$\mathcal{U}_1 = \exp\left(i\sum_{j=\pm}\Theta_j a_j^\dagger a_j\right) \tag{5.31}$$

where $\Theta_\pm = \pm\theta - \omega\tau$ is the argument of the complex eigenvalue $\lambda_\pm$ of $\mathbb{S}_1$, respectively, as in (4.44) and the field operators of the $\pm$ eigenmodes were defined by

$$\begin{pmatrix} a_+ \\ a_- \end{pmatrix} = \mathcal{V}\begin{pmatrix} a_R \\ a_L \end{pmatrix} = \frac{1}{\sqrt{2}}\begin{pmatrix} a_R e^{ik\xi} + a_L e^{-ik\xi} \\ a_R e^{ik\xi} - a_L e^{-ik\xi} \end{pmatrix} \tag{5.32}$$

The effect of $\mathcal{U}_1$ on the eigenmodes' field operators is found in analogy to the Heisenberg picture and one obtains

$$\mathcal{U}_1^\dagger a_\pm \mathcal{U}_1 = e^{i\Theta_\pm} a_\pm = e^{-i\omega\tau} e^{\pm i\theta} a_\pm \tag{5.33}$$

which exactly reproduces the action of $\mathbb{S}_1$ in the $\pm$ basis as requested in (5.30).
To recast $\mathcal{U}_1$ in the R/L-basis one simply has to insert the above expressions for $\Theta_\pm$ and $a_\pm$ and by identifying $\mathcal{U}_1 = \exp(-iH_1\tau/\hbar)$ we even obtain the Hamiltonian generating the time evolution of the electromagnetic fields for a single round trip

$$H_1 \equiv H_{\text{light}} = \hbar\omega\left(a_R^\dagger a_R + a_L^\dagger a_L\right) - \hbar\frac{\theta}{\tau}\left(a_R^\dagger a_L e^{-2ik\xi} + a_L^\dagger a_R e^{2ik\xi}\right) \tag{5.34}$$

Again, we recover the field Hamiltonian already found in sections 4.2 and 4.3.2. An interesting observation, however, is that this Hamiltonian does not generate the right time evolution for ξ and p, which becomes obvious when comparing $F = \dot{p} = -\partial H_1/\partial\xi$ to (5.21) and (5.29). This means that the the optomechanical force can in general not be described by a potential.

Force on PRM

The idea of $\mathcal{U}_1$ is that it generates a "stroboscopic" time evolution of the form $t \to t+\tau$, that is any operator $\mathcal{O}$ evolves in discrete time steps τ simply by applying $\mathcal{U}_1$ as it is also done for the usual time evolution operator in the Heisenberg picture

$$\mathcal{O}(t+\tau) = \mathcal{U}_1^\dagger \mathcal{O}(t)\mathcal{U}_1 \tag{5.35}$$

This means we promote $\mathcal{U}_1$ as giving the time evolution for the total system instead of its generator H_1. In the following, we will take a closer look at the action of $\mathcal{U}_1$ on p, the momentum operator of the PRM. The fact that we do not include the Hamiltonian of the oscillating PRM, H_m, results in the absence of the p-operator in $\mathcal{U}_1$ and thus represents the assumption of a "frozen" mirror, that is, the PRM position ξ is fixed during a single round trip. As mentioned before, this is only a good approximation if $\Omega_m\tau \ll 1$ (Ω_m is the angular frequency of the PRM's oscillation), which does hold for the system under consideration (cf. section 2). However, since $\mathcal{U}_1$ written in terms of $a_{R/L}$ contains the PRM's position operator ξ, its momentum operator p does evolve over one time step

$$p(t+\tau) = \mathcal{U}_1^\dagger p(t)\mathcal{U}_1 \tag{5.36}$$

This suggests a difference equation which we will approximate by a differential equation

$$\frac{dp}{dt} \approx \frac{\mathcal{U}_1^\dagger p(t)\mathcal{U}_1 - p(t)}{\tau} \tag{5.37}$$

to obtain an expression for the optomechanical force $F = dp/dt$. Adopting this procedure, we assume that the PRM is moving slowly and the PRM momentum change per time step is small, which is a good approximation since, for instance, the momentum transfer $2\hbar k$ of a reflected photon is rather tiny compared to the PRM momentum, as shown in section 3.1.1.

In order to explicitly calculate the action of $\mathcal{U}_1$ on p we have to use a little trick. The unitary time evolution operator is of the form $\mathcal{U} = \exp(i\theta A)$ where we neglected the part containing the photon numbers of the R and L-mode. We can do this since $[p, a^\dagger_{R/L} a_{R/L}] = 0$, hence the photon number terms do not contribute to the evolution of p. Specifically, we have

$$A = a_R^\dagger a_L e^{-2ik\xi} + a_L^\dagger a_R e^{2ik\xi} \tag{5.38}$$

We then rewrite

$$p(t+\tau) = p(\theta) = \exp(-i\theta A)\, p\, \exp(i\theta A) \tag{5.39}$$

whose derivative with respect to θ yields

$$\frac{dp}{d\theta} = i \exp(-i\theta A)[p, A] \exp(i\theta A) = \hbar \exp(-i\theta A) A' \exp(i\theta A) \tag{5.40}$$

where we used $p = -i\hbar\partial_\xi$ such that A' is the derivative of A with respect to the mirror position ξ. To work out the last expression in (5.40), we observe that A as well as A' are bilinear in a_R and a_L. Specifically speaking, A and A' only contain products of $a_{R/L}$ with their hermitian conjugates. Since $\mathcal{U}$ is a unitary operator we can insert $\mathbb{1} = \mathcal{U}\mathcal{U}^\dagger$ between the factors of these products and we therefore only have to consider terms like

$$\exp(-i\theta A) a_{R/L}^{(\dagger)} \exp(i\theta A) \tag{5.41}$$

From (5.30) one can see, that for the annihilation operators this is equal to the top and bottom entry of $\mathbb{S}$ applied to $(a_R, a_L)^T$, respectively, where θ as used in (5.41) determines the reflection and transmission coefficients in $\mathbb{S}$ via the relations $t = \cos\theta$ and $r = \sin\theta$. Besides, the fact that the operator $\mathcal{U}$ is used in (5.41), which is $\mathcal{U}_1$ with the photon number terms neglected, results in the application of $\mathbb{S}$ to $(a_R, a_L)^T$ rather than $\mathbb{S}_1 = \exp(-i\omega\tau)\mathbb{S}$. Thus, one finds

$$\exp(-i\theta A) a_R \exp(i\theta A) = t a_R + ir e^{-2ik\xi} a_L \tag{5.42}$$

$$\exp(-i\theta A) a_L \exp(i\theta A) = ir e^{2ik\xi} a_R + t a_L \tag{5.43}$$

As can be seen from

$$\left(\mathcal{U}^\dagger a_{R/L} \mathcal{U}\right)^\dagger = \mathcal{U}^\dagger a_{R/L}^\dagger \mathcal{U} \tag{5.44}$$

the corresponding transformation rules for $a^\dagger_{R/L}$ are simply given by the hermitian conjugates of (5.42) and (5.43), respectively.

We now have collected all information to evaluate (5.40). Then, integrating this from 0 to θ (this upper limit being the actual parameter for the PRM under consideration), one gets $p(\theta) - p(0)$, which is equivalent to $p(t+\tau) - p(t)$. If we now perform this calculation for A as given in (5.38) and employ (5.37), we finally arrive at

$$F = -\frac{2\hbar\omega}{L}\left[r^2\left(a_L^\dagger a_L - a_R^\dagger a_R\right) - irt\left(a_L^\dagger a_R e^{2ik\xi} - a_R^\dagger a_L e^{-2ik\xi}\right)\right] \tag{5.45}$$

As it should be, the whole procedure using the unitary time evolution operator for one round trip reveals the same force operator as found before. As already observed in the previous section, it is thus wrong to compute the force by using Heisenberg's equation of motion $[H_1, p]$.

5.2 Expansion into orders of PRM velocity

Until now, we have treated the PRM position ξ as a parameter which does not change during the round trip of the electromagnetic waves. Generally, of course, ξ is a dynamic variable of the micro-mechanical oscillator which changes due to the harmonic potential the oscillator is subject to and due also to the optomechanical effects of the light inside the ring cavity. The usage of ξ as a parameter corresponds to the assumption that the fields adiabatically follow the PRM position, which is approximately fulfilled in the "bad cavity limit" $\Omega_m \ll \kappa$. Later we want to calculate a friction force acting on the PRM due to the presence of the cavity modes, but a friction force can only arise from the non-adiabatic, time-delayed reaction of the field variables to the displacement of the PRM [34]. We focus on the low-velocity limit $kv \ll \kappa$, where $v = \dot{\xi}$ is the PRM velocity, i.e. the PRM moves much less than the wavelength on the time scale of the field dynamics. We can then treat the mirror motion as a perturbation and expand the field variables and the equations of motion into different orders of v and systematically solve the equations corresponding to each order of v. Following mainly the procedure used in [34] for atoms in an optical cavity, we apply the replacement

$$\frac{d}{dt} \longrightarrow \frac{\partial}{\partial t} + v\frac{\partial}{\partial \xi} \tag{5.46}$$

for the equations of motion, simultaneously expanding the field operators in orders of v

$$a_\pm = a_\pm^{(0)} + v a_\pm^{(1)} + \mathcal{O}(v^2) \tag{5.47}$$

where $a_\pm^{(0)}$ is the zeroth-order solution and $a_\pm^{(1)}$ represents the first-order correction to the field operators. Orders of v higher than the linear terms are neglected from now on. The basis for the following considerations is the Langevin equations for the field operators written in the $\pm$ basis and in a frame rotating at the pumping frequency, ω_p, which we derived generally in section 3.1.2 and 3.1.3

$$\dot{a}_+ = \left(-i\Delta_0 + i\frac{\theta}{\tau} - \frac{\kappa}{2}\right) a_+ + E_+ + \sqrt{\kappa}\, a_+^{\mathrm{in}} \tag{5.48}$$

$$\dot{a}_- = \left(-i\Delta_0 - i\frac{\theta}{\tau} - \frac{\kappa}{2}\right) a_- + E_- + \sqrt{\kappa}\, a_-^{\mathrm{in}} \tag{5.49}$$

where the damping (κ), the coherent driving ($E_\pm$) and the noise ($a_\pm^{\text{in}}$) is now included and we defined the detuning of the pump laser from the nth eigenfrequency of the ring cavity without the PRM, $\Delta_0 = \omega_n^{(0)} - \omega_p$. After the application of the replacements (5.46) and (5.47), one can identify the equations corresponding to different orders of the PRM velocity v which we are going to treat separately. The zeroth-order equations of motion are

$$\dot{a}_+^{(0)} = \left(-i\Delta_0 + i\frac{\theta}{\tau} - \frac{\kappa}{2}\right) a_+^{(0)} + E_+ + \sqrt{\kappa}\, a_+^{\text{in}} \tag{5.50}$$

$$\dot{a}_-^{(0)} = \left(-i\Delta_0 - i\frac{\theta}{\tau} - \frac{\kappa}{2}\right) a_-^{(0)} + E_- + \sqrt{\kappa}\, a_-^{\text{in}} \tag{5.51}$$

which is of course identical to the original Langevin equations for a mirror at rest. Here, the pumping and the input noise is already included and the results found in section 4.5 can thus immediately be applied to the zeroth-order solutions.

The equations of motion in first order of v, on the other hand, are found to be

$$\dot{a}_+^{(1)} = \left(-i\Delta_0 + i\frac{\theta}{\tau} - \frac{\kappa}{2}\right) a_+^{(1)} - \partial_\xi a_+^{(0)} \tag{5.52}$$

$$\dot{a}_-^{(1)} = \left(-i\Delta_0 - i\frac{\theta}{\tau} - \frac{\kappa}{2}\right) a_-^{(1)} - \partial_\xi a_-^{(0)} \tag{5.53}$$

and we see that the first-order corrections depend on the zeroth-order solutions.

In the previous sections, we derived the optomechanical force acting on the PRM due to the electromagnetic fields in the ring cavity. We arrived at

$$F = -\frac{2\hbar\omega}{L}\left[r^2\big(a_L^\dagger a_L - a_R^\dagger a_R\big) - irt\big(a_L^\dagger a_R e^{2ik\xi} - a_R^\dagger a_L e^{-2ik\xi}\big)\right] \tag{5.54}$$

which we now want to transfer into the $\pm$ basis using the transformation relation

$$a_\pm = \frac{1}{\sqrt{2}}\left(a_R e^{ik\xi} \pm a_L e^{-ik\xi}\right) \tag{5.55}$$

Substituting $a_{R/L}$ for the new field operators $a_\pm$, one obtains

$$F = \frac{2\hbar\omega}{L}\left[r^2\big(a_+^\dagger a_- + a_-^\dagger a_+\big) + irt\big(a_+^\dagger a_- - a_-^\dagger a_+\big)\right] \tag{5.56}$$

$$= \frac{4\hbar\omega}{L}\,\mathrm{Re}\left[\big(r^2 + irt\big) a_+^\dagger a_-\right] \tag{5.57}$$

We now apply the expansion (5.47) to the force, leading to

$$F = F^{(0)} + vF^{(1)} \tag{5.58}$$

Here, $F^{(0)}$ is a conservative force that will impose an additional fluctuating potential on the PRM and $F^{(1)}$ already represents a friction coefficient—at least if it is negative—since it is the proportionality factor of the part of the force which linearly depends on the PRM velocity. The friction coefficient is connected to a optically

induced dissipation rate, $\gamma_{\rm opt}$, by $\langle F^{(1)}\rangle = m\gamma_{\rm opt}$, where m is the motional mass of the micro-mechanical oscillator. One finds the expressions

$$F^{(0)} = \frac{2\hbar\omega}{L}\left[r^2\left(a_+^{(0)\dagger}a_-^{(0)} + a_-^{(0)\dagger}a_+^{(0)}\right) + irt\left(a_+^{(0)\dagger}a_-^{(0)} - a_-^{(0)\dagger}a_+^{(0)}\right)\right] \tag{5.59}$$

$$= \frac{4\hbar\omega}{L}\,\mathrm{Re}\left[\left(r^2 + irt\right)a_+^{(0)\dagger}a_-^{(0)}\right] \tag{5.60}$$

and

$$F^{(1)} = \frac{4\hbar\omega}{L}\,\mathrm{Re}\left[\left(r^2 + irt\right)\left(a_+^{(0)\dagger}a_-^{(1)} + a_+^{(1)\dagger}a_-^{(0)}\right)\right] \tag{5.61}$$

$$\tag{5.62}$$

Our aim is to investigate the expectation values of the conservative force $F^{(0)}$ as well as the friction coefficient $F^{(1)}$ and we will take a closer look at the fluctuations of the force originating from the fluctuations of the cavity fields. In the following subsections, we will successively determine and evaluate these parts of the force F.

5.2.1 Conservative part – 0th order in v

As mentioned above, the zeroth order completely neglects the motion of the PRM and treats the PRM position ξ as a parameter. The Langevin equations for the field operators (5.50) and (5.51) are equivalent to the ones considered in section 4.5 and thus all results derived there also hold for the zeroth-order field operators. In particular, adopting the ansatz

$$a_\pm^{(0)} = \alpha_\pm^{(0)} + \delta a_\pm \tag{5.63}$$

for the solutions of the Langevin equations (5.50) and (5.51), where we do not use a superscript for the fluctuation operators as those will be the only ones under consideration, we found the steady-state amplitudes

$$\alpha_\pm^{(0)} = \frac{E_\pm}{i\Delta_0 \mp i\frac{\theta}{\tau} + \frac{\kappa}{2}} \tag{5.64}$$

and the only non-vanishing correlation functions of the field fluctuations were given by

$$\left\langle \delta a_\pm(t)\delta a_\pm^\dagger(t')\right\rangle = \exp\left[-i\Delta_\pm(t-t')\right]\exp\left(-\frac{\kappa}{2}|t-t'|\right) \tag{5.65}$$

which will be important for the correlations of the force fluctuations. The cross-correlations do not contribute, since in section 4.5.1 we applied the assumption of non-correlated pump lasers.

Before going into detail, we would like to mention another general observation. According to the assumption (5.63), the steady-state field operators can be written as small fluctuations $\delta a_\pm$ around a steady-state value $\alpha_\pm = \langle a_\pm\rangle$. Both the mean of these fluctuations $\langle\delta a_\pm\rangle$ and the expectation value of the corresponding photon number $\langle\delta a_\pm^\dagger\delta a_\pm\rangle$ are equal to zero, since in (4.126) we assumed a zero-temperature

field and no laser noise. This implies that the noise contributions vanish whenever one considers the steady-state expectation value of any normally ordered product of field operators, such as the optomechanical force F. Explicitly, one then only has to replace the field operators by their respective steady-state values to obtain the expectation value of the normally ordered operator under consideration, i.e. $a_\pm \to \alpha_\pm$.

If one now applies the ansatz (5.63) to the force operator of zeroth order (5.60), it also exhibits small fluctuations around a steady-state value

$$F^{(0)} = \langle F^{(0)} \rangle + \delta F \tag{5.66}$$

where the steady-state expectation value is given by

$$\langle F^{(0)} \rangle = \frac{4\hbar\omega}{L} \operatorname{Re}\left[\big(r^2 + irt\big) \alpha_+^{(0)^*} \alpha_-^{(0)} \right] \tag{5.67}$$

according to the the simple replacement for a normally ordered product of field operators. The force fluctuation operator is found to be

$$\delta F = \frac{4\hbar\omega}{L} \operatorname{Re}\left[\big(r^2 + irt\big) \left(\alpha_+^{(0)^*} \delta a_- + \alpha_-^{(0)} \delta a_+^\dagger \right) \right] \tag{5.68}$$

where we neglected 2-fold products of the field fluctuations as those represent higher-order corrections.

Expectation value of force in steady state

As explained in section 4.5.1, the pumping amplitudes in the $\pm$ basis are defined by

$$E_\pm = \frac{1}{\sqrt{2}} \left(E_R e^{ik\xi} \pm E_L e^{-ik\xi} \right) \tag{5.69}$$

and the simultaneous driving of the clockwise and counterclockwise travelling modes has the form

$$E_R = E_R^0 e^{i\varphi_R}, \qquad E_L = E_L^0 e^{-i\varphi_L} \tag{5.70}$$

respectively, where the pumping amplitude $E_{R/L}^0$ depends on the power $P_{R/L}$ of the external pumping laser via $E_{R/L}^0 = (\kappa P_{R/L}/\hbar\omega_p)^{1/2}$. Under these circumstances, we saw that

$$E_+^* E_- = \frac{1}{2} \left[(E_R^0)^2 - (E_L^0)^2 + 2i E_R^0 E_L^0 \sin(2k\xi + \phi) \right] \tag{5.71}$$

where we introduced the phase difference of the pump lasers, $\phi = \varphi_R + \varphi_L$. Also recall from section 4.5.1, that $\phi = 0\,(\pi)$ corresponds to mainly pumping the $+\,(-)$ mode and $\phi = \pi/2$ roughly excited both modes equally, if using comparable pump amplitudes.

Combining equations (5.67), (5.64) and (5.71), we get the zeroth-order force

$$\langle F^{(0)} \rangle = F_{\mathrm{rp}} + F_{\mathrm{dip}} \tag{5.72}$$

the components of which are the radiation pressure

$$F_{\mathrm{rp}} = \frac{2\hbar\omega}{L} \cdot \frac{r^2 A + rtB}{A^2 + B^2} \left[(E_R^0)^2 - (E_L^0)^2 \right] \tag{5.73}$$

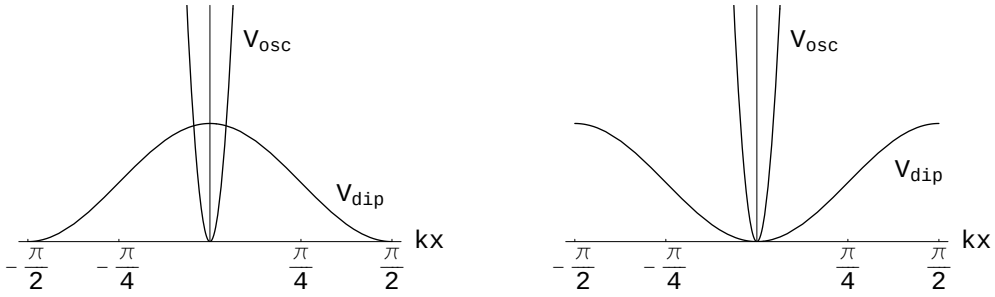

Figure 5.2: Schematic plots of the dipole potential V_{dip} and the harmonic confinement of the PRM. The left (right) panel shows the case where the PRM sits at a maximum (minimum) of the dipole potential. The narrow mirror potential results in very small PRM displacements, i.e. $k\xi \ll 1$.

and the dipole force

$$F_{\mathrm{dip}} = \frac{4\hbar\omega}{L} \cdot \frac{r^2 B - rtA}{A^2 + B^2} E_R^0 E_L^0 \sin(2k\xi + \phi) \tag{5.74}$$

where

$$A = \Delta_0^2 - \frac{\theta^2}{\tau^2} + \frac{\kappa^2}{4}, \qquad B = \frac{\kappa\theta}{\tau} \tag{5.75}$$

We keep r and t in the expressions of F_{rp} and F_{dip}, but bear in mind that these actually depend on the reflection parameter θ as well, such that $r^2 = \sin^2\theta$ and $2rt = \sin 2\theta$.

As mentioned in section 4.5.1, we will mainly focus on amplitude-symmetric pumping, i.e. $E_R^0 = E_L^0 = E_0$, whereby the radiation pressure due to photon reflection at the PRM vanishes. Therefore, we will first analyze the dipole force—also introducing some notation—and then come back to the effect of the constant radiation pressure (constant with respect to ξ).

In the following we consider the cases $\phi = 0, \pi$, which implies that the PRM sits at the extreme points of the dipole potential defined by $F_{\mathrm{dip}} = -\partial V_{\mathrm{dip}}/\partial\xi$. The dipole potential is thus given by

$$V_{\mathrm{dip}} = \pm\frac{2c\hbar}{L} \cdot \frac{r^2 B - rtA}{A^2 + B^2} E_R^0 E_L^0 \cos(2k\xi) \tag{5.76}$$

where the upper (lower) sign corresponds to $\phi = 0\,(\pi)$. Figure 5.2 schematically shows the dipole potential and the confining harmonic potential of the mechanical oscillator and illustrates both possible cases, namely, that the PRM sits at a minimum/maximum of the dipole potential. Note the very narrow harmonic potential, which reflects the fact that the mirror displacement is much smaller than the wavelength of the cavity fields, i.e. $k\xi \ll 1$, as shown in section 3.1.1. We can therefore linearize F_{dip} in ξ or, equivalently, replace the cosine in (5.76) by $-(2k\xi)^2/2$, where we dropped the constant "1", since a potential is only defined up to a constant offset.

One then obtains

$$F_{\text{dip}} = K(\Delta_0, \theta) \cdot k\xi \tag{5.77}$$

$$V_{\text{dip}} = -\frac{1}{2} K(\Delta_0, \theta) \cdot k\xi^2 \tag{5.78}$$

where

$$K(\Delta_0, \theta) = \pm \frac{8\hbar\omega}{L} \cdot \frac{r^2 \frac{\kappa\theta}{\tau} - rt\left(\Delta_0^2 - \frac{\theta^2}{\tau^2} + \frac{\kappa^2}{4}\right)}{\left(\frac{\kappa\theta}{\tau}\right)^2 + \left(\Delta_0^2 - \frac{\theta^2}{\tau^2} + \frac{\kappa^2}{4}\right)^2} \cdot E_R^0 E_L^0 \tag{5.79}$$

and the upper (lower) sign corresponds to $\phi = 0\,(\pi)$. Around the extreme points of the dipole potential, F_{dip} can thus be described as a harmonic potential whose curvature is determined by the quantity kK. Equivalently, kK plays the role of an optical spring constant, which depends on the cavity detuning Δ_0 and the PRM reflectivity θ. The function $K(\Delta_0, \theta)$ has the dimension of a force as it is the spring constant corresponding to the dimensionless PRM displacement $k\xi$ and when plotting it, we therefore normalize it by the magnitude of the force exerted on the PRM by one photon reflection per round trip, i.e. $F_{1\text{ph}} = 2\hbar\omega/L = 2\hbar k/\tau$, which becomes $F_{1\text{ph}} \sim 10^{-17}\,\text{N}$ when applying the reference values stated in section 2.

We expect significant values of $K(\Delta_0, \theta)$ if the positive denominator in (5.79) becomes small. We consider the denominator normalized by $1/\kappa^4$

$$\tilde{D} = \left(\tilde{\Delta}_0^2 - \frac{\theta^2}{T^2} + \frac{1}{4}\right)^2 + \left(\frac{\theta}{T}\right)^2 \tag{5.80}$$

where $\tilde{\Delta}_0 = \Delta_0/\kappa$ and we used the relation $\kappa\tau = T$ found in (4.71), where T is the transmittivity of the incoupling mirror (CM). The minima of $\tilde{D}$ are given by

$$\frac{\partial \tilde{D}}{\partial \tilde{\Delta}_0} = 4\left(\tilde{\Delta}_0^2 - \frac{\theta^2}{T^2} + \frac{1}{4}\right) \stackrel{!}{=} 0 \tag{5.81}$$

$$\Longrightarrow \quad \tilde{\Delta}_0^2 = \frac{\theta^2}{T^2} - \frac{1}{4} \tag{5.82}$$

In section 4.5.2 we discovered that the $\pm$modes are well separated if $\theta \gg T/2$, which is already fulfilled even for very low PRM reflectivities, since we assume $T \sim 10^{-3}$. In that regime, we can neglect the $-1/4$ in (5.82) and we thus expect to find large values of K if

$$\Delta_0 \approx \pm \frac{\theta}{\tau} \tag{5.83}$$

Observe that in these cases $\Delta_\pm \approx 0$, respectively, which implies that non-vanishing forces may only be expected around the eingenfrequencies $\omega_\pm$.

The plots of K over different ranges of Δ_0 and θ are shown in figure 5.3 and 5.4, where we applied amplitude-symmetric pumping to all of them, i.e. $E_R^0 = E_L^0 = E_0$. Note that in this case K is proportional to E_0^2 and different pumping intensities would thus only scale the optical spring constant, but would not affect its dependence on Δ_0 and θ. In plot (a) of figure 5.3 we find, indeed, that non-vanishing values

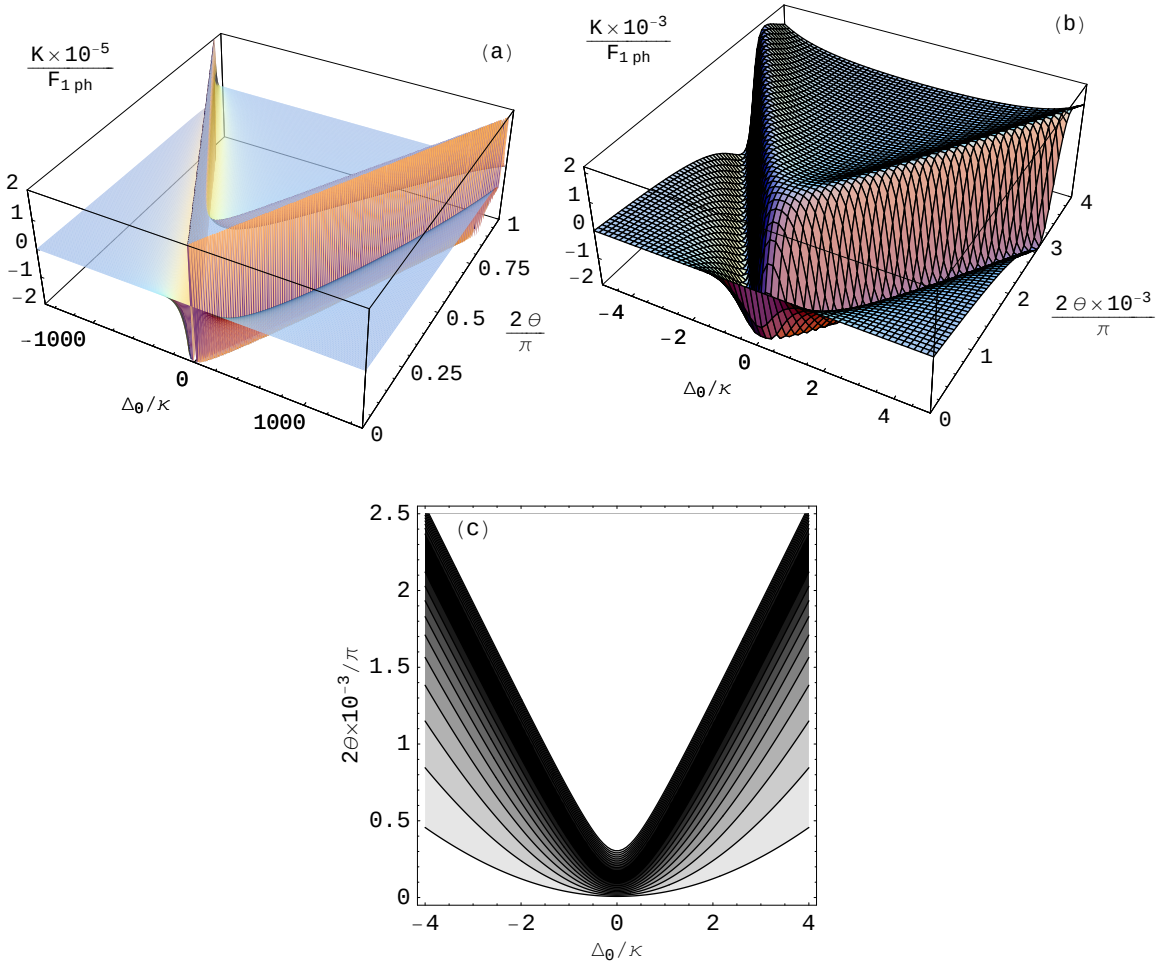

Figure 5.3: Plots of the normalized spring constant $K/F_{1\mathrm{ph}}$. Panel (a) shows K over the whole range of Δ_0 and θ, where the vertical range was chosen to be rather small in order to illustrate the characteristic V-shape. Panel (b) corresponds to very small θ to show the tip of the "V" in detail. The shaded areas of the contour plot (c) correspond to $K < 0$, i.e. the optomechanical force is restoring, and the darker the shading the larger the magnitude of K. In (c) we chose the range of parameters similar to (b). For all plots we used $\phi = 0$, $E_R^0 = E_L^0 = \kappa$ and $T = 10^{-3}$.

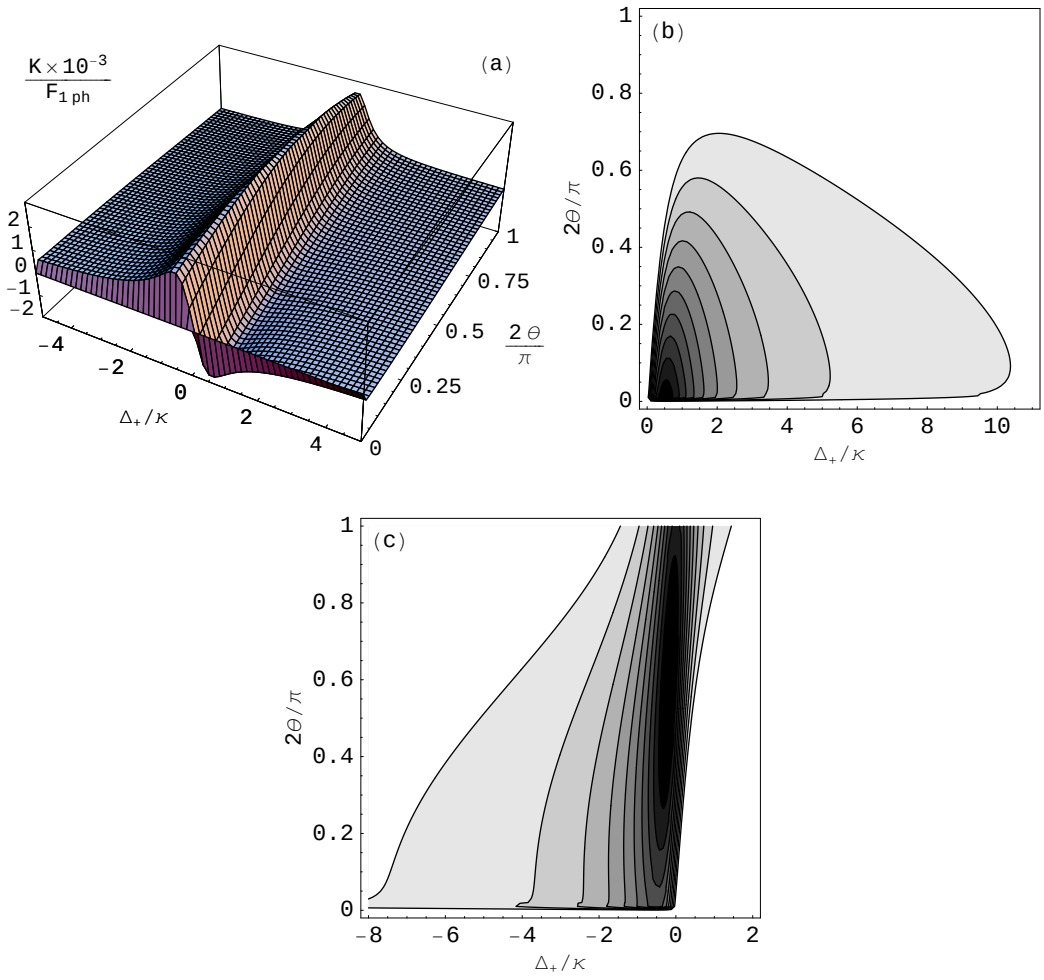

Figure 5.4: Plots of the normalized spring constant $K/F_{1\mathrm{ph}}$. Panel (a) shows $K(\Delta_+, \theta)$, i.e. the values of K around the resonance frequency ω_+, which corresponds to the right branch of plot (a) in figure 5.3. The contour plots reveal parameter domains where $K < 0$. The panels (a) and (b) correspond to $\phi = 0$, whereas we used $\phi = \pi$ to obtain (c). Moreover, $E_R^0 = E_L^0 = \kappa$ and $T = 10^{-3}$ for all plots.

of K are concentrated around the eigenfrequencies $\omega_\pm = \omega_n^{(0)} \mp \theta/\tau$ and the plots therefore show a characteristic V-shape. Note that the right (left) branch follows the eigenfrequency ω_+ (ω_-). Moreover, K can be both negative and positive depending on the particular values of Δ_0 and θ. This means that the dipole force can amplify and diminish the harmonic potential of the micro-mechanical oscillator, respectively, which is illustrated in figure 5.2. As one is, however, interested in increasing the oscillation frequencies of mechanical oscillators in order to approach the quantum regime thereof, the areas of a negative spring constant seem more interesting and are therefore shown in the contour plots of figure 5.3 and 5.4. The optomechanical force is then restoring and has thus the effect of a harmonic trap.

For the sake of a better visibility, figure 5.4 presents the plot of $K(\Delta_+, \theta)$, i.e. the variation of K with the detuning from the eigenfrequency ω_+ defined by $\Delta_+ = \omega_+ - \omega_p = \Delta_0 - \theta/\tau$. The contour plot (b) in figure 5.4 reveals that for $\phi = 0$ one finds trapping only for rather small PRM reflectivities up to $\theta \approx \pi/4$ and red-detuned pump laser frequencies, i.e. $\Delta_+ > 0$. Interestingly, we find an equivalent behaviour around the cavity resonance ω_- even though $\phi = 0$, in which case mainly the + mode is pumped, as we discovered in section 4.5.1. One could therefore tend to expect no significant forces around ω_- if $\phi = 0$. However, as we have seen in section 4.5.2, despite the fact that $\phi = 0$, small PRM displacements also lead to an excitation of the $-$ mode, which is the reason for the non-vanishing forces in the vicinity of ω_-. In particular, we find K to be invariant under the replacement $\Delta_+ \to -\Delta_-$, where $\Delta_- = \omega_- - \omega_p = \Delta_0 + \theta/\tau$ is the detuning from the eigenfrequency ω_-. This shows the equivalence of the forces around $\omega_\pm$, respectively, apart from a reflection due to the minus sign appearing in the replacement. That is, areas of negative K are also found for $\Delta_- < 0$ and $\theta \lesssim \pi/4$ if $\phi = 0$. This mirror-symmetry of $K(\Delta_0, \theta)$ with respect to $\Delta_0 = 0$ can also be seen in the plots (a)-(c) of figure 5.3.

The effect of $\phi = \pi$—as already indicated by (5.79)—is simply a change of the sign of K. That is, areas of a repelling dipole force now correspond to a restoring force and vice versa. This fact is shown in the contour plot (c) in figure 5.4. As opposed to the case of $\phi = 0$, one now finds the principle possibility of trapping over almost the whole range of θ and for small $\Delta_+ \lesssim 0$.

As discovered above, if $\phi = 0, \pi$, the dipole force generates an additional harmonic potential to the the already present one of the micro-mechanical mirror. One can therefore define an effective spring constant, k_{eff}, which is simply the sum of the two respective ones, and applying the general relation $k_{\text{eff}} = m\Omega_{\text{eff}}^2$, we find the effective frequency

$$\Omega_{\text{eff}}^2 = \Omega_m^2 + \Omega_{\text{opt}}^2 = \Omega_m^2 - \frac{kK(\Delta_0, \theta)}{m} \tag{5.84}$$

From the plots of K in figure 5.3, where we used $E_0 = \kappa$, we extract typical values of $\lesssim 10^{-3} F_{1\text{ph}}\,\text{N} \sim 10^{-20}\,\text{N}$. As K is proportional to E_0^2 we can therefore generally write $K \lesssim 10^{-20} E_0^2/\kappa^2\,\text{N}$ and applying the typical oscillator values presented in section 2, this leads to an optically induced mechanical frequency $\Omega_{\text{opt}} \lesssim 10^{-1} E_0/\kappa\,\text{s}^{-1}$. Compared to $\Omega_m \sim 10^5\,\text{s}^{-1}$ we see that the optical "trap" is rather inefficient in increasing the oscillation frequency of the PRM even if one uses strong pumping lasers with $E_0 \approx 10^3\kappa$ ($P_0 \approx \mu$W).

We now return to the case of asymmetric pumping with respect to the pump amplitudes, i.e. $E_R^0 \neq E_L^0$. In that case, we found the component F_{rp} of the total optomechanical force given by (5.73), which is independent of ξ and proportional to the intensity difference of the pump lasers. The mean total force in zeroth order acting on the mirror is then

$$\begin{aligned} \left\langle F_{\mathrm{tot}}^{(0)}(\xi)\right\rangle &= F_{\mathrm{rp}} + F_{\mathrm{dip}}(\xi) + F_m(\xi) && (5.85)\\ &= F_{\mathrm{rp}} - m\Omega_{\mathrm{eff}}^2\xi && (5.86)\end{aligned}$$

which of course only holds for $\phi = 0, \pi$. The PRM will then be dragged to a position ξ_0 where the mean total force vanishes

$$\xi_0 = \frac{F_{\mathrm{rp}}}{m\Omega_{\mathrm{eff}}^2} \approx \frac{F_{\mathrm{rp}}}{m\Omega_m^2} \tag{5.87}$$

where we applied that the optical spring constant is negligible in comparison with the mechanical one. One finally finds

$$\xi_0 = \frac{2\hbar\omega}{m\Omega_m^2 L}\, \frac{r^2\left(\Delta_0^2 - \frac{\theta^2}{\tau^2} + \frac{\kappa^2}{4}\right) + rt\left(\frac{\kappa\theta}{\tau}\right)}{\left(\Delta_0^2 - \frac{\theta^2}{\tau^2} + \frac{\kappa^2}{4}\right)^2 + \left(\frac{\kappa\theta}{\tau}\right)^2} \left[(E_R^0)^2 - (E_L^0)^2\right] \tag{5.88}$$

Using the typical values stated in section 2, we observe that the PRM may even be displaced by several wavelengths if the difference of the pump intensities is large, e.g. if $(E_R^0)^2 - (E_L^0)^2 \sim \kappa^2$. This would of course violate one of our main approximations $k\xi \ll 1$, which is why we rather focus on a symmetric pumping scheme.

Fluctuations of force and diffusion

As we have seen, the presence of an electromagnetic field inside the cavity induces an optomechanical force acting on the PRM. According to section 3.1.2 and 4.5, the coupling of the cavity fields to the "outside world" leads to fluctuations of the fields and, consequently, the PRM is subject to force fluctuations given by (5.68). By construction, $\langle \delta a_\pm \rangle = 0$ immediately implies $\langle \delta F \rangle = 0$, that is, the total force indeed consists of small fluctuations around the steady-state value discussed above. In the following, we investigate the correlation function of these force fluctuations and can thereby derive a momentum diffusion coefficient D_p, which generally leads to heating of the PRM and thus counteracts a possible friction coefficient.

Exploiting $\langle \delta F \rangle = 0$, we deduce from (5.66) that

$$\left\langle F^{(0)}(t)F^{(0)}(t')\right\rangle - \left\langle F^{(0)}(t)\right\rangle\left\langle F^{(0)}(t')\right\rangle = \left\langle \delta F(t)\delta F(t')\right\rangle \tag{5.89}$$

and using the results for the correlation of the field fluctuations (4.145) one finds the correlation function of the force fluctuations to be

$$\begin{aligned} C_{\delta F}(t,t') &:= \left\langle \delta F(t)\delta F(t')\right\rangle && (5.90)\\ &= r^2F_{1\mathrm{ph}}^2\Big(|\alpha_+|^2\left\langle \delta a_-(t)\delta a_-(t')\right\rangle + |\alpha_-|^2\left\langle \delta a_+(t)\delta a_+(t')\right\rangle\Big) && (5.91)\\ &= r^2F_{1\mathrm{ph}}^2 e^{-\frac{\kappa}{2}|t-t'|}e^{-i\Delta_0(t-t')}\left(|\alpha_+|^2e^{-i\frac{\theta}{\tau}(t-t')} + |\alpha_-|^2e^{i\frac{\theta}{\tau}(t-t')}\right) && (5.92)\\ &= C_{\delta F}(t-t') && (5.93)\end{aligned}$$

which shows that we are still dealing with a stationary process, i.e. $C_{\delta F}$ only depends on the time difference $t - t'$. However, the force fluctuations are not δ-correlated and therefore represent coloured noise, as we have also seen for the field noise. Due to the exponential decay, the typical correlation time is $\tau_{\mathrm{corr}} \approx \kappa^{-1}$, which is short compared to the time scale of interest in the bad cavity limit $\Omega_m \ll \kappa$. Thus, on the time scale of the PRM dynamics, Ω_m^{-1}, we can approximate the correlation function to be δ-correlated and we can then identify

$$\mathrm{Re}\left\{C_{\delta F}(t-t')\right\} = 2D_p\,\delta(t-t') \tag{5.94}$$

where D_p is the momentum diffusion coefficient. Altogether we have[1]

$$\begin{aligned} D_p &= \mathrm{Re}\int_0^\infty dt\; C_{\delta F}(t) && (5.99)\\ &= r^2F_{1\mathrm{ph}}^2\,\mathrm{Re}\left\{\frac{|\alpha_+|^2}{\frac{\kappa}{2}+i\Delta_-}+\frac{|\alpha_-|^2}{\frac{\kappa}{2}+i\Delta_+}\right\} && (5.100)\\ &= \frac{1}{2}\kappa r^2F_{1\mathrm{ph}}^2\left[\frac{|\alpha_+|^2}{\frac{\kappa^2}{4}+\Delta_-^2}+\frac{|\alpha_-|^2}{\frac{\kappa^2}{4}+\Delta_+^2}\right] && (5.101)\\ &= D_p^+ + D_p^- && (5.102)\end{aligned}$$

That is, the total diffusion coefficient caused by the force fluctuations is the sum of the diffusion coefficients resulting from field fluctuations of the + and − mode, respectively. Inserting the steady-state values (5.64) and the corresponding expressions of the pump parameters (4.128) yields the interesting result

$$D_p = \frac{\kappa r^2F_{1\mathrm{ph}}^2}{2\left(\frac{\kappa^2}{4}+\Delta_+^2\right)\left(\frac{\kappa^2}{4}+\Delta_-^2\right)}\left[(E_R^0)^2+(E_L^0)^2\right] \tag{5.103}$$

where the parts of $|E_\pm|^2$ depending on ξ and ϕ have cancelled each other and D_p does therefore neither depend on the PRM position nor on the phase difference of the pump lasers. This feature is also found for an atom in a standing wave [35]. Also observe the proportionality to the pump intensity E_0^2 when pumping symmetrically, i.e. $E_R^0 = E_L^0 = E_0$. The dependence of the momentum diffusion coefficient on the PRM reflectivity and the detuning from the cavity resonances is shown in figure 5.5. Again, one finds non-vanishing values only in the vicinity of the cavity

[1] One can also generally derive relation (5.99) without assuming a δ-correlation, but with the assumptions of a monochromatic field, negligible velocity and quasi-stationary conditions [35]. In that case, one finds

$$\begin{aligned} D_p &= \frac{1}{2}\frac{d}{dt}\big(\langle p\cdot p\rangle - \langle p\rangle\langle p\rangle\big) && (5.95)\\ &= \mathrm{Re}\left[\langle F\cdot p\rangle - \langle F\rangle\langle p\rangle\right] && (5.96)\\ &= \mathrm{Re}\int_{-\infty}^0 dt\left[\langle F(0)F(t)\rangle - \langle F(0)\rangle\langle F(t)\rangle\right] && (5.97)\\ &= \mathrm{Re}\int_0^\infty dt\; C_{\delta F}(t) && (5.98)\end{aligned}$$

where one uses $F = dp/dt$ and stationarity of the correlation. The time zero is arbitrary and the time minus infinity is an exaggeration since the correlation time of the force is of the order of κ^{-1}.

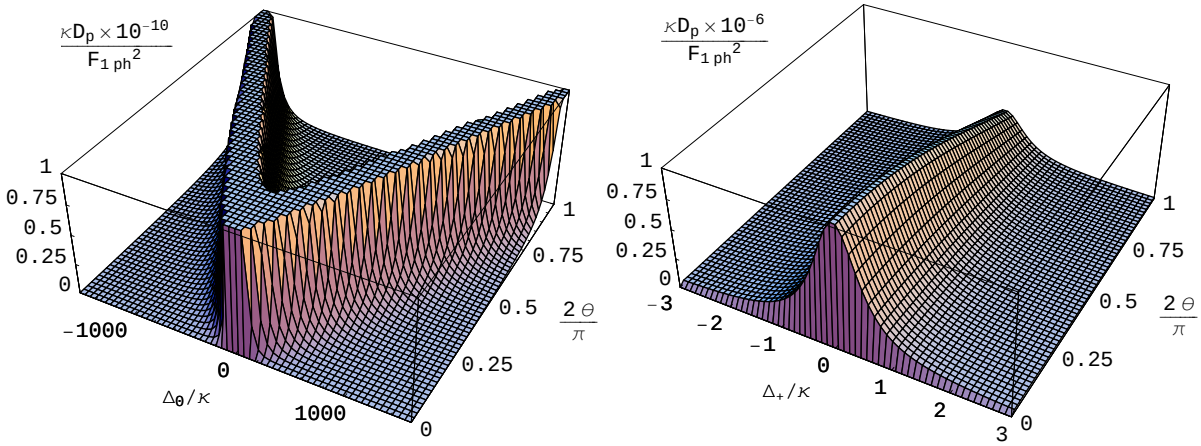

Figure 5.5: Dependence of momentum diffusion coefficient D_p normalized by $F_{1\mathrm{ph}}^2/\kappa$ on θ and Δ_0 (left panel) or Δ_+ (right panel). For these plots $E_R^0 = E_L^0 = \kappa$ and $T = 10^{-3}$ was used.

eigenfrequencies $\omega_\pm$ leading to the familiar V-shape. Actually, D_p is maximal along the cavity resonances, which is again due to the lorentzian response function of a damped harmonic oscillator. This is, of course, not true for $\theta \to 0$ since a vanishing PRM reflectivity lets D_p decay to zero, as one would expect.

5.2.2 Friction force – 1st order in v

In the present section we analyze the friction coefficient $F^{(1)}$ defined in (5.61), which is responsible for a friction force experienced by the PRM if it is moving within the cavity fields. Domokos [34] argues that the non-adiabatic dynamics of the internal variables—in our case these are the field operators—which is the origin of the friction force, does not substantially depend on the noise. We will therefore solve equations (5.52) and (5.53) for their steady-state solutions $\alpha_\pm^{(1)} = \langle a_\pm^{(1)} \rangle$, which are given by

$$\alpha_+^{(1)} = \frac{\partial_\xi \alpha_+^{(0)}}{\frac{\kappa}{2} + i\Delta_+} \tag{5.104}$$

$$\alpha_-^{(1)} = \frac{\partial_\xi \alpha_-^{(0)}}{\frac{\kappa}{2} + i\Delta_-} \tag{5.105}$$

Another argument is that the friction force as well as the conservative part of the force only contains normally ordered products of the field operators. As before, due to their correlations, any first-order fluctuations would not contribute when investigating the steady-state expectation value of the friction force. By taking a look at the pumping terms $E_\pm$ in (5.69) we see that

$$\partial_\xi \alpha_\pm^{(0)} \propto \partial_\xi E_\pm = ikE_\mp \tag{5.106}$$

which leaves us with the first-order steady-state solutions

$$\alpha_+^{(1)} = \frac{ikE_-}{\left(\frac{\kappa}{2} + i\Delta_+\right)^2} \tag{5.107}$$

$$\alpha_-^{(1)} = \frac{ikE_+}{\left(\frac{\kappa}{2} + i\Delta_-\right)^2} \tag{5.108}$$

Inserting this and all relevant expressions into the steady-state expectation of (5.61), we finally obtain the quite lengthy expression

$$\langle F^{(1)}\rangle = -\frac{4c\hbar k^2}{c_+c_-L}\left\{\frac{1}{2}(A_+ + A_-)\left[(E_R^0)^2 + (E_L^0)^2\right] - (A_+ - A_-)E_R^0E_L^0\cos(2k\xi + \phi)\right\} \tag{5.109}$$

where we use the abbreviations

$$A_\pm := \frac{r^2a_\pm \mp rtb_\pm}{c_\pm} \tag{5.110}$$

and

$$a_\pm := \Delta_\mp\left(\frac{\kappa^2}{4} - \Delta_\pm^2\right) - \Delta_\pm\frac{\kappa^2}{2} \tag{5.111}$$

$$b_\pm := \frac{\kappa}{2}\left(\frac{\kappa^2}{4} - \Delta_\pm^2\right) + \kappa\Delta_\pm\Delta_\mp \tag{5.112}$$

$$c_\pm := \frac{\kappa^2}{4} + \Delta_\pm^2 \tag{5.113}$$

The cases $\phi = 0, \pi$ simply alter the sign of the second term of (5.109) and by linearizing the expression in $k\xi$ the cosine then becomes 1. That is, the friction coefficient, as well as the diffusion coefficient, does essentially not depend on the PRM displacement if $\phi = 0, \pi$. Moreover, we see that if one applies amplitude-symmetric pumping $E_R^0 = E_L^0 = E_0$, the friction coefficient is also proportional to the pump intensity E_0^2.

Again, we look for ranges of the parameters Δ_0 and θ where the friction coefficient $\langle F^{(1)}\rangle$ is negative, since then the PRM looses energy due to friction resulting in the cooling of the PRM motion. If $\langle F^{(1)}\rangle > 0$, the PRM gains energy from the cavity modes, which then results in the heating of the PRM. However, in order to observe quantum behaviour of such micro-mechanical oscillators, one is aiming at further decreasing the oscillator's temperature. Figures 5.6 and 5.7 present plots of $\langle F^{(1)}\rangle$ for $\phi = 0$ and $\phi = \pi$, respectively, and also show the areas where $\langle F^{(1)}\rangle < 0$. We observe that the friction is most effective if one selects ϕ to drive the $+\,(-)$ mode, however, with a pump frequency near the resonance frequency ω_- (ω_+), whereas driving one mode at its own eigenfrequency implies a relatively ineffective friction or even heating. In detail, we see from panel (a) in figure 5.6 that driving the $+$ mode around its eigenfrequency ω_+ introduces heating for almost any value of Δ_+ and θ. If one, however, drives the $+$ mode ($\phi = 0$) slightly above the eigenfrequency ω_-, one finds the most effective dissipation in that case, but only for small θ. The

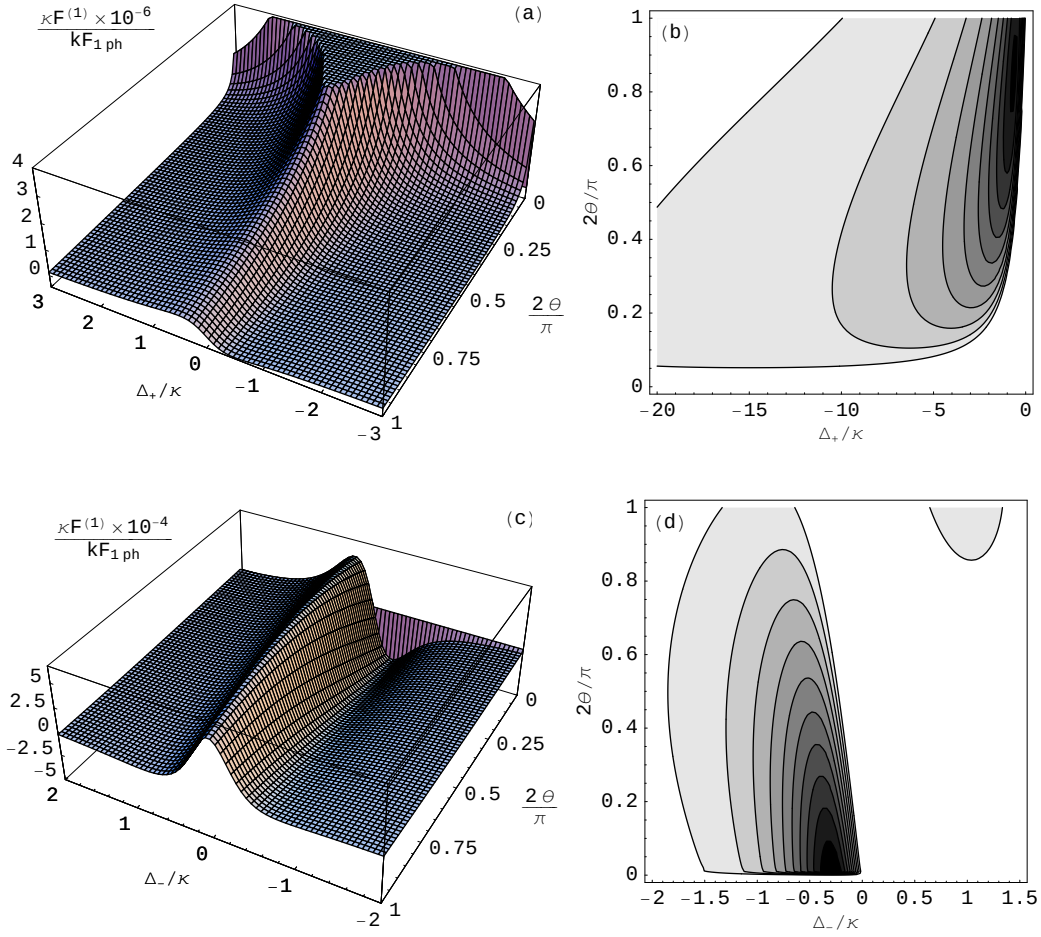

Figure 5.6: Plots of friction coefficient $\langle F^{(1)} \rangle$ normalized by $kF_{1\mathrm{ph}}/\kappa$ for $\phi = 0$, i.e. mainly driving the + mode. The panels (a) and (b) show the plots near the eigenfrequency ω_+ and the panels (c) and (d) correspond to detunings around ω_-. The contour plots correspond to $\langle F^{(1)} \rangle < 0$, i.e. the kinetic energy of the PRM is dissipated into the cavity modes. Again, $E_R^0 = E_L^0 = \kappa$ and $T = 10^{-3}$ was used for all plots. Note, that we turned the 3-dimensional plots around for a better visibility.

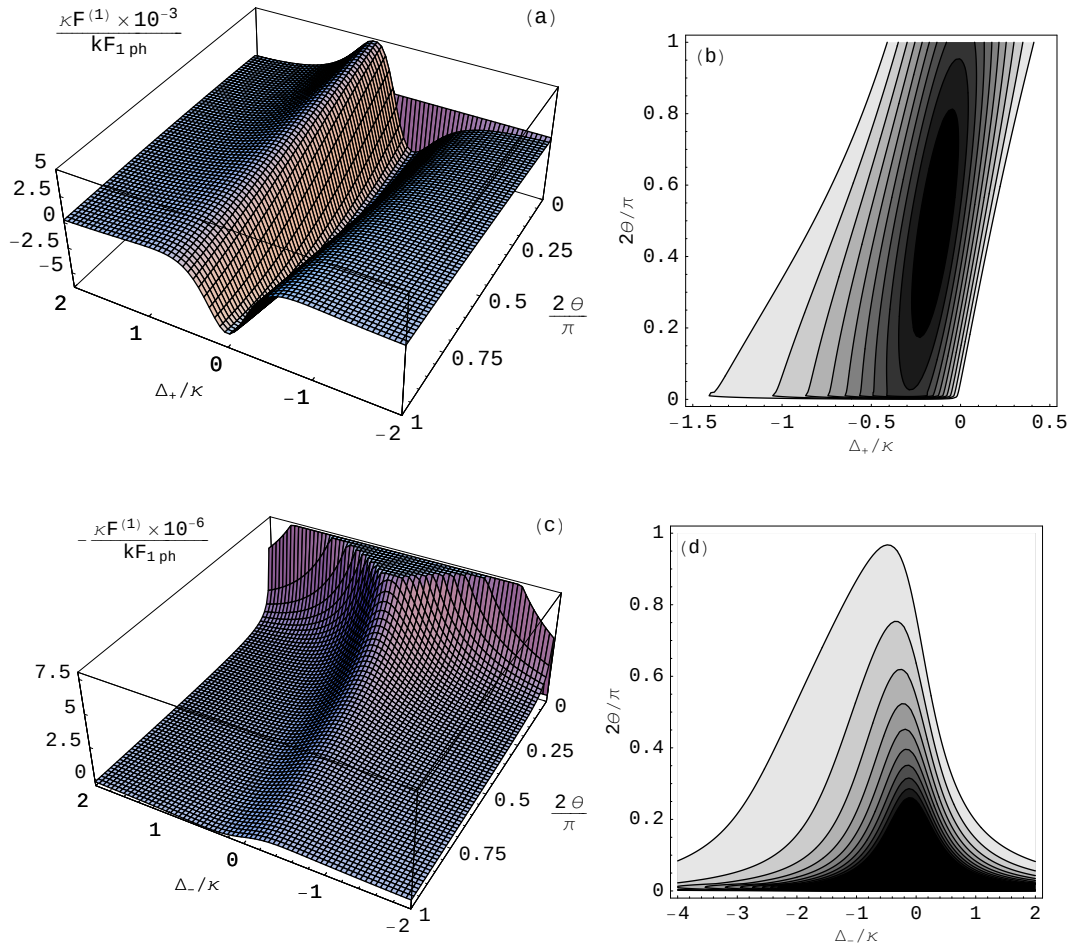

Figure 5.7: Plots of friction coefficient $\langle F^{(1)} \rangle$ normalized by $kF_{1\mathrm{ph}}/\kappa$ for $\phi = \pi$, i.e. mainly driving the $-$ mode. The panels (a) and (b) show the plots near the eigenfrequency ω_+ and the panels (c) and (d) correspond to detunings around ω_-. The contour plots correspond to $\langle F^{(1)} \rangle < 0$, i.e. the kinetic energy of the PRM is dissipated into the cavity modes. Again, $E_R^0 = E_L^0 = \kappa$ and $T = 10^{-3}$ was used for all plots. Note, that we turned the 3-dimensional plots around and that panel (c) actually shows $-\langle F^{(1)} \rangle$, for the sake of a better visibility.

largest magnitudes of the friction coefficient are found in panel (a) of figure 5.7 for $\phi = \pi$ and pumping frequencies slightly above ω_+. Moreover, we then observe that the dissipation does not only take place for small θ, but over the whole range of θ. Around frequencies ω_-, one also discovers negative values of $\langle F^{(1)} \rangle$, but the magnitudes are much smaller and almost completely vanish for large PRM reflectivities θ.

The reason for this particular behaviour could be that some of the few photons of the $+(-)$ mode driven near ω_- (ω_+) are reflected into the $-(+)$ mode, as these are coupled by the PRM. Thereby, some energy is transferred from the PRM to the photons, which then leak out of the cavity through the incoupling mirror.

5.2.3 Cooling and limit temperature

As we have discovered above, the PRM is subject to optomechanical forces which can be separated into a conservative part that produces an additional potential, force fluctuations that are responsible for momentum diffusion and a velocity-dependent force leading to dissipation for some ranges of the parameters Δ_0 and θ. The fluctuations and the friction force eventually determine the equilibrium temperature to which the PRM can be cooled. As we have shown in section 3.1.1, the mean energy of a harmonic oscillator in a thermal state at temperature T_0 in the high-temperature limit is equal to $k_B T_0$ and it consists to equal amounts of the mean potential energy and the mean kinetic energy of the oscillator. The latter is proportional to $\langle p^2 \rangle$ whose steady-state value is governed by the momentum diffusion and the friction coefficient and one can therefore estimate the oscillator's equilibrium temperature to be

$$k_B T_e = \frac{D_p^{\mathrm{tot}}}{2\beta^{\mathrm{tot}}} \tag{5.114}$$

where the total momentum diffusion coefficient is given by the sum of the oscillator's diffusion coefficient at initial temperature T_0 and the optically induced diffusion coefficient

$$D_p^{\mathrm{tot}} = D_p^m(T_0) + D_p(\Delta_0, \theta, E_0) \tag{5.115}$$

and similarly for the total friction coefficient

$$\beta^{\mathrm{tot}} = \beta_m - \left\langle F^{(1)}(\Delta_0, \theta, E_0) \right\rangle \tag{5.116}$$

Note, that one can simply obtain expression (5.114) from equation (1.1) of the introduction. Using our reference values $m \sim 10^{-11}\,\mathrm{kg}$, $\Omega_m \sim 10^5\,\mathrm{s}^{-1}$ and $Q_m \sim 10^6$ from section 2, we find an intrinsic friction coefficient

$$\beta_m = m\gamma_m = m\frac{\Omega_m}{Q_m} \sim 10^{-12}\,\mathrm{kg\,s}^{-1} \tag{5.117}$$

where γ_m is the oscillator's intrinsic dissipation rate, which is connected to the quality Q_m of the mechanical oscillator. The intrinsic diffusion coefficient for an oscillator at thermal equilibrium with its environment at temperature T_0 can be estimated using (5.114) without the optically induced terms and one obtains

$$D_p^m(T_0) = \frac{m\Omega_m k_B T_0}{Q_m} \sim 10^{-35}\frac{T_0}{\mathrm{K}}\,\mathrm{N^2 s} \tag{5.118}$$

In the following, we will assume a feasible initial temperature for such membranes of $T_0 \sim 10^{-1}\,\mathrm{K}$ [17]. From our analysis of the preceding sections we have the typical values

$$D_p(\Delta_0, \theta, E_0) \lesssim 10^{-47} \frac{E_0^2}{\kappa^2}\,\mathrm{N^2 s} \tag{5.119}$$

$$-\left\langle F^{(1)}(\Delta_0, \theta, E_0)\right\rangle \lesssim 10^{-19} \frac{E_0^2}{\kappa^2}\,\mathrm{kg\,s^{-1}} \tag{5.120}$$

and applying strong pumping $E_0 \sim 10^3\kappa$ as suggested by [17], we find the relations

$$D_p \lesssim 10^{-5} D_p^m(T_0) \tag{5.121}$$

$$-\left\langle F^{(1)}\right\rangle \lesssim 10^{-1}\beta_m \tag{5.122}$$

That is, the diffusion due to fluctuations of the optomechanical force is very small compared to the thermal diffusion at the initial temperature T_0, whereas the optically induced friction is almost comparable to the intrinsic one. According to (5.114), this should in principle give us the possibility of cooling the PRM. If one neglects the intrinsic diffusion and dissipation of the micro-mechanical oscillator[2], one can estimate the principle limit temperature of the cooling scheme under consideration. From the values given in (5.119) and (5.120) we deduce the limit temperature

$$T_{\mathrm{limit}} \sim 10^{-5}\,\mathrm{K} \tag{5.123}$$

For comparison, the famous Doppler (cooling) limit for atoms is given by $k_B T_D = \hbar\Gamma$, where Γ is the spontaneous decay rate of the atom. As explained in [34], the energy transfer channel for Doppler cooling is the atomic spontaneous decay, and equilibrium temperatures can be as low as the width of this channel. In our case, the energy transfer channel is the cavity decay, and the temperature should thus be limited by the cavity decay rate κ. Comparing (5.123) to $T = \hbar\kappa/k_B \sim 10^{-4}\,\mathrm{K}$ indeed roughly verifies this estimate.

Also note that throughout this thesis we apply only vacuum fluctuations from outside of the cavity. If one also allows for thermal fluctuations of the fields at temperature $T \neq 0$, the diffusion coefficient would be increased and the efficiency of the cooling process would thus be decreased.

However, due to the relative small changes of the diffusion and dissipation from the intrinsic values of the oscillator (cf. (5.121) and (5.122)), the temperature drop is not expected to be very large. Moreover, as the relative change of the diffusion coefficient is much smaller than the relative change of the friction coefficient—also known as "cold friction"—the latter one will essentially determine the dependence of the temperature change on the parameters Δ_0 and θ.

The plots of the relative temperature change for amplitude-symmetric pumping with $E_0 = 10^3\kappa$ are shown in figure 5.8 and 5.9 for $\phi = 0$ and $\phi = \pi$, respectively.

[2]This is of course not realistic as it requires the oscillator to be completely isolated from its environment or to be cooled to $T = 0$. Moreover, the quality of the oscillator Q_m would have to be increased by several orders of magnitude

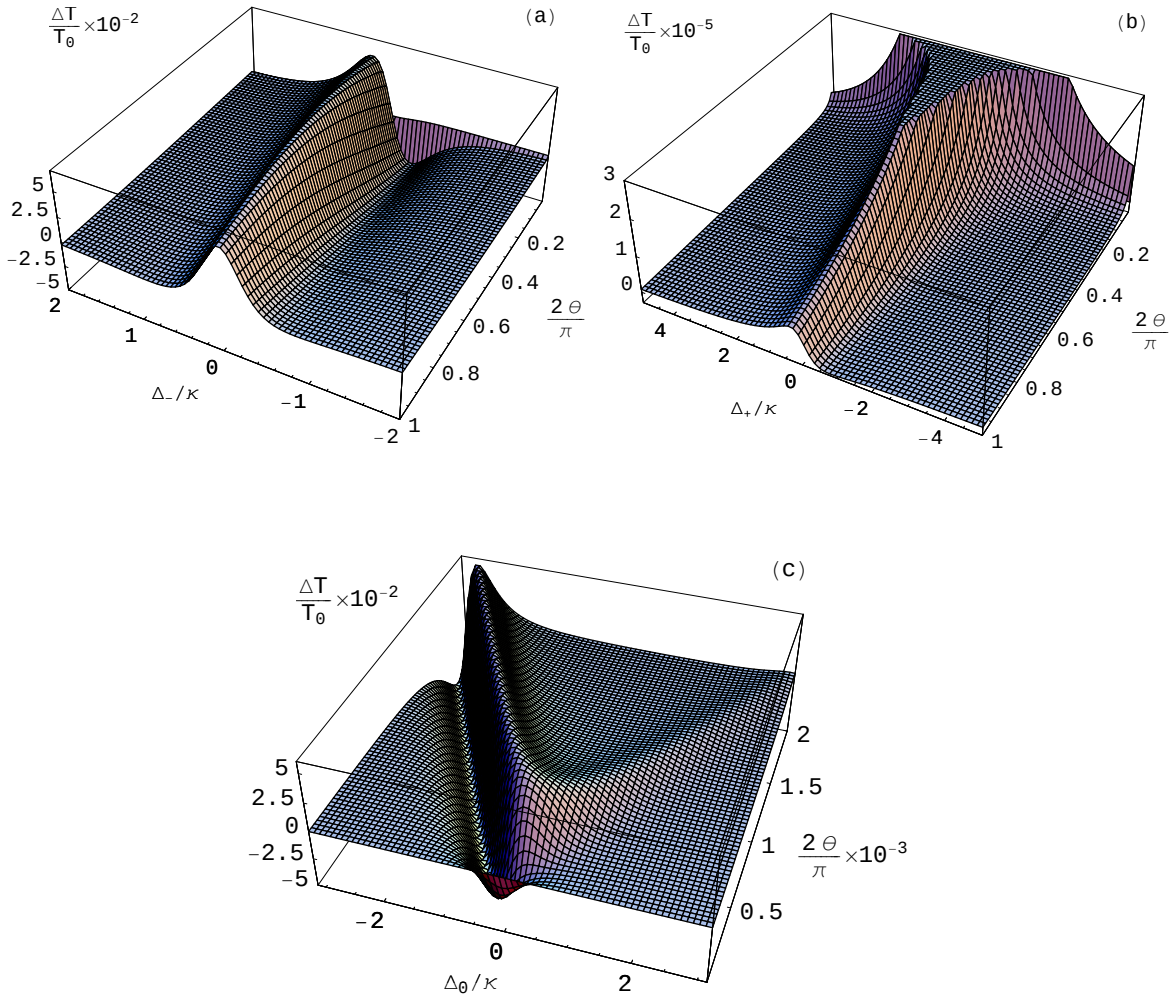

Figure 5.8: Plots of the relative temperature change for $\phi = 0$ starting from the initial temperature $T_0 = 10^{-1}\,\mathrm{K}$. Panel (a) and (b) show plots around the eigenfrequency ω_- and ω_+, respectively. Panel (c) shows the tip of the "V" in detail. For these plots $E_R^0 = E_L^0 = 10^3\kappa$ and $T = 10^{-3}$ was used.

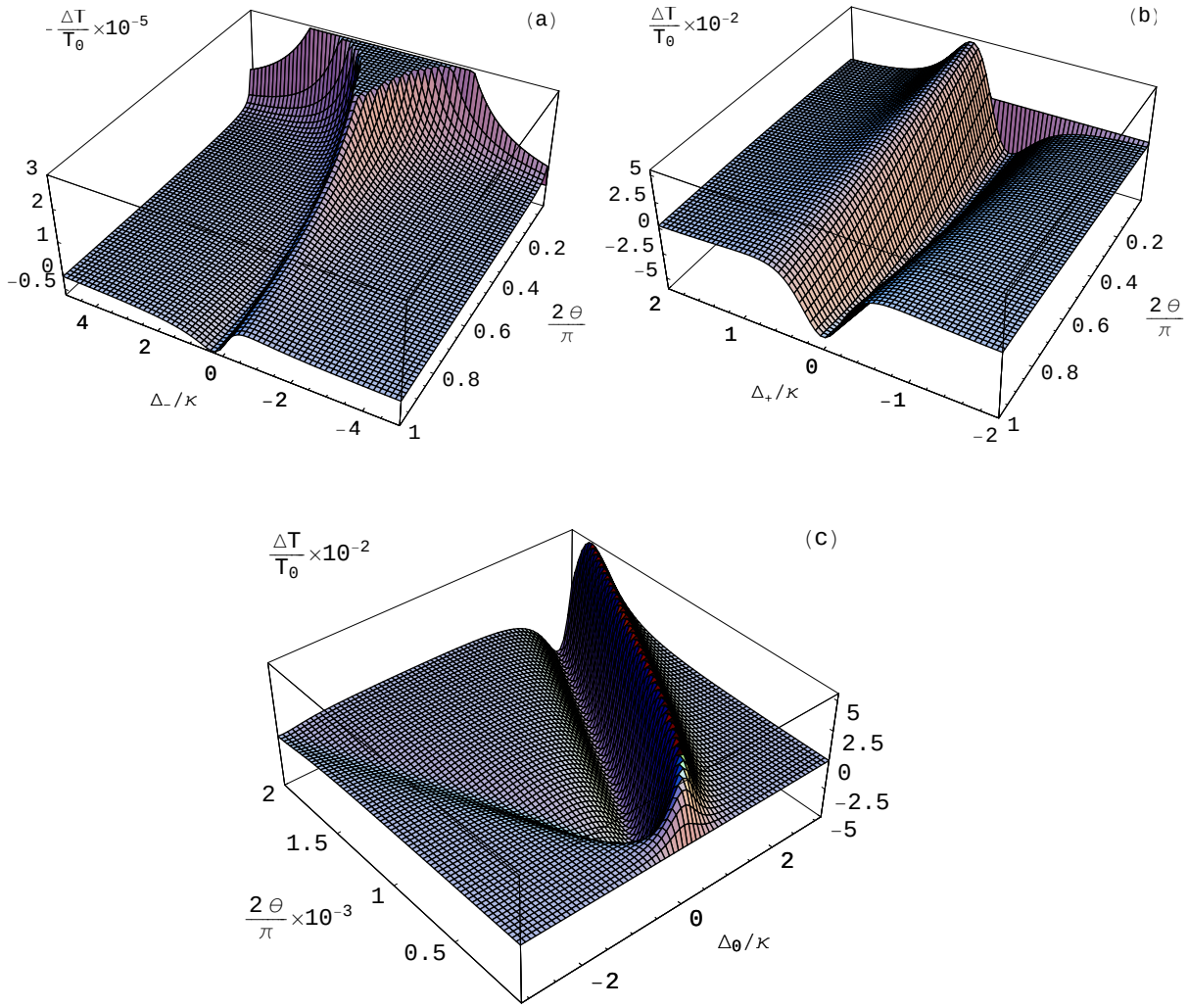

Figure 5.9: Plots of the relative temperature change for $\phi = \pi$ starting from the initial temperature $T_0 = 10^{-1}\,\mathrm{K}$. Panel (a) and (b) show plots around the eigenfrequency ω_- and ω_+, respectively. Note that for a better view, panel (a) depicts the negative temperature change. Panel (c) shows the tip of the "V" in detail. For these plots $E_R^0 = E_L^0 = 10^3\kappa$ and $T = 10^{-3}$ was used.

Indeed, the plots are qualitatively almost equivalent to the behaviour of the friction coefficients shown in figure 5.6 and 5.7. We therefore do not present any contour plots of the relative temperature change, as the areas of cooling basically coincide with the areas where one finds a negative friction coefficient $\langle F^{(1)} \rangle$. Hence, also the comments on the features of the friction force can be applied here. That is, the cooling is most effective when choosing the pump laser phase difference to excite mainly the $+\,(-)$ mode and at the same time tuning the pump laser frequency ω_p to be slightly larger than the eigenfrequency ω_- (ω_+). In general, exciting mainly the $-$ mode, i.e. $\phi = \pi$, leads to a more effective cooling, especially for large PRM reflectivities θ, whereas the highest temperature drop when pumping the $+$ mode is found only for very small θ. Altogether, the maximal relative temperature decrease found in panel (a) of figure 5.9 is $\approx 6 \times 10^{-2}$, which corresponds to a cooling of almost 10 mK when starting at the temperature $T_0 = 100\,\mathrm{mK}$. That is, despite the fact that we already considered relatively large pump intensities $E_0 = 10^3\kappa$, which implies a pump laser power $\sim \mu$W, the cooling of the movable PRM inside a ring cavity is of only moderate efficiency compared to other cooling schemes, e.g. [17].

The cooling effect of the ring cavity could be improved by using even stronger pump lasers (up to $\sim 1\,\mathrm{mW}$). However, one has to take care that the high laser power does not lead to heating or even destruction of the PRM due to absorption. Another option would be to decrease the decay rate of the cavity, but at some point this violates the bad cavity limit $\Omega_m \ll \kappa$. Probably the best way is to further decrease the initial temperature of the micro-mechanical oscillator and to improve its quality, which is a very challenging task, too.

Chapter 6

Conclusion and outlook

The aim of this thesis was to derive and investigate the optomechanical forces acting on a partially reflecting micro-mechanical movable mirror (PRM) placed into the beam line of a ring cavity opposed to the incoupling mirror. In chapter 4, we found in which form the travelling plane wave cavity modes are coupled by the PRM, which was done by applying a transfer/scattering matrix formalism suggested by the known scattering matrix of a conservative beam splitter of arbitrary reflectivity. With that technique, a single spatial round trip along the ring was performed and we could thereby extract the cavity eigenmodes and eigenfrequencies, the latter of which only depend on the PRM reflectivity θ, but due to translational symmetry of the ring cavity, they are independent of the PRM displacement ξ. The cavity eigenmodes are given by even and odd mode functions with respect to the PRM and they correspond to a lower and higher resonance frequency, respectively, which merge into the eigenfrequency of an empty ring cavity as $\theta \to 0$. This can be explained by different dielectric polarization energies of the PRM in the even and odd cavity fields, respectively—a parallel to the formation of band gaps in photonic crystals. The above mentioned matrix formalism also led us to a discrete time evolution of the cavity fields in steps of the round trip time τ, under the realistic assumption that the mirror position does not change during that time ($\Omega_m \tau \ll 1$). From that we then deduced the corresponding Langevin equations describing the dynamics of the cavity fields of the open quantum system "ring cavity" on a larger time scale. At that point, the mirror position only enters as a parameter. We discovered that the coupling and thus the field dynamics of the cavity fields in the ideal ring cavity are governed by the Hamiltonian $H_{\text{light}}(\xi)$, which does, however, not generate the correct dynamics of the PRM position and momentum operator. Moreover, we discussed that with particular choices of the pump laser phase difference and frequency one can excite one of the cavity eigenmodes and analyzed the dependence of the steady-state fields on the experimental parameters like detuning and PRM reflection and position. The cavity resonances have, of course, a lorentzian shape due to the dissipative nature of the ring cavity and non-vanishing mirror displacements break the symmetry of the system and thus lead also to the excitation of the undriven mode.

As mentioned above, the mirror dynamics are not simply obtained by plugging H_{light} into Heisenberg's equation of motion and we thus first had to derive the force operator $F = dp/dt$, which was the subject of Chapter 5. This has been done in three

different ways, which all led to the same expression. We were able to identify the two components radiation pressure and dipole force, the first of which is only present for asymmetric pump amplitudes. The dipole force depends on the PRM displacement and can possibly also be interpreted in terms of the dielectric polarization energy of the PRM by the cavity fields. However, further work must be done in this direction to completely understand the emergence of the dipole force. We then allowed for a moving PRM by expanding the equations of motion as well as the mode operators to linear order in the PRM velocity v and solved the resulting equations separately. The optomechanical force thereby splits into a conservative force, imposing an additional fluctuating harmonic potential for suitably chosen pump parameters, and a friction force, which leads to cooling of the mirror motion for particular ranges of detuning and PRM reflectivity. That is, we discovered the possibility of trapping and cooling the micro-mechanical mirror, as is required for observing quantum effects of macroscopic objects. However, the fluctuations of the conservative part of the force, which originate from the vacuum fluctuations of the electromagnetic field outside of the ring cavity, induce momentum diffusion and thus limit the final temperature of the present cooling scheme. Neglecting the intrinsic dissipation and diffusion of the oscillator, we found a limit temperature of about $10^{-5}\,\mathrm{K}$ for the oscillating membranes particularly considered in this work and for pump laser powers in the μW range. This temperature is roughly of the order of $\hbar\kappa/k_B$, that is, it mainly seems to be limited by the bandwidth of the loss channel of the system, which is the cavity decay at rate κ. This is in analogy with the famous Doppler limit. Altogether, we see that the trapping and cooling of the micro-mechanical oscillator is not as effective as with traditional setups using linear cavities. This is probably due to the fact that the eigenfrequencies of the cavity do not change with the PRM position. The effects are in principle scalable by the pump laser power and one could possibly increase it up to the mW range, but at some point nonlinear effects arise and the in reality inevitable absorption of light by the PRM eventually leads to heating or even destruction of the oscillator. As we mentioned in the introduction, the advantage of the ring geometry is the possibility of the cancellation of pump laser phase noise [19], which already questions the feasibility of ground state cooling of macroscopic objects in linear cavities. As we did not discuss the effects of pump laser noise in this thesis, further investigation has to be done on that matter. The effect of using squeezed pump light would also be interesting.

Bibliography

[1] W. H. Zurek, Phys. Today **44**, 36 (1991).

[2] E. Schrödinger, Proc. Cambr. Phil. Soc. **31**, 555 (1935).

[3] D. Bouwmeester, A. Ekert and A. Zeilinger, *The Physics of Quantum Information*, Springer, Berlin, 2000.

[4] *Quantum Entanglement and Information Processing*, edited by D. Estève, J.-M. Raimond and J. Dalibard, Elsevier, Amsterdam, 2003.

[5] M. Nielsen and I. Chuang, *Quantum Computation and Quantum Information*, Cambridge University Press, 2000.

[6] D. Vitali, S. Gigan, A. Ferreira, H. R. Böhm, P. Tombesi, A. Guerreiro, V. Vedral, A. Zeilinger and M. Aspelmeyer, Phys. Rev. Lett. **98**, 030405 (2007).

[7] M. Paternostro, D. Vitali, S. Gigan, M. S. Kim, C. Brukner, J. Eisert and M. Aspelmeyer, Phys. Rev. Lett. **99**, 250401 (2007).

[8] M. Pinard, A. Dantan, D. Vitali, O. Arcizet, T. Briant and A. Heidmann, Europhys. Lett. **72**, 747 (2005).

[9] M. Bhattacharya and P. Meystre, Phys. Rev. Lett. **99**, 073601 (2007).

[10] M. Bhattacharya, H. Uys and P. Meystre, Phys. Rev. A **77**, 033819 (2008).

[11] W. H. Zurek, Rev. Mod. Phys., **75**, 715 (2003).

[12] E. Joos, H. D. Zeh, C. Kiefer, D. Guilini, J. Kupsch and I.-O. Stamatescu, *Decoherence and the Appearance of a Classical World in Quantum Theory*, Springer-Verlag Berlin Heidelberg, 2003.

[13] D. Kleckner, W. Marshall, M. J. A. de Dood, K. N. Dinyari, B.-J. Tors, W. T. M. Irvine and D. Bouwmeester, Phys. Rev. Lett. **96**, 173901 (2006).

[14] D. Kleckner and D. Bouwmeester, Nature **444**, 75 (2006).

[15] T. Corbitt, Y. Chen, E. Innerhofer, H. Müller-Ebhardt, D. Ottaway, H. Rehbein, D. Sigg, S. Whitcomb, C. Wipf and N. Mavalvala, Phys. Rev. Lett. **98**, 150802 (2007).

[16] O. Arcizet, P.-F. Cohadon, T. Briant, M. Pinard and A. Heidmann, Nature **444**, 75 (2006).

[17] J. D. Thompson, B. M. Zwickl, A. M. Jayich, F. Marquardt, S. M. Girvin and J. G. E. Harris, Nature **452**, 72 (2008).

[18] C. Henkel, M. Nest, P. Domokos and R. Folman, Phys. Rev. A **70**, 023810 (2004).

[19] L. Diósi, arXiv:0803.3760v2 (2008).

[20] M. Blencowe, Physics Reports **395**, 159 (2004).

[21] S. Bose, K. Jacobs and P. L. Knight, Phys. Rev. A **59**, 3204 (1999).

[22] V. B. Braginsky and F. Ya. Khalili, *Quantum Measurement*, Cambridge University Press, 1992.

[23] R. J. Glauber, Phys. Rev. **130**, 2529 (1963); R. J. Glauber, Phys. Rev. Lett. **10**, 84 (1963).

[24] E. C. G. Sudarshan, Phys. Rev. Lett. **10**, 277 (1963).

[25] M. Orszag, *Quantum Optics*, Springer-Verlag Berlin Heidelberg, 2000.

[26] M. O. Scully and M. S. Zubairy, *Quantum Optics*, Cambridge University Press, 1997.

[27] D. F. Walls and G. J. Milburn, *Quantum Optics*, Springer-Verlag Berlin Heidelberg, 1994.

[28] M. Pinard, Y. Hadjar and A. Heidmann, Eur. Phys. J. D **7**, 107 (1999)

[29] U. Leonhardt, Phys. Rev. A **48**, 3265 (1993).

[30] R. J. C. Spreeuw, R. Centeno Neelen, N. J. van Druten, E. R. Eliel and J. P. Woerdman, Phys. Rev. A **42**, 4315 (1990).

[31] G. Barton and A. Calogeracos, Ann. Phys. (NY) **238**, 227 (1995).

[32] L. Mandel and E. Wolf, *Optical Coherence and Quantum Optics*, Cambridge University Press, 1995.

[33] J. D. Jackson, *Classical Electrodynamics (3rd ed.)*, Wiley, New York, 1998.

[34] P. Domokos and H. Ritsch, J. Opt. Soc. Am. B **20**, 1098 (2003).

[35] J. P. Gordon and A. Ashkin, Phys. Rev. A **21**, 1606 (1980).

Selbständigkeitserklärung

Hiermit versichere ich, dass ich die vorliegende Arbeit mit dem Titel “Forces on mobile optical elements in a ring cavity” selbständig verfasst und keine anderen als die angegebenen Quellen und Hilfsmittel benutzt habe und dass die Arbeit in gleicher oder ähnlicher Form noch keiner Prüfungsbehörde vorgelegt wurde.

Marc Herzog
Potsdam, den 17.04.2008